Thermal Spray Coatings on Water-Wall Tubes of Bagasse-Fired Boilers by Ni-based Alloys for Enhancing Corrosion Prevention Capacity

Adama Science and Technology University

Ephrem Beyene Duressa

A Thesis submitted to
The Department of Materials Science and Engineering

School of Chemical, Mechanical, and Materials Engineering

Submitted in Partial Fulfillment of the Requirement for the Degree of Master's in Materials Science and Engineering

Office of Graduate Studies

Adama Science and Technology University

December 2021

Adama, Ethiopia

Thermal Spray Coatings on Water-Wall Tubes of Bagasse-Fired Boilers by Ni-based Alloys for Enhancing Corrosion Prevention Capacity

Ephrem Beyene Duressa

Advisor: Thothadri Ganesh (Ph.D.)

Co-advisor: Dinsefa Mensur (Ph.D.)

A Thesis submitted to The Department of Materials Science and Engineering

School of Chemical, Mechanical and Materials Engineering

Presented in Partial Fulfillment of the Requirement for the Degree of

Master's in Materials Science and Engineering

Office of Graduate Studies

Adama Science and Technology University

December 2021

Adama, Ethiopia

Declaration

I hereby declare that this Master Thesis entitled "**Thermal Spray Coatings on Furnace Wall Tubes of Bagasse Fired Boilers by Ni-based Alloys for Enhancing Corrosion Prevention Capacity**" is my original work. That is, it has not been submitted for the award of any academic degree, diploma, or certificate in any other university. All sources of materials that are used for this thesis have been duly acknowledged through citation.

_____	_____	_____
Name of Student	**Signature**	**Date**

Recommendation

I/we, the advisor(s) of this thesis, hereby certify that I/we have read the revised version of the thesis entitled "**Thermal Spray Coatings on Furnace Wall Tubes of Bagasse-Fired Boilers by Ni-based Alloys for Enhancing Corrosion Prevention Capacity**" prepared under my/our guidance by Ephrem Beyene submitted in partial fulfillment of the requirements for the degree of masters of Science in Materials Science and Engineering. Therefore, I/we recommend the submission of a revised version of the thesis to the department following the applicable procedures.

_____	_____	_____
Major Advisor	Signature	Date
_____	_____	_____
Co-advisor	Signature	Date

Approval Page of the Thesis

I/we, the advisors of the thesis entitled "**Thermal Spray Coatings on Furnace Wall Tubes of Bagasse-Fired Boilers by Ni-based Alloys for Enhancing Corrosion Prevention Capacity**" and developed by Ephrem Beyene, hereby certify that the recommendation and suggestions made by the board of examiners are appropriately incorporated into the final version of the thesis.

_____	_____	_____
Major Advisor	Signature	Date
_____	_____	_____
Co-advisor	Signature	Date

We, the undersigned, members of the Board of Examiners of the thesis by Ephrem Beyene have read and evaluated the thesis "**Thermal Spray Coatings on Furnace Wall Tubes of Bagasse-Fired Boilers by Ni-based Alloys for Enhancing Corrosion Prevention Capacity**" and examined the candidate during the open defense. This is, therefore, to certify that the thesis is accepted for partial fulfillment of the requirement of the degree of Master of Science in Materials and Engineering.

_____	_____	_____
Chairperson	Signature	Date
_____	_____	_____
Internal Examiner	Signature	Date
_____	_____	_____
External Examiner	Signature	Date

Finally, approval and acceptance of the thesis are contingent upon submission of its final copy to the Office of Postgraduate Studies (OPGS) through the Department Graduate Council (DGC) and School Graduate Committee (SGC).

Department Head	Signature	Date
School Dean	Signature	Date
Office of Postgraduate Studies	Dean Signature	Date

Acknowledgement

There are many individuals who have assisted me during my present work. I would like to extend my lofty gratitude -- first and foremost to Jesus Christ my Lord for His abundant grace.

My first vote of thanks must go to Dr. Thothadri Ganesh for his unceasing enthusiasm, interest, constructive criticism and practical hand on assistance with the Powder Flame Thermal Spray System and for putting up with me until the end. His expertise, availability to discuss ideas and willingness to give his knowledge were instrumental in the completion of this thesis. I owe him too much gratitude for all his unreserved efforts till the completion of the work.

I would like to express my sincere thanks to Dr. Dinsefa Mensur, for whom I have the greatest respect and admiration. His guidance and supervision were invaluable. I am extremely grateful for all his advises and suggestions towards solving the problems and fueling me forward to finalize the work and granting me to all access to all department services as department head.

I will be sincerely indebted to Mr. Girum Asfaw, Mr. Fiseha Tarekegn, & Mr. Tilahun Zeleke from Ethiopian Sugar Research Center (ESRC) who assisted me in the laboratory activities so that the paper will be applied in the sugar sector wherein I work as research engineer. Without their support and encouragement, this research would not have been done.

I would like to acknowledge workshop staffs at WSSF Mr. Hiluf Hagos (welder), Mr. Yismu Getachew (Machine Shop and Fabrication Head) for their technical help and discussions at various stages of the work. Special thanks also goes to my brother Mr. Fasil Beyene (Prod'n Mgr., FSF) for his regular support and assistance in getting the samples from Finchaa Sugar Factory (FSF).

I am grateful to Mr. Demeke Tesfaye (laboratory coordinator at ASTU, MSED) Yeshitla Tsegaw, Ermias Tafa, Mintesinot Tamiru and other colleagues for supporting me from the laboratory centers of MSED, ASTU for their assistance in the synthesis and characterization of the project.

Last but not certainly the least, my gratitude is extended to my family, especially my beloved mother, father, and elder brother who have given their utmost support throughout my life so far. They have inspired me whole-heartedly since childhood to advance in my educational career.

Contents

List of Acronyms

AAS – Atomic Absorption Spectrometer

AC – Alternating Current

CS – Carbon Steel

EDS – Electron Dispersion Spectroscopy

EIS – Electrochemical Impedance Spectroscopy

FSF – Finchaa Sugar Factory

FTIR – Fourier Transform Infrared

FWT – Furnace Wall Tubes

MSE – Materials Science and Engineering

PFTS – Powder Flame Thermal Spray

PSI – Pounds per Square Inch

SCC – Stress Corrosion Cracking

SEM – Scanning Electron Microscopy

TCD – Tons of Cane Crushed per Day

UTG – Ultrasonic Thickness Gauge

WTE – Waste to Energy

WLM – Weight Loss Method

WSSF – Wonji Shoa Sugar factory

WWT – Water Wall Tubes

XRD – X-Ray Powder Diffraction

List of Figures

List of Tables

Abstract

Bagasse-fired boilers heavily suffer from high temperature corrosion despite the importance of sustainable boiler operation in the sugar industries. The failure and downtime of boilers is a big threat to the effectiveness of steam power plants, juice process plants, and distilleries. Corrosion related failures cost a huge percentage in the yearly maintenance cost involved in Ethiopian sugar industries. The coating of a compact and adherent Ni-based alloys by using powder flame thermal spray technique is a fail-safe approach to extend the component's service-time and, hence, increase the thermal, and electrical efficiency of the boilers. In this research, Ni-based coatings of Ni20Cr, Ni50Cr, Ni50Al, and Cr_3C_2-30(Ni20Cr) – sprayed by using powder-flame thermal spray coating has been investigated through detailed laboratory studies in 3.5wt% NaCl and 0.5N H_3PO_4-NaOH environments. The pristine and corroded carbon steel substrate (SA210-A1) was characterized by OM, SEM, TGA, DTA, and while the coated samples were characterized by XRD, EIS, and weight loss and the results were consistent. The physical properties of the sample has also been studied using weight loss, thickness loss, particle density, and hardness. The exposures were conducted in a simulated boiler environment at 600 ˚C for up to 120h with and without NaCl salt. The applied coatings were highly protective in all environments due to formation of corresponding protective layers of Cr_2O_3 and Al_2O_3 on the substrate surface. The oxide scale formed by powder flame thermal spray techniques with Ni-based alloys coatings has lowered the corrosion rate because the created oxide was continuous, adherent, and rich in chromium. With the use of 0.5N H_3PO_4-NaOH, pH = 11 as an electrolyte has decreased the rate of corrosion because of its alkalinity as it is the standard pH value for the supply of boiler water. A percentage drop in the corrosion rate of 11.48% was attained with coating performed by Ni20Cr. The performance of the coatings in the tested environment was ranked (from highest to lowest corrosion resistance); Ni20Cr > Ni50Cr > Ni50Al > Cr_3C_2-30(Ni20Cr).

Keywords: Corrosion, Boilers, Alloys, Powder-Flame Thermal Spray Coating, Furnace Wall Tubes, Dispersed Oxide, Microstructures

CHAPTER 1

INTRODUCTION

Corrosion is a serious problem in many industrial machinery components resulting in catastrophic failure, economic loss and personal injury [1-3]. In this regard, the power generation industry has been rapidly shifting towards utilization of more ecologically compliant biomass and waste fuels, like bagasse, straw and municipal solid wastes (MSW) to reduce the usage of fossil fuels, and accordingly the emissions of CO_2[4]. Unlike the fossil fuels, biomass and waste fuels are firstly considered CO_2-neutral, i.e. the carbon released during combustion in the form of CO_2 emission can be re-used for new plant growth. Thus, no net increase in the greenhouse gases is yielded. Secondly, burning such inexpensive fuels to produce electricity/heat diminishes waste landfill and minimizes the amount of foreign currency needed to purchase it in developing countries like Ethiopia. Even though there are several incentives to utilize such fuels, these fuels contain high concentrations of corrosive species such as chlorine (Cl_2), water vapor, hydrogen chloride (HCl) and alkali chlorides (e.g., KCl, or NaCl), which are released along with the hot fuel gas and accelerate corrosion of boiler components, especially furnace-wall and superheater tubes [5]. When the boilers are in operation, these corrosive compounds are deposited on the boiler parts, thereby not only curtailing the heat transfer but also triggering corrosion mechanisms. Corrosion reduces the thermal/electrical efficiency of the boiler and causes high maintenance, retubing and replacement, and outage costs [6].

To address these problems many efforts have been made to produce high performance Ni-based coatings providing improved corrosion resistance to components. Nickel is an ideal base for corrosion resistant alloys. Not only is it inherently resistant to certain chemicals, but also it can be highly alloyed with elements known to enhance corrosion performance, such as chromium, copper, molybdenum and aluminum while retaining its ductile face-centered cubic structure [7].

In addition to commercially pure nickel, four binary alloy systems also provide exceptional corrosion resistance. These include nickel-chromium (Ni-Cr), nickel-copper (Ni-Cu), nickel-aluminum (Ni-Al), and nickel-molybdenum (Ni-Mo). Chromium enhances the resistance of nickel to oxidizing acids by triggering the formation of passive films. Copper is very helpful in seawater, brackish water, and reducing acids, in particular hydrofluoric. Aluminum resists corrosion due to

its tendency to form a compact oxide layer over the surface. Molybdenum is extremely beneficial in all reducing acids[7, 8].

Most of the industrial machinery parts in general and sugar factory components in particular currently being utilized can potentially degrade or catastrophically fail in service due to such phenomena as wear, corrosion, and fatigue. Thus serviceable engineering components not only rely on their bulk material properties, but also on the design and characteristics of their surface. Surface engineering involves the application of traditional and innovative coating technologies to engineering components and materials to improve their characteristics [9].

There are quite a number of processes to apply coatings, as well as a nearly unlimited number of coating materials. To select the correct combination for the respective application, the knowledge of specialists is usually required. Thermal spraying process is one of the most successful of all the advanced coating techniques because of the wide range of coating materials and substances to which it can be applied. Metals and carbides are mostly used as base materials, although spraying of polymers has been researched [10, 11].

Along with the microstructure, the content of coating materials also plays a critical role in corrosion protection mechanisms [12, 13]. Ni-based coatings with the addition of protective scale-forming elements, e.g., Cr and/or Al, have demonstrated reasonable high temperature corrosion protection and have been studied both in commercial boilers and in laboratory furnaces with simulated corrosive environments [14, 15]. However, the corrosive agents have been found to diffuse through some of the coatings, accompanied by depletion of Cr or/and Al [16].

Table 1 below lists principal coating processes, the typical coating thicknesses attainable, common coating materials, and sample applications. Some processes are not suitable for certain coating materials; also, the necessary coating thicknesses are not attainable with all methods. Beyond that, the equipment necessary for some processes can be quite complex and, therefore costly. The use of cost analysis can determine whether a coating is a noble practical solution. Today's regulations require that ecological criteria of the respective coating processes must also be examined, as not all methods are environmentally friendly.

Table 1 Principal Coating Processes and Characteristics [17]

Coating Process	Typical Coating Thickness	Coating Material	Characteristics	Examples
PVD	1 - 5µm	Ti(C,N)	Wear resistance	Machine tools
CVD	1 – 50 µm	SiC	Wear resistance	Fiber coatings
Baked Polymers	1 – 10 µm	Polymers	Corrosion resistance, aesthetics	Automobile
Thermal Spray	0.04 – 3 mm	Ceramic and metallic alloys	Wear, tear resistance, Corrosion resistance	Bearings, tubes
Hard Chromium Plate	10 – 100 µm	Chrome	Wear resistance	Rolls
Weld Overlay	0.5 – 5 mm	Steel, Stellite	Wear resistance	Valves
Galvanize	1 - 5 µm	Zinc	Corrosion resistance	Steel sheet
Braze Overlay	10 - 100 µm	Ni-Cr-B-Si alloys	Very hard, dense surface	Shafts

The coating process having the greatest range of coating materials, coating thicknesses and possible coating characteristics is thermal spray as illustrated in **Table 1**. Thermal spray is defined as "Applying coatings takes place by means of special devices/systems through which melted or molten spray material is propelled at high speed onto a cleaned and prepared component surface [18]. Thermally sprayed coatings are used to protect components from different types wear and corrosion [19-21]. Various base metals are also coated with a low thermal conductivity material to increase its application [22, 23]. There are several different processes used to apply a thermal sprayed coating such as flame spray, electric arc wire spray, plasma spray, and high velocity oxy-fuel spray (HVOF).

The conventional flame spray can be either wire flame spray or powder flame spray. In the wire flame spray system, the wire spray material is melted in a gaseous oxygen-fuel flame. The fuel gas can be acetylene, propane or hydrogen. The wire is fed concentrically into the flame, where it is melted and atomized by the addition of compressed air that also directs the melted material towards the workpiece/substrate surface. On the other hand, the powder flame coating process is based on the same operational principle as the wire flame spray process, with the difference that the coating material is a spray powder. Thus, a larger selection of spray materials is available, as not all spray materials can be manufactured in wire form[18].

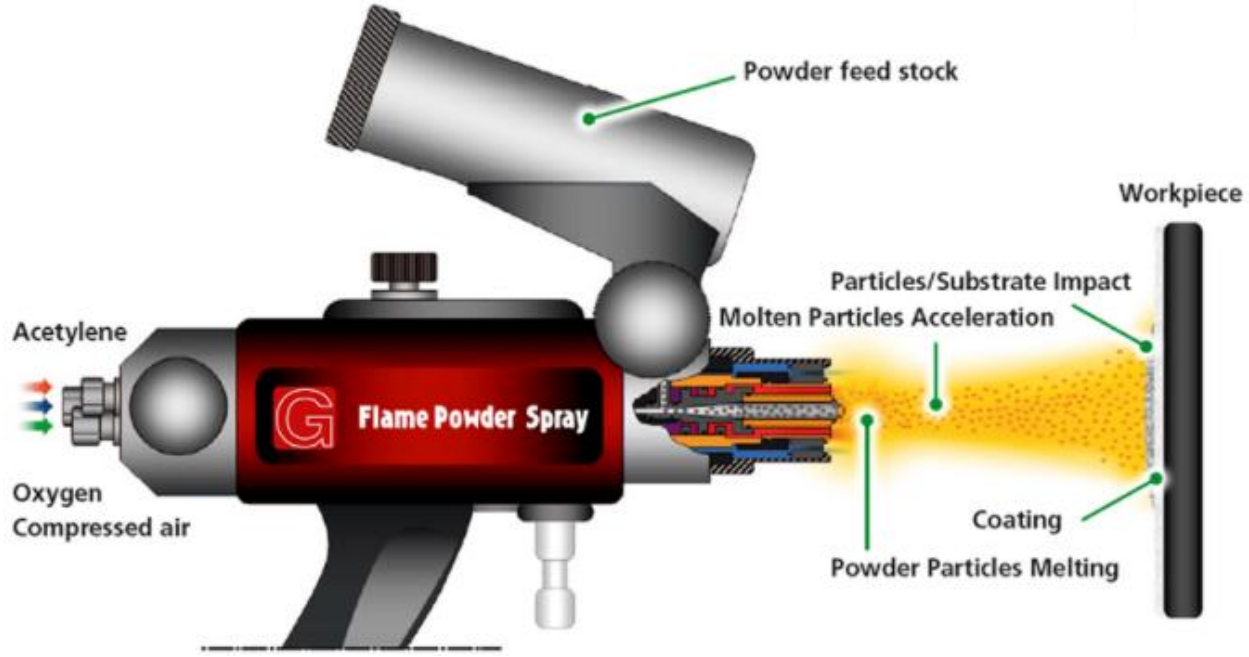

Figure 1 Schematic diagram of powder flame spray coating process [24]

1.1 Thesis Outline

This thesis consists of five chapters, including this introduction which illustrates the scope and limitations of the work, as well as the structure of the research work and the outline of the thesis. The scope and limitations of the work, as well as the research questions addressed, are discussed at the end of this chapter. **Chapter 2** provides the review of literature and background information, to illustrate a better understanding of the main motivation behind this study and why this research work is relevant to the scientific society, specifically to the thermal society. This chapter begins with a review of power plant boilers utilizing biomass and waste fuels, and the encountered high temperature corrosion problems. A literature review on previous works performed to reduce corrosion using coatings in power plants is illustrated. However the main focus is on coatings produced with various thermal spray processes. In **Chapter 3**, the coating materials utilized in this research have been discussed in detail. The choice of Nickel as a base metal and other alloying elements like chromium, aluminum, cermets have been discussed in detail. **Chapter 4** discusses the experimental procedures utilized to produce the coatings and investigate them before and after high temperature corrosion exposures. The different corrosion test methods and equipment's set up and the procedures needed for the set up formation are also described in detail. In Chapter 4, the effect of coating composition, microstructure, and architecture on high temperature corrosion behaviour is illustrated in detail. In **Chapter 5**, the characterization of the results obtained from

the research are discussed in detail. **Chapter 6 and 7** give conclusions and recommendations for future work, respectively.

1.2 Objectives

1.2.1 General Objectives

The objective of this study was to enhance the corrosion resistance capacity of furnace-wall tubes by application of thermal sprayed coatings of Ni-based alloys.

1.2.2 Specific Objectives

- To redesign, and modify the conventional oxy-acetylene cutting/welding torch in local machine shops so that it can be utilized for the purpose of powder flame thermal spray coating so that it can be used for boiler tube application.
- To evaluate and select the corrosion resistant materials that can be effective in preventing the corrosion of boiler tubes in sugar mills context.
- To enhance the corrosion resistance of Ni-based alloy coatings in a simulated boiler environment, and hence enhance the corrosion prevention capacity of the tubes in the boilers in general and water-wall tubes in particular.

1.3 Statement of Problems

In most of the steam generation plants of Ethiopian sugar mills, boilers are subjected to recurrent outages caused by frequent rupture of tubes caused by corrosion which resulted in ~8% of the total downtime of power generation plant. On the one hand, the contamination of water with juice (pH≈5.4) which creates acidic environment is another critical factor that contributes a lot to aggravate the effect of corrosion on the boiler tubes. On the other hand, the substandard operation of deaeration and entrainment of oxygen and carbon dioxide is the other factors that aggravate the problem of corrosion in the boiler. In the year 2016/17, the retubing project of the existing boiler of Finchaa Sugar Factory (FSF) costed about ETB 90M after a total service of 18years. Therefore, even though researchers made tremendous effort to rectify the problem by treatment of boiler water; the problem of corrosion in the boiler tubes is still unresolved.

1.4 Scope and Limitations

1.4.1 Scope

This particular research was an experiment-based research targeted to examine the thermal spray coatings against high temperature corrosion for bagasse-fired water-tube boiler applications.

1.4.2 Limitations

Certain limitations should be taken into consideration if the results of this research should be applied to other thermal spraying techniques for coating applications. The limitations of this current research are summarized as follows:

i. Coating Materials

Only Ni-based coating materials (Ni50Cr, Ni20Cr, Ni50Al, and Cr_3C_2-30Ni20Cr) were investigated in this particular project. For the substrate material, I selected a commercially available carbon steel ASTM SA210-GrA1 which is a common material for boiler tubes in FSF.

ii. Coating Applications

This project was focused on Ni-based powder flame thermal spray coatings for bagasse-fired water tube boilers specifically on water-wall tubes.

iii. Spraying Techniques

The spraying of coatings was mainly executed using oxy-acetylene flame powder spray coating technique. Even though thermal spraying techniques were briefly explored in this research, the coating process of the furnace-wall tubes was conducted using oxy-acetylene powder-flame thermal spray coating by small modification on the tip of the cutting torch.

iv. Coating Characterization Techniques

Experimental coating characterization performed in this project was limited to the characterization techniques (hardness, particle density, thermal analysis, weight loss, thickness loss, electrochemical impedance spectroscopy (EIS), surface roughness, microstructure analysis performed using optical microscope, scanning electron microscope (SEM). The phases formed before and after the corrosion exposures were evaluated using X-ray diffractometer (XRD).

CHAPTER 2

LITERATURE REVIEW

2.1 Introduction

Surface coating methods are available in a wide variety due to the enormous diversity of applications and needs in different fields. These processes consist of many different on-line/off-line parameters while giving way to many different outcomes in the form of material microstructure, effectiveness, suitability, and durability. However, coating methods are useful in specific applications according to the desired functionality among which corrosion and wear protection are the most important[25]. The property of a material is greatly dependent upon its surface, the environment and its operating conditions. Surface engineering can be defined as the branch of science that deals with methods for achieving desired surface requirements and behaviour in service for industrial machinery components[26].

The surface of any component may be selected on the basis of texture and color, but engineering components generally demand a lot more than this. Surface properties of the component used in a particular working environment have to be designed with that environment in mind. Surface engineering in today's production world embraces the design, evaluation and performance in service of a component including a substrate, through the interface, to the surface of a coating [27]. Coating technology can be tailored to suit certain environments. A variety of bulk materials, such as ferrous and non-ferrous metals, alloys, ceramics and cermets can be coated to achieve adequate resistance to wear, corrosion and friction.

2.2 Reliable Coating Techniques

A coating may be defined as a near surface region, having properties different from the bulk material it is deposited on. Coating methods provide protection to a specific part or area of a structure exposed to harsh and corrosive environments in different fields ranging from aerospace and the automotive industry to tiny biomedical devices and implants inside the human body[28]. Thus the material system (coating and substrate) forms a composite, where one set of properties is obtained from the bulk substrate and another from the coating itself. Coatings may be applied to the surface of materials in order to protect the surface from the environment that may produce corrosion or other deteriorative reactions and/or to improve the surface's appearance[9].

The selection of specific deposition process depends on several factors, including:

1. Chemical, process, and mechanical compatibility of the coating material with the substrate [29],
2. Rate of deposition required,
3. The ability of the substrate to withstand the required processing[30],
4. Limitations imposed by the substrate (for example maximum allowable deposition temperature),
5. Adhesion of the deposited material to the substrate,
6. Process energy,
7. Purity of the target material (this will influence the purity content of the film),
8. Requirement and availability of the apparatus,
9. Cost,
10. Ecological considerations.

Despite the fact that there are different types of coatings, the coating technique having the greatest range of coating materials, coating thicknesses, good coating characteristics are few **(Figure 3)**. These techniques are divided into two common groups, metallic and non-metallic. Metallic coating deposition has three categories, hard facing being the most important in the context of this research. Hard facing is used to deposit thick coatings of hard and wear and corrosion resistant materials on either a worn component or new component, which is subjected to wear in service. There are three techniques of hard facing available: welding, cladding, and thermal spraying. Thermal spraying is of the most importance in this research, hence the following section concentrates on this technique[9].

a) b)

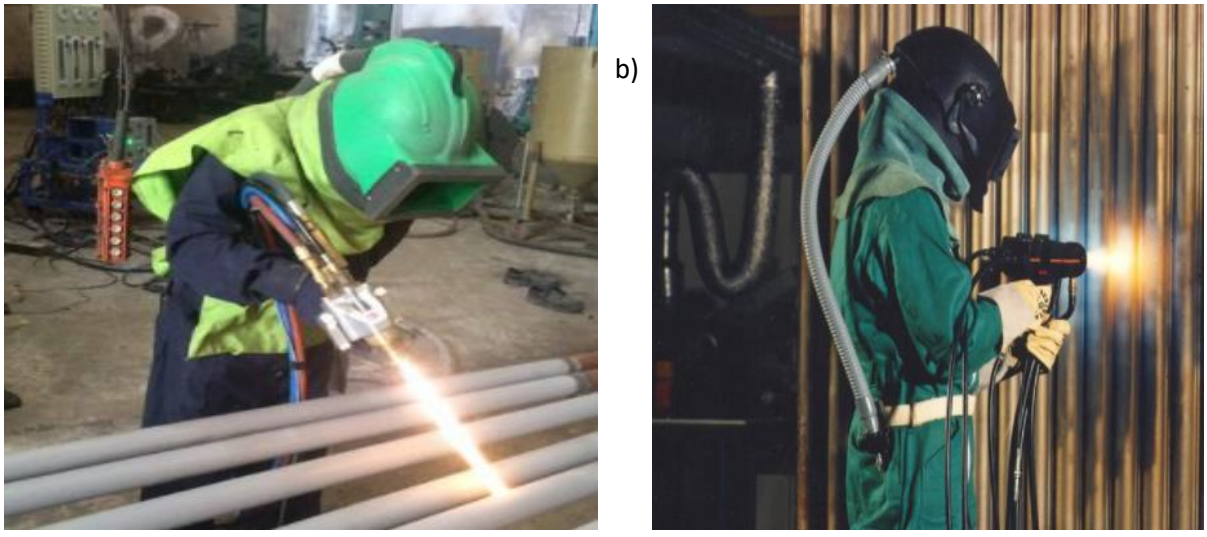

Figure 2 Schematic showing thermal spraying of boiler tubes [31]

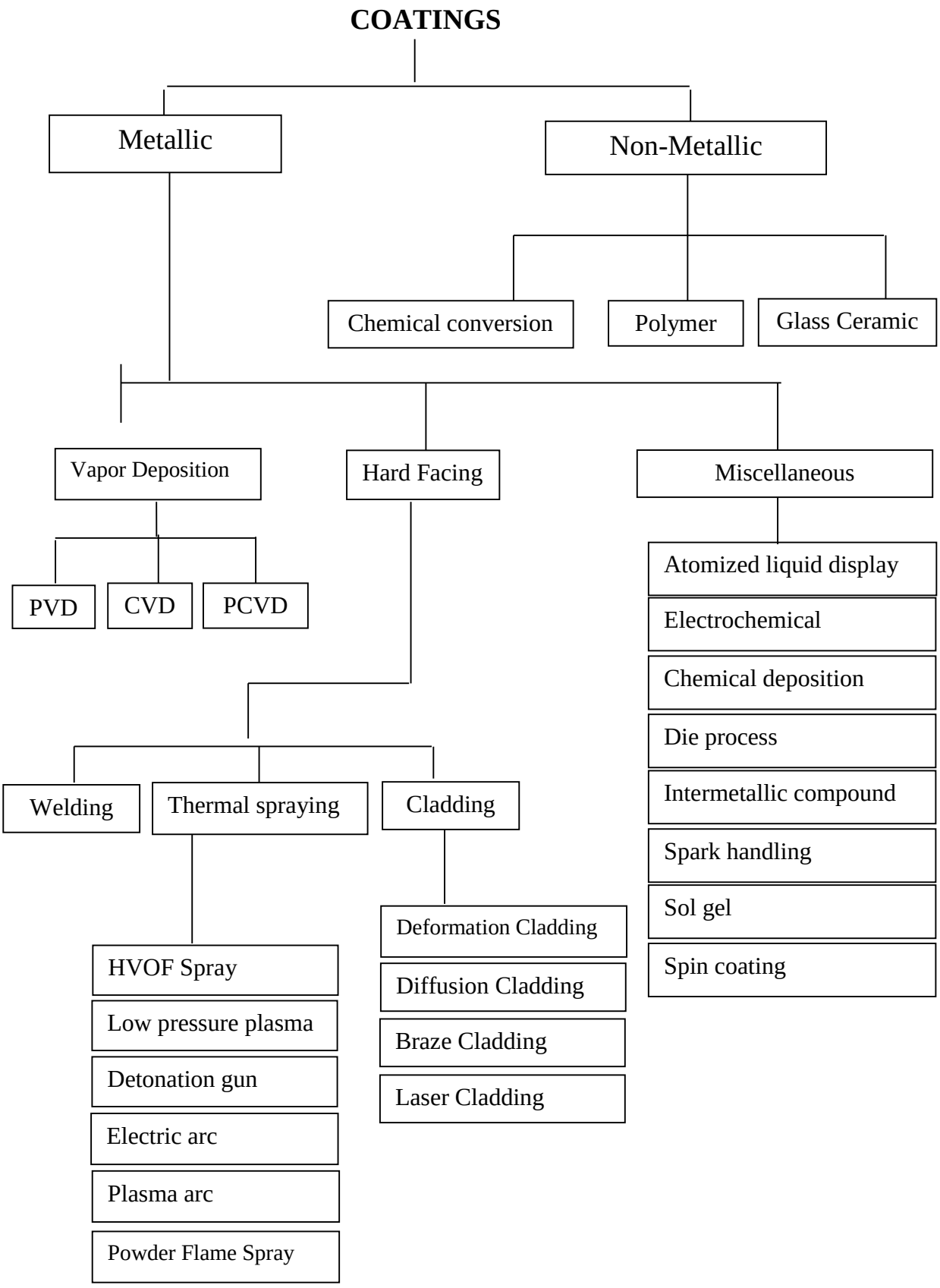

Figure 3 Coating Deposition Techniques [32]

2.3 Thermal Spray Techniques

In addition to the new innovative patents registered in 1882 and 1899, new other patents on tin and lead coating on metal surfaces have been attained with thermal spraying by Dr. Max Schoop [33]. The rate of progress of thermal spray was slow after the inception of Schoop, then it increased at a modest rate until 1950s. At that time a variety of what then was known as modern plasmatrons appeared, which boosted the development considerably[34]. In particular, the D-gun coatings, developed by Praxair Surface Technology found a receptive market in the aerospace industry and a large proportion of subsequent technological growth was due to plasma based thermal barrier coatings [34].

Thermal Spraying is a group of processes wherein a feedstock material is heated and propelled as individual particles or droplets onto a surface. As the materials are heated, they are changed to a plastic or molten state and are confined and accelerated by a compressed gas stream to the substrate. The particles strike the substrate, flatten, and form thin platelets (splats) that conform and adhere to the irregularities of the prepared substrate and to each other[35].

Thermal spraying comprises a number of techniques that are widely and industrially used to obtain coatings on many different types of substrates and for many different applications. These techniques are flexible and provide high quality coatings with a fraction of the cost that other fractions have[36, 37]. In 1988 Sulzer **METCO** introduced Powder Flame thermal spray system, which is the process under investigation in the current research and which is described in detail later in this report[34].

Thermal spraying is a process whereby a coating material is fed into a heating zone to become molten (or semi-molten), and is then propelled from there to base material (substrate)[38]. The industrial benefit of the thermal spray coatings is the achievement of cost-effective solutions to minimize wear and corrosion, including thermal barrier coatings. The tailoring of components, or specific areas, to counteract damaging effects, prolongs new parts or provides cost-effective restoration of worn parts. Substrate materials such as low and medium carbon steel can be thermally sprayed with thin layers of nickel alloys to provide a cost-effective product with high corrosion resistance[39].

The heat energy that is used to melt the coating material, may be divided into two categories, electrical and flame heating. There are three processes by which electrical heating is utilized to melt the coating material. They are:

a) Electric arc process,
b) Plasma arc process,
c) Low pressure plasma spraying,

Additional information has been illustrated by Stokes on those techniques[40], hence this is not described here. The second type is flame heating with the following three processes:

a) Flame spraying process,
b) Spray and fuse process,
c) HVOF thermal spray process.

The flame spraying process is relevant to this study, hence this flame heating process is investigated in detail in this research.

2.3.1 Flame Spraying Process

Thermal spray processes may be categorized as either combustion or electric processes. Combustion processes include flame spraying, HVOC spraying, and detonation flame spraying. Electric processes include arc spraying and plasma spraying.

a. Combustion Processes

(1) Flame Spraying

The oldest form of thermal spray, flame spraying, may be used to apply a wide variety of feedstock materials including metal wires, ceramic rods, and metallic and non-metallic powders. In flame spraying, the feedstock material is fed continuously to the tip of the spray gun where it is melted in a fuel gas flame and propelled to the substrate in a stream of atomizing gas. Common fuel gases are acetylene, propane, and methyl acetylene-propadiene.

Air is typically used as the atomization gas. Oxy-acetylene flames are used extensively for a wire flame spraying because of the degree of control and the high temperatures offered by these gases. By gauging its appearance, the flame can be easily adjusted to be an oxidizing, neutral, or reducing flame. The lower temperature propane flame can be used for lower melting metals such as aluminum and zinc as well as polymer feedstock. The basic components of a flame spray system include the flame spray gun, feedstock material and feeding mechanism, oxygen and fuel gases with flowmeters and pressure regulators, and an air compressor and regulator.

(a) Wire flame spraying

Wire flame spray is the flame process of greatest interest to the Corps of Engineers. CEGS-09971 allows for the application of aluminum, zinc, and zinc/aluminum alloy coatings using the flame spray method. **Figure 4** shows a schematic of a typical oxy-fuel flame spray system. **Figure 5** depicts a typical wire flame spray gun. Compared with arc spraying, wire flame spraying is generally slower and more costly because of the relatively high cost of the oxygen-fuel gas mixture compared with the cost of electricity. However, flame spraying systems, at only one-third to one-half the cost of wire arc spray systems, are significantly cheaper. Flame spray systems are field portable and may be used to apply quality metal coatings for corrosion protection. This is the type of thermal spray technology that we can apply industries with many sub-plants like sugar factories to minimize the effect of corrosion.

(b) Powder flame spraying

Powder flame operates in much the same way as wire flame spray except that a powder feedstock material is used rather than wire and there is no atomizing air system. The melted coating material is atomized and propelled to the surface in the stream of burning fuel gas. The powder is stored in either a gravity type hopper attached to the top of a spray gun or a larger air or inert gas entrainment type detached hopper. Powder flame spray guns are lighter and smaller than other types of thermal spray guns. Production rates for powder flame spray are generally less than for wire flame spray or arc spray. Particle velocities are lower for flame spray, and the applied coatings are generally less dense and not as adherent as those applied by other thermal spray methods. **Figure 4** illustrates a typical combustion powder gun installation, and **Figure 5** shows a powder gun cross section.

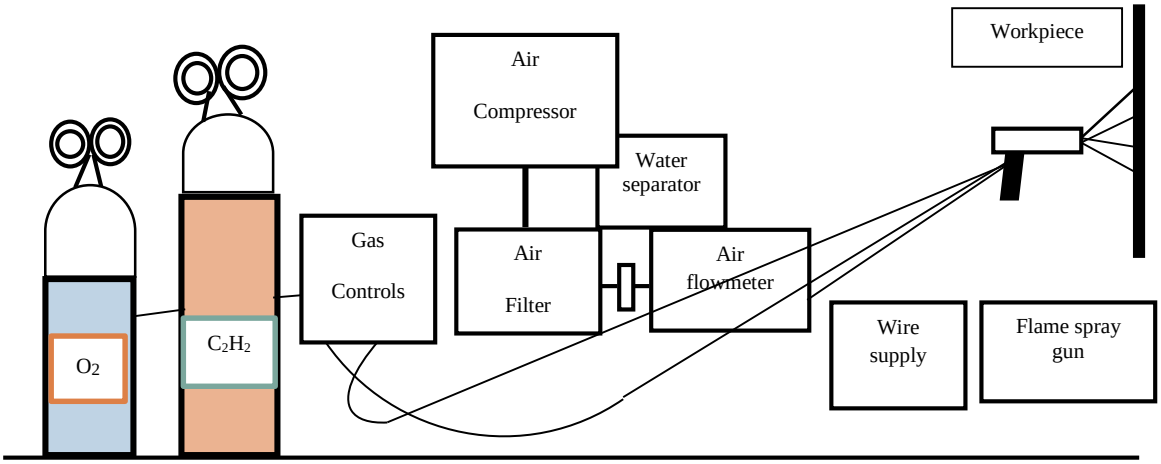

Figure 4 Typical (wire) flame spray System

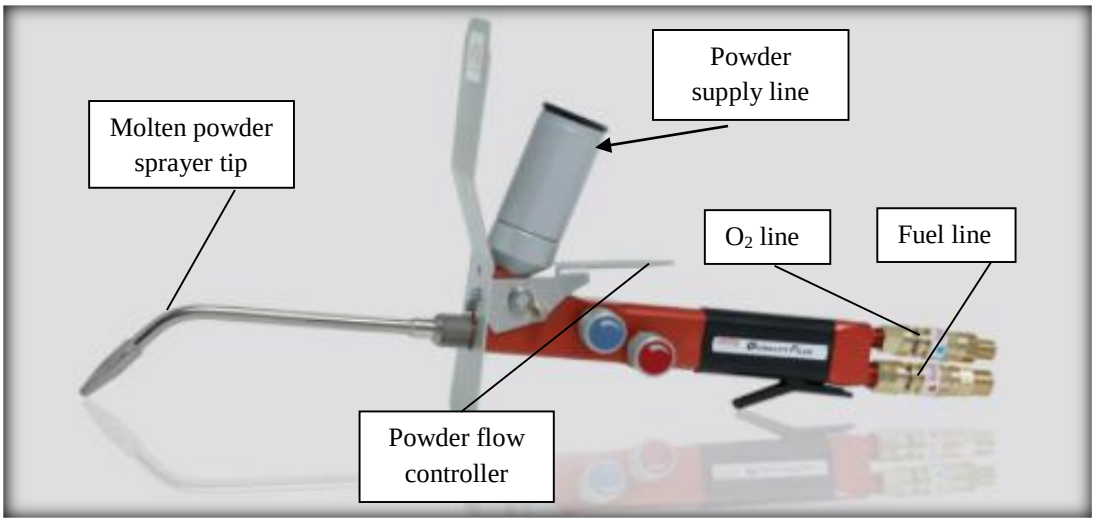

Figure 5 Typical (powder) flame thermal spraying gun

2.4 The Oxy-Acetylene Flame Spray Process

Oxygen and acetylene together in a flame provide the heat necessary to melt most metals. This combines with a neutral welding atmosphere and suitable filler material allows a skilled operator to weld most metals. Oxy-fuel welding, commonly referred to as oxy welding or gas welding is a process of joining metals by application of heat created by gas flame. The fuel gas commonly acetylene, when mixed with proper proportion of oxygen in a mixing chamber of welding torch, produces a very hot flame of about 5700-5800˚F. With this flame, it is possible to bring any of the so-called commercial metals, namely: cast iron, steel, copper, and aluminum, to a molten state and cause a fusion of the two pieces of like metals in such a manner that the point of fusion will very closely approach the strength of the metal fused [41].

2.4.1 Chemistry of Oxy-Acetylene Process

The most common fuel used in welding is acetylene. It has a two stage reaction; the first stage primary reaction involves the acetylene disassociating in the presence of oxygen to produce heat, carbon monoxide, and hydrogen gas.

$2C_2H_2 + 2O_2 = 4CO + 2H_2 + Energy$ ---------- (2.1)

A secondary reaction follows where the carbon monoxide and hydrogen combine with more oxygen to produce carbon dioxide and steam.

$4CO + 2H_2 + 3O_2 = 4CO_2 + Steam + Energy$ ---------- (2.2)

When you combine equations (1) and (2) you will notice that about 5 parts of oxygen is necessary to consume 2 parts of acetylene,

$2C_2H_2 + 5O_2 = 4CO_2 + Steam + Energy$ ---------- (2.3)

Or we can say about 2.5 parts of oxygen is necessary to achieve complete combustion of acetylene. In operation, one part of oxygen is supplied through the torch and the remaining 1.5 parts is obtained from the surrounding air atmosphere (secondary reaction). When the secondary reaction does not burn all of the reactants from the primary reaction, the welding processes produces large amounts of carbon monoxide, and it often does. Because of the need for supplemental oxygen from the atmosphere, the acetylene oxygen flame cannot be used inside of pipes or structures subjected to oxygen depletion from gas welding. By varying the relative amounts of acetylene and oxygen, a welder can produce different flame atmospheres and temperatures as he requires[41]. At the end of nineteen century, a discovery was made which was to have a big effect on the metal fabrication industry. The flame produced by burning acetylene with oxygen was hotter than other familiar processes previously known. The flame was quickly adapted to heat and weld metal. **Table 2** below sets out the flame temperatures of various fuel gases. From this, it can be seen that it is the hottest of all flames in commercial use.

Table 2 Fuel gases - temperatures [24, 42-46]

Fuel gas	**Maximum flame with air (˚C)**	**Temperature with oxygen (˚C)**
Acetylene	2630	3130
Hydrogen	2210	2660
Coal gas	1920	2450
Propane	1925	2700

2.4.2 Combustion Dynamics of Oxy-Fuel Spray System

The oxygen and acetylene flame has been used in gas welding and cutting for many years. In this process of combustion, oxygen and fuel gas at certain pressures, are firstly mixed in the mixing zone and then directed towards the combustion zone. After ignition with an external igniter, a chemical reaction takes place that releases heat energy. The pressure increases with an increase in temperature, and this results in the high gas velocities [47, 48]. In flame spraying conducted using acetylene and oxygen, the simple chemical reaction of gases is as follows[49]:

Acetylene + Oxygen = Steam (water) + Gas (Carbon Dioxide) + Energy ---------- (2.4)

Stoichiometric (theoretically required for complete combustion) oxygen to fuel ratio is 4.5 to 1. The energy released by the chemical reaction of the gases is used to heat and accelerate both the emerging gases and the spraying powder. Because of excessively high deposition temperatures, the water produced in the combustion reaction evaporates. The resulting gas velocity is a function of pressure, temperature, density, gas composition, and the area through which gas travels. But the sound velocity affects the maximum obtainable gas velocity through the minimum cross sectional area.

Variation of spray parameters, such as the powder feed rate, flow rate ratio of oxygen to fuel, flow rate of the compressed air and spray distance also affects the Oxy-fuel flame sprayed deposition thickness and properties. With a decrease in the oxygen to fuel ratio, the deposition temperature increases (as shown in **Figure 6**) [50]. This in turn increases residual build-up in the coatings, (as will be indicated by equation 2.2 later). With an increase in the spray distance, the flight time of the particles from the gun to the substrate is increased, which results in lower particle velocities and lower impact temperatures. This decrease in particle velocities and temperature causes lower deposition thickness and lower residual stress in the coatings[51]. Thus with an increase in the flow rate of the compressed air, the particle velocities increase inside the gun, as well as from the gun to the substrate. Higher particle velocities also decrease premature solidification of coating material before impact with the substrate.

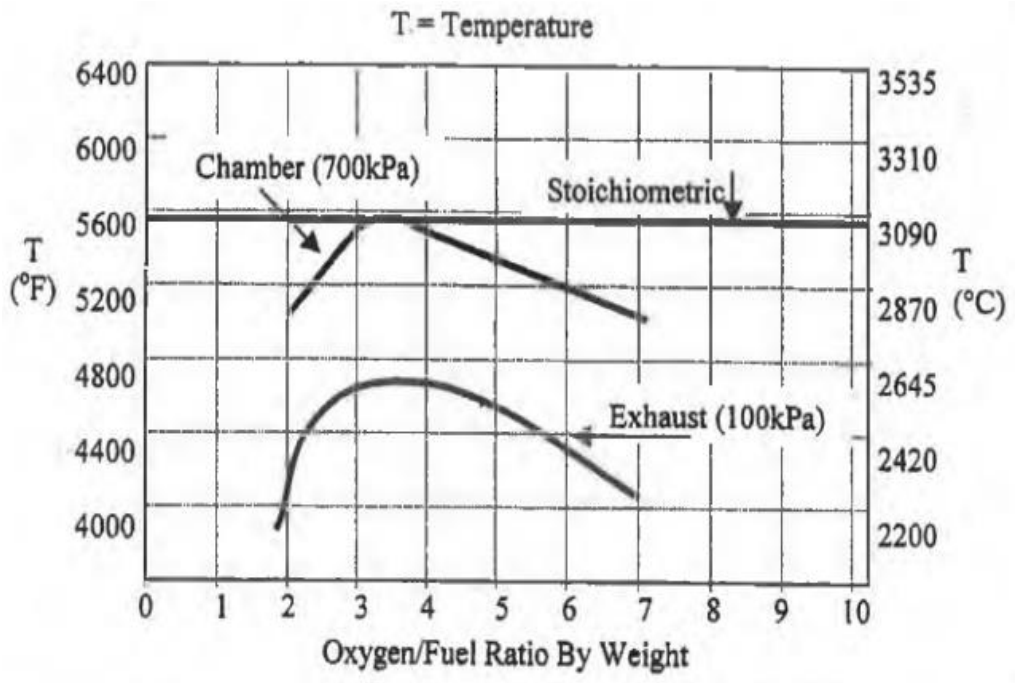

Figure 6 Theoretical flame temperature against oxygen/fuel ratio [12, 34, 43, 52]

2.4.3 Merits of Oxy-Fuel Spray Coating

Though particle velocity is the very essential parameter in the thermal spray process, availability of the spray gun system is another constraint that limits [53]. This is because particles have less time to cool down at high velocities. The oxy-acetylene process is designed around producing high velocities and this confers many of the advantages that oxy-acetylene has over other thermal spraying techniques which include [54].

- Equipment set-up is simple;
- Does not require electricity;
- Ease of availability in any metals workshop;
- Equipment is readily available and portable;
- Has wide range of applications;
- Lower capital cost and ease of use compared to other processes;
- Oxyacetylene process is ideally suited to the welding of thin sheet, tubes, and small diameter pipe. It is also used for repair work, maintenance and in body shops;
- Dissimilar metals can easily be joined;
- Can also be used for preheating, cutting metal, case hardening, soldering and annealing.

Table 3 summarizes some of the reasons why Oxy-Fuel flame spraying process produces such high quality coatings.

Table 3 Benefits of using oxy-fuel flae spray coating [50, 55-57]

S/n	Coating Benefits	Main reasons for this benefit
1	Improved corrosion resistance	Less porosity
2	Higher hardness ratings	Better bonding and less degradation
3	Better adhesive strength	Improved particle bonding
4	Lower oxide content	Less in flight exposure time to air
5	Thicker coatings	Less residual stress
6	Smoother as sprayed surface	Higher impact energies
7	Higher density (lower porosity)	Higher impact energy

2.4.4 Limitations of the Oxy-Fuel Spray System

- Large heat-affected zone (distortion);
- Acetylene and oxygen are expensive gases;

- Acetylene becomes dangerous if used above 15 pounds pressure. Pure acetylene is self-explosive if stored in the free state under a pressure of 29.4 pounds per square inch (psi);
- More safety is recommended in oxy-fuel welding process;
- The process is typically slower than the electric arc-welding and HVOF processes [41].

2.5 Bagasse-Fired Water-tube Boilers

Boiler has emerged as an important tool of an industry with high degree of versatility. As a source of hot water and/ or steam it has found enormous application at home and in a variety of industries like sugar, pulp, paper, textile, aluminum, automobiles, concrete blocks and bricks, ceramics glass, organic and inorganic chemicals etc. Broadly speaking, a boiler is a device used for generating [58]:

a. Steam for power generation process,
b. Hot water for heating purpose.

Steam boilers can be commonly classified as fire tube boiler where the fire is inside the tube and the water is in the shell and water tube boiler where the water is inside the tube and the fire or the flue gas is inside the shell. The sample selected for investigation in this particular research is a water-tube boiler (**Figure 8**). The primary purpose of a boiler is the generation of steam above that of atmosphere. The steam produced due to the transfer of heat from combustion process which take place within the boiler, from resistance heaters in the case of electric boilers, from nuclear reaction, or from other fuels in the case of waste heat boilers [59].

Bagasse boilers can utilize bagasse and wood including furnace oil as an auxiliary fuel. However, furnace oil which is the residue of petroleum is used seldom when dry bagasse is in short supply or during winter season when the extracted bagasse from the milling or diffusion plants (in the context of sugar factories) has higher amount of moisture (<50%). The operating conditions of different boilers (temperature, flue gas composition, and fly ash, etc.) depend on the fuels and the operating process parameters, and may differ inside the boiler [60]. The combustion of such complex fuels leads to very harsh conditions and may cause fouling, slagging, and high temperature corrosion of metallic heat exchangers and eventually a failure, see **Figure 7**.

Corrosion can lead to severe material damage and tube leakage, resulting in serious operational efficiency problems and expensive consequences such as unplanned shutdowns of the plant, high maintenance costs, reduced availability of the plant for power generation, and shortened lifetime

of the boiler tubes. Additionally, the demand for higher electricity/heat efficiency of the boilers requires an increase in steam temperature of boiler tubes, leading to even more severe corrosion problems, especially for furnace-wall tube components [46, 61].

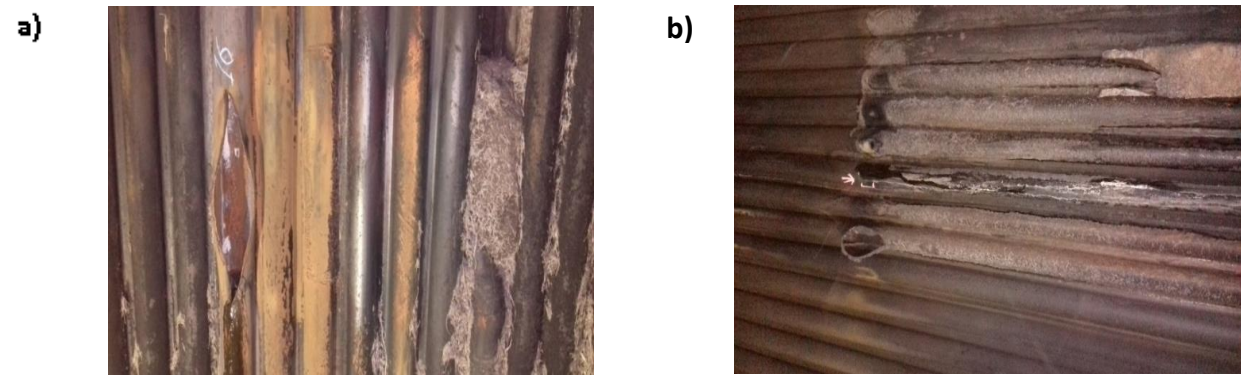

Figure 7 Sample failed tubes taken by photograph from the water-wall tubes in FSF

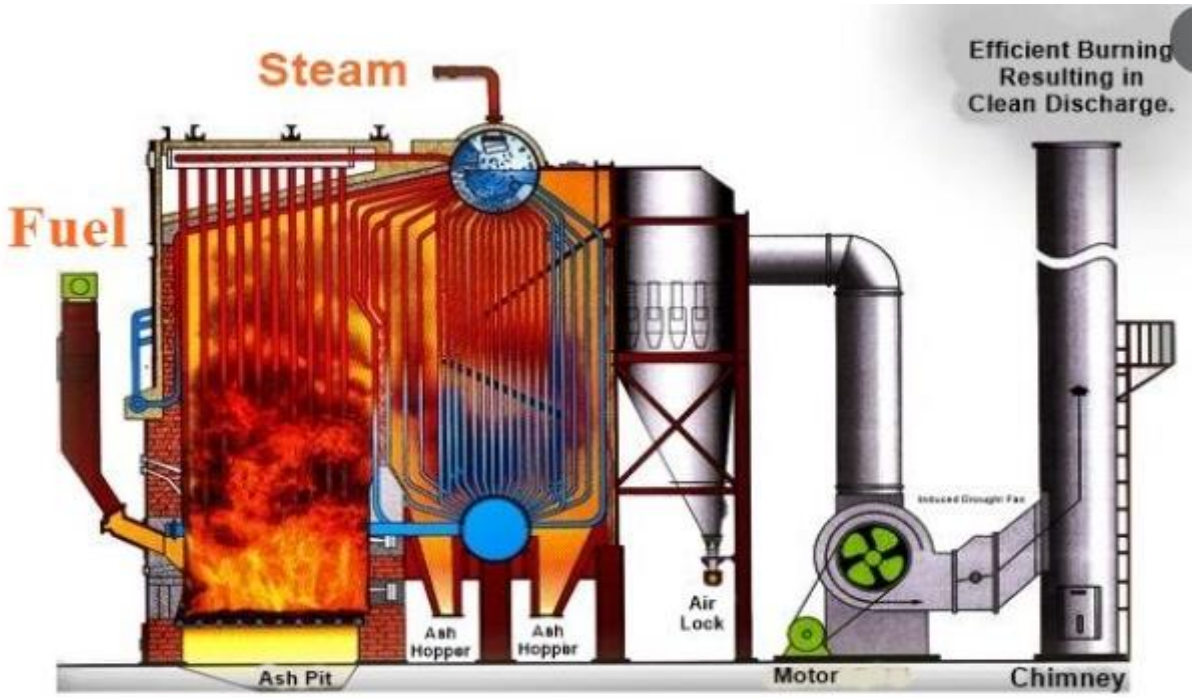

Figure 8 Typical schematic diagram of bagasse-fired water-tube boiler [17, 62-65]

2.6 Corrosion in Bagasse-fired Boilers

Corrosion is widely recognized as a major problem in the sugar industry which tends to reduce the service life and reliability of metallic materials [66]. Corrosion processes occur due to different factors or conditions that define the corrosive characteristics of the media in which the carbon steel

metal elements of the sugar industry are exposed. Corrosive in sugar factories can arise mainly due to [45]:

- Acidic environment- which is produced due to the presence of some acids and other impurities in sugar cane juice.
- Abrasion, erosion, and fretting wear- The rate of corrosion increases with increasing rate of abrasion, erosion, and fretting wear [62]. Abrasion and corrosion together would significantly shorten the service life of a component.
- Use of chemicals which produces stronger electrolytes that can increase the rate of corrosion and acidic water vapor from return condensate.

These corrosion problems have an adverse effect on productivity. Moreover, repeated chemical cleaning of boilers, heat exchangers, evaporators, reactors, condensers, and process vessels can lead to corrosion effects which may damage to the equipment and endanger the operating personnel [67]. Besides, the other important factor that would contribute a lot to the cause of corrosion is the combustion material utilized which is bagasse.

Bagasse contains carbon (C), hydrogen (H), oxygen (O), nitrogen (N), sulphur (S), and chlorine (Cl), as well as major ash-forming elements (Al, a Fe, K, Mg, Na, P, Si, Ti) and minor ash-forming elements (As, Ba, Cd, Co, Cr, Cu, Hg, Mn, Mo, Ni, Pb, Ti, V, Zn). The content of each species has little variation depending on the variety of cane used in the boiler. During the combustion in boilers, Cl contained in the bagasse mainly forms gaseous HCl, or alkali chlorides (e.g., KCl and NaCl) [68]. Due to the subsequent cooling of the flue gas in the boiler, a large part of Cl condenses as salts on the heat exchanger surfaces or on fly ash particles in the flue gas. The main consequences of Cl are the corrosive effect of chloride salts and HCl on metal surfaces in the boiler [69], and acidic pollutant emissions (e.g., HCl) [70], but also causes corrosion problems when they are deposited on metal surfaces.

Due to large number of gaseous, solid, and even liquid compounds present in boilers, various competing reactions can occur. Hence, prediction of corrosion rates or the type of corrosion attacks is challenging. However, with a combination of simplified and controlled laboratory exposures, significant features associated with fireside corrosion of furnace wall tubes in full-scale steam generation plants can be highlighted. Even though SO_2-containing compounds [71] might also have an impact on alloy performance, the main mechanisms associated with oxide breakdown are

associated with the presence of Cl-containing compounds present in the gaseous, liquid, or solid state, which are briefly illustrated below:

2.6.1 Cl-induced corrosion

Tube deterioration due to corrosion problems related to bagasse-fired boilers have been reported to be mainly caused by Cl. Several corrosion mechanisms proposed concerning the effect of Cl. However only two of them are addressed in this particular research. According to Nielsen [5], the level of HCl when firing biomass fuels usually ranges between 100 and 1000 ppm and, during waste incineration, it is even higher [72]. In atmospheres containing both HCl and O_2, accelerated corrosion has been observed. A conventional understanding is that Cl_2 forms according to the Deacon reaction (Eq. 1) [73]. During combustion of waste, alkali chlorides are deposited on the boiler tubes and formation of Cl_2 may take place based on:

$$2HCL + \frac{1}{2}O_2 = Cl_2 + H_2O \qquad \Delta G_f^{\circ}(Cl_2) \approx 0.4\,KJ/mol\ at\ 600\ ℃ ------(2.5)$$

It was also proposed by Lee and MacNallan [74] and further investigated by by Grabke and Zahs [70] that the Cl-containing compounds, e.g., KCl, react with the alloying elements present in the boiler components, and trigger rapid corrosion in **Figure 9.**

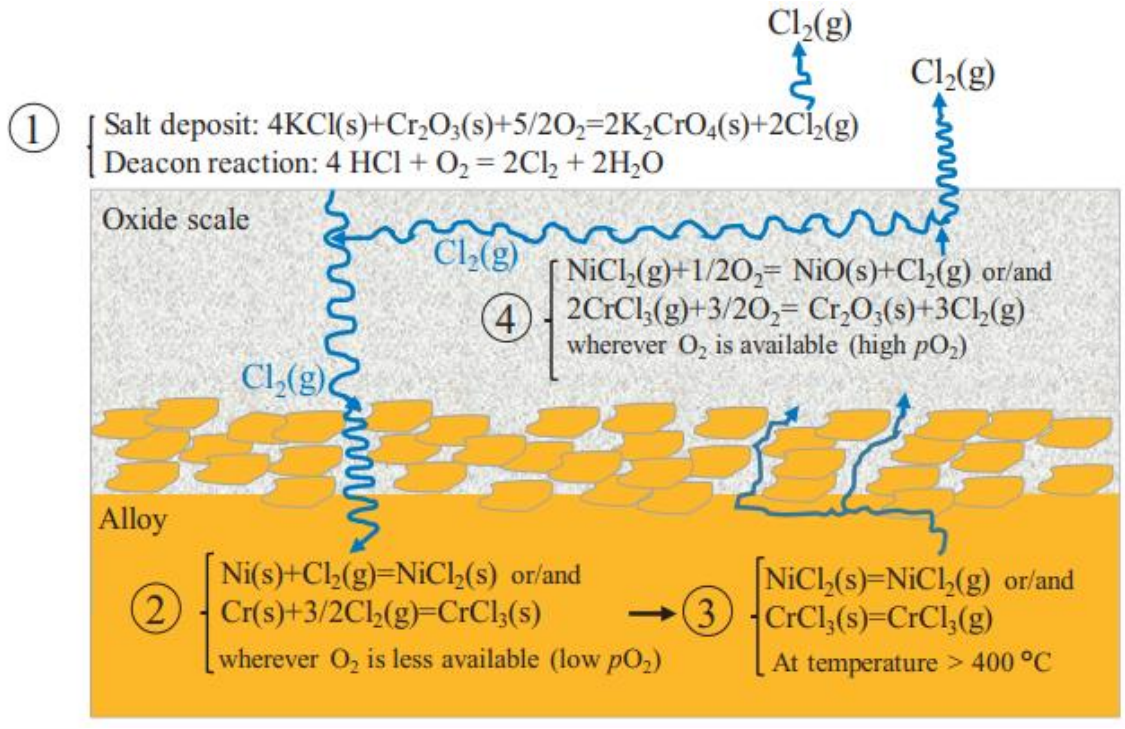

Figure 9 Schematics of "chlorine-induced active corrosion" mechanism [4, 75, 76]

Chemical analyses of corrosion products formed in oxidizing-chloridizing environments have confirmed that metal chlorides are frequently observed at the metal/deposit interface (low pO_2), while the outer part of the deposit (high pO_2) contains mainly metal oxides [77]. In other words, there is an inward diffusion of Cl_2 through the scale and a subsequent accumulation of Cl_2 at the metal/deposit interface. In this case, the molecular Cl_2 must diffuse through the oxide layer, presumably through cracks and pores.

2.6.2 Corrosion due to Water Vapor

At temperature below 400˚C, the effect of mechanical surface treatment on oxidation in dry steam is negligible. Above that temperature, surface-hardened stainless steels corrode considerably less than the same steels when pickled [78]. Ni-based coatings alloyed with ≈ 20 wt% Cr [79] are widely used for protecting components against oxidation in dry environments as an oxide scale of Cr_2O_3 [80] can potentially protect the coating and substrate from further oxidation. However, water vapor is present in many environments of industrial relevance in general and in sugar factory boilers in particular.

The high chromium content of the oxide is thought to be responsible for the excellent corrosion protective effect in metals. Electron probe microanalysis of metal layers hardened by mechanical treatment showed that the chromium diffused towards the surface to form the protective oxide, whereas in an annealed specimen chromium diffusion was restricted to the immediate vicinity of the grain junction [78].

It is generally accepted that ferrous hydroxide is formed in the course of the oxidation reaction of steels in water which is given as follows:

$$Fe + 2H_2O = Fe(OH)_2 + H_2 \quad \text{----------} \quad (2.6)$$

This ferrous hydroxide has a high solubility in relation to other iron oxides. Various authors have measured the product which is soluble when heated and found values between 10^{-16} and 10^{-14} [81, 82]. Ferrous hydroxide is also converted into magnetite (Shikorr's Reaction) at high temperatures:

$$3Fe(OH)_2 = Fe_3O_4 + H_2 + 2H_2O \quad \text{----------} \quad (2.7)$$

It is worth noting that sizable literature is available on the role of H_2O (g); however, the exact effect of water vapor on the extent of degradation is still a controversial issue [83].

2.7 Corrosion of Thermally Sprayed Coatings

Though it can be difficult to eradicate corrosion in its totality, the extent of its impact can be reduced by altering the composition, microstructure, and architecture of the coatings. Major alloying elements like Ni and minor alloying elements, e.g., protective scale-forming elements (Al or/and Cr) can alter the corrosion mechanisms [84]. Microstructural features in the coating, such as pores and splat boundaries, can also significantly affect the corrosion performance [85]. The coating microstructure can be varied by selection of spraying process, spraying parameters, or post-spray treatment [86, 87]. Besides, it is possible to reduce the impact of corrosion by varying the architecture of the coating either by creating a new coating design, such as what has already been achieved in multilayered or functionally graded coatings [88] or by incorporating certain oxygen-active elements into coatings to fabricate composite structures [89].

Various efforts have focused on the oxidation behaviour Ni-based coatings deposited by commonly used thermal spraying techniques such as high velocity oxy-fuel spray (HVOF) and atmospheric plasma spray (APS) [90]. Nevertheless, the coating features associated other techniques, pores and *in situ* formed oxides [17], lead to the formation of a discontinuous oxide scale with less bond strength and greater porosity. Other effective coating methods are reported though inconvenient for boiler applications. The high amount of interconnected pores as well as poor splat cohesion due to the oxides and/or voids formed at the splat boundaries in the coatings have an adverse effect on the oxidation resistance of the coating materials [91].

Previously published research results while claiming that the oxy-acetylene flame-sprayed Ni-based coatings could provide oxidation protection [13, 92], showed that oxidation occurred through the splat boundaries and the pores of tube coatings. Due to its availability, portability, versatility, and controllability of the essential parameters that it offers powder-flame thermal spraying method is chosen for this particular research. In this paper, the influence of the variation in powder flame spray parameters to obtain a Ni-Cr/Al metallic coating on carbon steel (ASTM SA210-A1) substrate was studied. Besides, preceding researches were focused dominantly on coal fired boilers and the spraying technology they utilized was dominantly electric-driven technologies like plasma spraying which is more expensive than powder-flame thermal spraying technology. Furthermore, powder-flame thermal spraying technology renders higher impact energy, improved particle bonding, thicker range of coating thickness, and better adhesive strength than other methods for bagasse-fired water-tube boilers in sugar mills context.

CHAPTER 3

COATING MATERIALS SELECTION

3.1 Introduction

Currently, the need to enhance or develop high temperature capabilities of structural materials for advanced bagasse-fired steam power plants. These materials require a combination of high temperature strength, creep resistance in the oxygen-rich and hydrogen-rich high pressure environments. Structural materials with enhanced high temperature capabilities can improve the efficiency of these power plants, thus decreasing the greenhouse gas emissions. One way of attaining this objective is to develop ultra-super-critical power plants in which some of the components would need to withstand a high temperature close to 760˚C under stresses [93].

Furthermore, the architecture, composition, and microstructure of the coatings need to be tailored in order to endure high temperature corrosion environment prevailing in boilers. In this chapter, the importance of coating composition (e.g., alloying elements), microstructure and architecture in corrosive environments, particularly in boiler environment is briefly explained.

3.2 Chemical Composition

3.2.1 Nickel (Ni) as Base Matrix

Nickel base super alloys are the best candidates for high temperature resistance, high corrosion and wear resistance applications. Nickel-based coatings often display a good resistance to high temperature corrosion. Ni-based coatings often display a good resistance to high temperature corrosion. The Ni-matrix is preferred over other metal matrices like Fe in Cl-containing environments, as formation of $NiCl_2$ is less thermodynamically favored (with higher Gibbs free energy) than the other detrimental metallic chlorides such as $FeCl_2$, see Eqs. 1 and 2 [14]:

$$Fe\ (S) + \ Cl_2\ (g) = FeCl_2\ (s) \qquad \Delta G_f^{\circ}\ (FeCl_2)\ \approx\ -231.8\ kJ/mol\ at\ 600\ ℃ - -(3.1)$$

$$Ni\ (s) + \ Cl_2\ (g) = NiCl_2\ (s) \qquad \Delta G_f^{\circ}(NiCl_2)\ \approx\ -173.9\ kJ/mol\ at\ 600\ ℃ - -(3.2)$$

In addition to this, Nickel and nickel alloys have useful resistance to a wide variety of corrosive environments typically encountered in various industrial processes. In many instances, the corrosive conditions are too severe to be handled by other commercially available materials, including stainless and superstainless steels. Nickel by itself is a very versatile corrosion-resistant

metal, finding many useful applications in industry. More importantly, its metallurgical compatibility over a considerable composition range with a number of other metals as alloying elements has become the basis for many binary, ternary, and other complex nickel-base alloy systems, having very unique and specific corrosion-resistant and high-temperature resistant properties for managing the modern-day corrosive environments of chemical process, sugar, petrochemical, marine, pulp and paper, agrichemicals, oil and gas, heat treatment, energy conversion and many other industries [94].

Furthermore, Ni-base alloys are used in numerous demanding applications which require corrosion and high temperature strength (**Figure 10**), and can also be used as coatings which exhibit these environmental resistance. The melting point for nickel is 1453˚C and nickel has relatively low thermal and electrical conductivity, high resistance to oxidation and corrosion, excellent strength and toughness at elevated temperatures. The density of nickel at 25˚C is 8.902g.cm^{-3}. About 65% of Ni is used as an alloying addition to stainless steels and about 20% is used in other steels and non-ferrous alloys, including superalloys [95]. Nickel-based alloys can be used for higher fractions of the melting point than other elements [96].

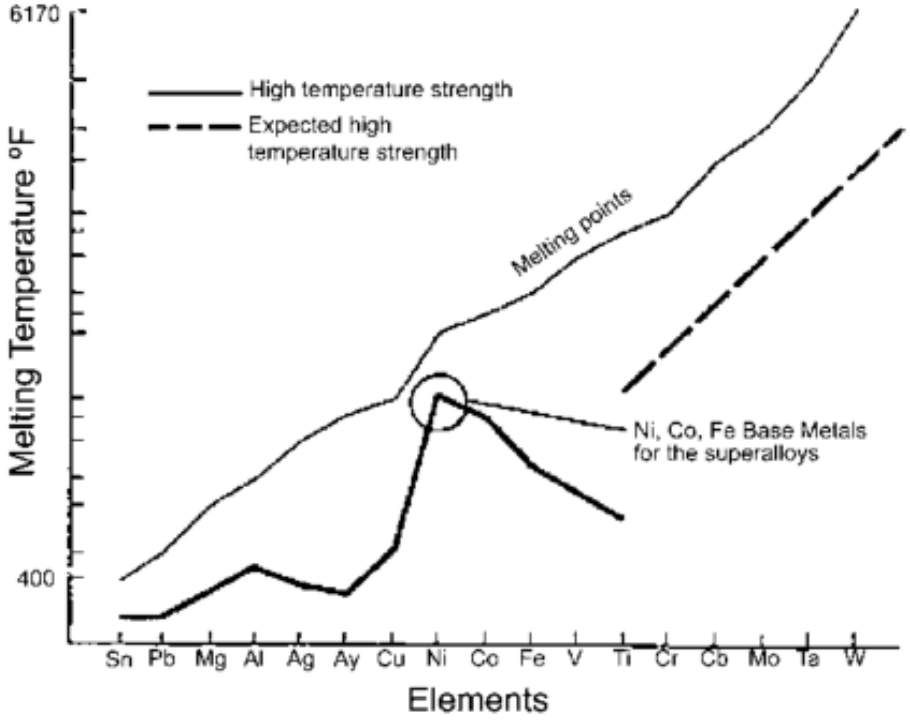

Figure 10 Maximum melting temperature of elements in the periodic table [84]

3.2.2 Alloying Element

Elemental nickel is utilized principally as a base alloying matrix to increase the corrosion resistance of commercial iron and copper alloys. The addition of sufficient nickel to turns steel

into what is called austenitic stainless steel, which is tougher and harder than conventional carbon steels. The most essential elements for forming protective oxide layers at high temperatures are Cr, Co, Fe, Mo, Al, Si, and Cu.

3.2.2.1 Chromium (Cr)

Chromium is a lustrous, brittle, and hard metal which does not tarnish in air, when heated it burns and forms green chromic oxide. Chromium is unstable in oxygen, it immediately produces a thin oxide layer that is impermeable to oxygen and protects the substrate metal under it. Besides, Cr is a very important and common alloying element in materials for high temperature applications and forms the stable oxide (Cr_2O_3) with the hexagonal corundum structure. Diffusion of corrosive species through Cr_2O_3 is rather slow, thus it is considered as a protective oxide. As long as the oxide scale is well attached to the underlying alloy, and growth rate of the scale is controlled by diffusion of ions through the scale, oxidation follows a parabolic rate [97]. **Figure 11** shows the ternary phase diagram of the Cr-O-Cl system at 600˚C illustrating that various corrosion products that can form depending upon the availability of Cl and O. The most aggressive condition used in this study thermodynamically favors formation of Cr_2O_3 [98].

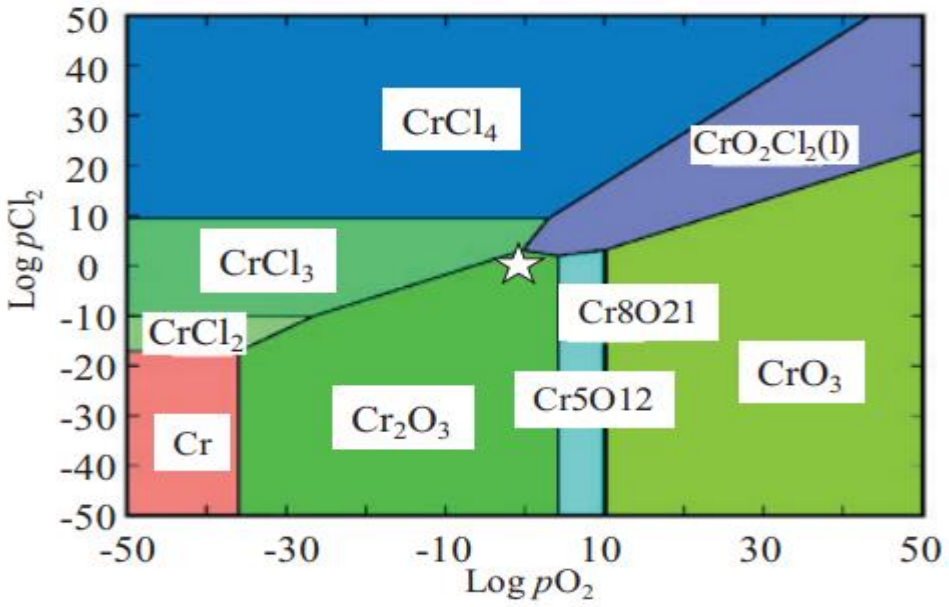

Figure 11 Predominance diagram for Cr-O-Cl system produced at 600 ˚C [79]

3.2.2.2 Aluminum (Al)

Aluminum (Al) metal has a density lower than those of other common metals, at approximately one third that of steel having a great affinity towards oxygen, and forms a protective layer of oxide

when exposed to air. It forms only one thermodynamically stable oxide, α-Al_2O_3, which has the hexagonal corundum structure. The α-Al_2O_3 has excellent protective properties with a lower growth rate than the other oxides found on engineering alloys. However, during the transient oxidation of Al, other crystal structures such as θ-Al_2O_3, γ-Al_2O_3, and δ-Al_2O_3 may also form [99]. These transient oxides are less protective so that Al_2O_3-forming alloys should be pre-oxidized in controlled atmospheres to ensure formation of protective α-Al_2O_3.

Nickel-based alloys are traditionally composed of nickel and chromium. However, these materials lack the creep strength needed for longevity when they are being used as an advanced tube alloy. Aluminum, titanium and niobium are added to provide high temperature strength and precipitation hardening. The nickel-aluminum alloys are superior to the commercial alloys, especially in the field of high-temperature properties, in an oxidizing and carburizing environments. The most attractive properties of the nickel-aluminum intermetallic include [100]:

- A high tensile and compression strength at temperature of 650-1100˚C;
- An increase of flow stress with increasing temperature-an anomalous positive temperature dependence of the yield strength (at 600-900 ˚C) is characteristic feature of the Ni-Al phase and its alloys;
- A high corrosion resistance in oxygen and carbon enriched atmospheres up to 1100˚C, due to a formation of a continuous surface alumina (Al_2O_3) layer;
- A high corrosion resistance in organic acids (oxalic and acetic acids), bases (sodium and ammonium hydroxides), and sodium-chloride solution;
- A high fatigue strength resulting from the elimination of stress concentrations on the second phase particles (e.g., carbides);

However, Ni-Al alloys (as well as other intermetallics) also have a number of common drawbacks-mainly related to their low susceptibility to plastic deformation and a high tendency to brittle cracking-that limits their industrial usefulness, especially as components with a minimal linear dimension (a thickness below 400μm) [101].

3.2.3 Chrome-Carbides/Cermets

Cermets combine the most favorable characteristics of ceramics and metals, namely the high hardness, high oxidation, and temperature resistance, and the ductility and toughness. As a consequence, these materials have found widespread application in a broad range of demanding

wear and/or corrosion applications, as both bulk materials and coatings. Common cermet and hardmetal uses include tooling for grinding, cutting, and machining; mechanical seals; friction surfaces; aerospace coatings; etc. The most ubiquitous examples of these ceramic–metal composites are 'hardmetals', which are based on chrome carbides, WC–Co, and have been actively developed for nearly 100 years. Somewhat more recently, lighter weight cermet systems, based on alternate carbides, borides and/or nitrides, have grown in prominence [102].

The mechanical, tribological, and corrosion properties of these cermets are highly dependent upon both their composition and microstructure, and there is a continuing emphasis on the improvement of these characteristics for new generations of these materials. There is also an increasing drive towards the development of nanostructured cermets, particularly for improvements that can be achieved in terms of their wear response. In many usage scenarios, combined tribo-corrosion environments are also encountered; in such instances, the simultaneous physical and chemical demands on the materials can be extreme [103].

Consequently, there is a growing demand for new cermet systems especially those alloyed with other supper alloy like Ni-Cr, and this is reflected in a continuing emphasis on research in these materials for high temperature resistance, high strength, and corrosion resistance applications. The primary aim of this special issue on cermets is therefore to provide a platform for researchers to overview the current state-of-the-art in the development, characterization, and applications of high performance ceramic–metal composites and metallic alloys. Chromium carbide-based coatings are widely utilized for high temperature and high wear resistance applications where tungsten carbides are no longer suitable especially in bagasse-fired steam generation plants. Indeed, at temperatures exceeding 540˚C, tungsten carbide coatings' hardness and oxidation resistance drop rapidly [104]. While those microstructural changes would happen in service for the Cr_3C_2-NiCr coatings intended for high temperature applications, most of the studies replicate this condition by heat treating the coatings prior to testing.

3.3 Coating Morphology

3.3.1 Splat Boundaries

The inter-splat boundaries, elemental segregation zones, and pores are the defect sites with localized stress concentration, leading to premature coating failure of spray coatings on the substrate. Splat is a term given to a single impacted particle, as depicted in **Figure 12**. Many overlapped splats, solidified and adhered to one another form a thermal sprayed coating. Thus, the

splat is the basic structural building block in thermal spray coatings. The splats are formed when the accelerated particles impact a surface. The arriving molten droplets are generally spherical, and on impact with the substrate surface, they flatten and spread in the form of disk-like structures (splats) and fill the underlying interstices (free spaces). The splat shape shows the degree of particle melting achieved in flight as well as deformation under impact (if the particle do not melt completely). The degree of melting indicated by these splats, largely determines the adhesion, cohesion, porosity, and subsequent corrosion properties of the coating [84].

The high temperature tube corrosion failure in the thermal spray coatings indicates that the attack at intersplat boundaries is the major corrosion mechanism, most likely due to the fact that they represent short-circuit diffusion paths for O_2 or Cl_2 shown in **Figure 12**. Thus, the most severe corrosion failure happens along the boundaries of rounded, unmelted particles and, more generally, along the boundaries [105]. These areas are important in corrosion protection due to various reasons. Primarily, poor splat cohesion (lack of intimate contact between splats) causes the splat boundaries to act as corrosion spots: hence, passivation is prohibited and corrosion processes can be triggered [106, 107]. Secondly, in situ oxidation of the feedstock particles leads to the presence of oxides around the splats [108].

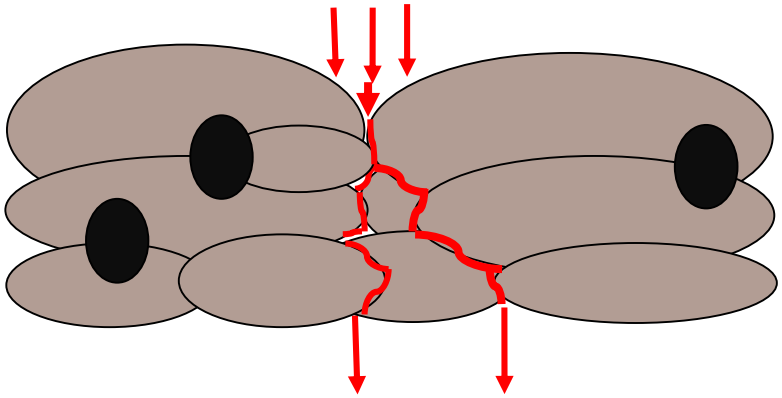

Figure 12 Mechanisms of splat boundaries in corrosion resistant coatings

3.3.2 Coatings Porosity

Porosity or void fraction is a measure of the empty spaces in a material, and is a fraction of the volume of voids over the total volume, between 0 and 1. The most common cause of porosity in a powder coating film is trapped air or contamination on the substrate. A formed metal surface, galvanized steel surface, cast substrate or any surface with existing metal porosity can cause outgassing (release of trapped air) during the cure cycle. The most familiar source of coating is trapped, or unmelted particles in the process of spray coating [109].

The liquid state particles flow easily and fill most voids. On the other hand, solid or partially melted particles are plastically deformed on impact. Solid particles, some of which may re-bound from the solid surface or become trapped in the coatings by the next arriving particles. These undeformed particles are not well bonded, nor are they in intimate contact with the underlying splat, which creates voids [110].

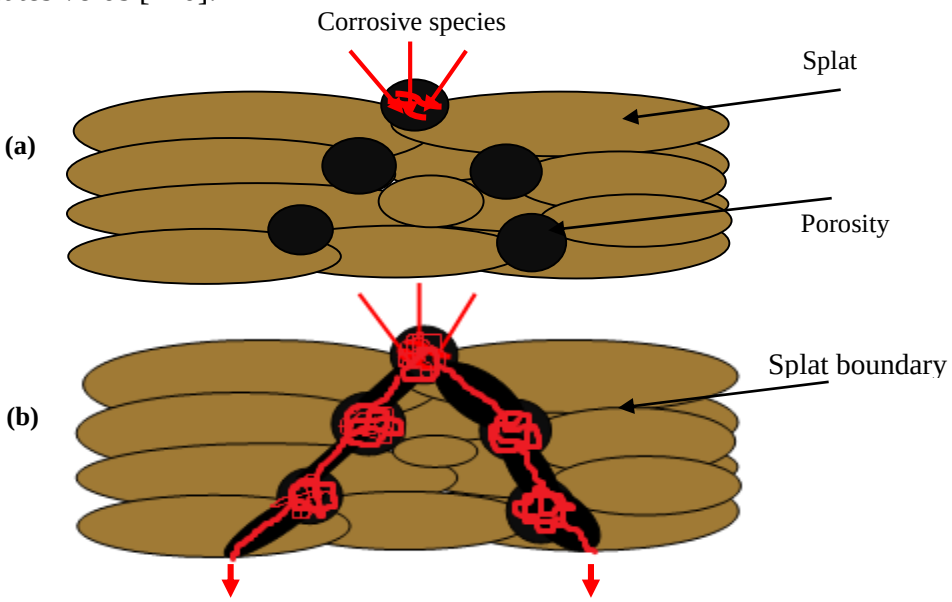

Figure 13 The effect of different types of porosity on corrosion behaviour of coatings

(a) Closed porosity (b) Interconnected porosity

It is widely known that the corrosion resistance of coatings highly relies on the content of pores [55, 64, 111-115]. If coatings are porous, the corrosive species can easily penetrate the coating through the pores and reach the substrate. In such cases, the coating delaminates in a short time and its ability to impart protection is lost. Porosity can be categorized as interconnected and closed porosity, and each of these plays roles of varying importance in determining the corrosion behavior of the coatings, as shown in **Figure 13**. If the pores are interconnected, it leads to a rapid corrosion by attacking the substrate. Compared to closed porosity, interconnected porosity is much more sensitive to corrosion as it forms direct channels between the corrosive environment and the substrate material [116].

When long-term corrosion reaction takes place, the chemical/electrochemical reaction in the area surrounding the pores makes the isolated pores grow and eventually interconnect with nearby pores. In this manner, open channels can also be created that facilitate the corrosive medium in reaching the coating/substrate interface [117].

CHAPTER 4

MATERIALS & METHODS

4.1 Introduction

This particular research investigates an innovative modification of the powder flame thermal spray process using oxy-acetylene cutting torch system. This required development of the current oxy-acetylene facility to spray Ni-based alloy powders to improve the corrosion prevention capacity of boiler tubes, carrying out a series of spray tests at range of parameters and characterize resulting coatings. In this chapter, the PFTS coating facility used and the characterization methods used are discussed in details, along with the design modification of a powder feed hopper system needed to deposit the powder coatings.

The powder flame thermal sprayed (PFTS) facility used in this particular project is a manually controlled modified oxy-acetylene powder flame thermal spray system. It consists of four parts: the oxygen and acetylene bottles, the hoses, the cutting/welding torch, and the powder supply and control system. All parts are integrated together, so that the spraying system should be perfect and continuous. **Figure 14** shows the whole PFTS thermal spray system available in the Electromechanical Workshop of Wonji-Shoa Sugar Factory (WSSF). The PFTS thermal spray system shown in figure 14 is modified in the current project in order to spray any powder for coating metals for enhancing corrosion prevention capacity of metals.

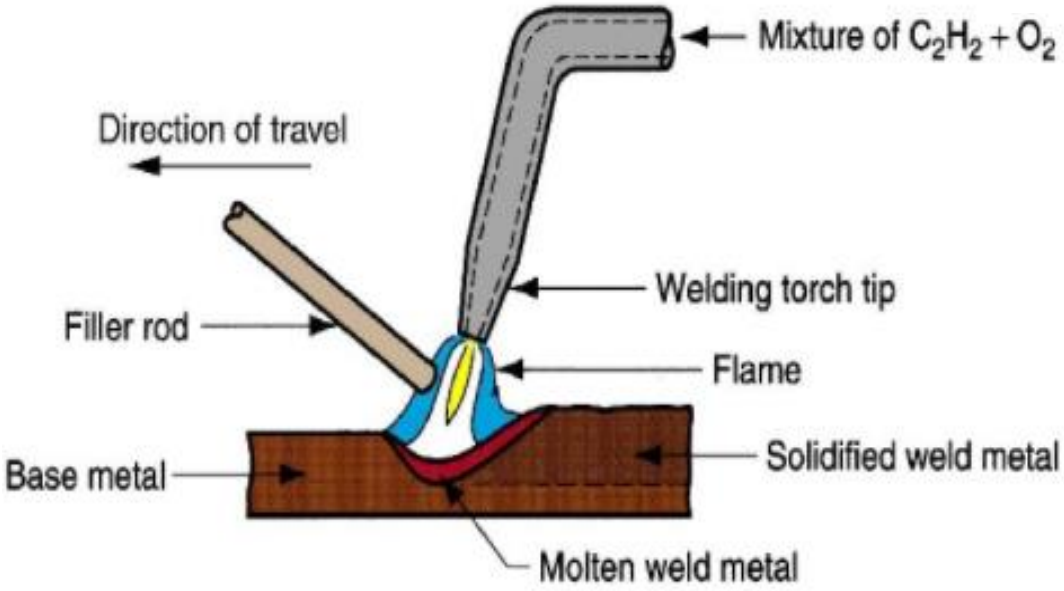

Figure 14 Typical oxy-acetylene welding system [56]

4.2 Location of Research

The research is conducted in the mechanical workshop of Wonji Shoa Sugar Factory (WSSF), quality control laboratory of Finchaa Sugar Factory (FSF), and the research laboratories of Adama Science and Technology University (ASTU), School of Mechanical, Chemical, and Materials Engineering, department of Materials Science and Engineering (MSE).

4.3 The Oxy-Acetylene Spraying System

The oxy-acetylene flame spraying system consists of the following components:

1. Gas carrier hoses,
2. Powder supply unit,
3. Pressure Regulators,
4. Welding torch and blowpipes,
5. Oxygen and acetylene cylinders,

4.3.1 Gas carrier hoses

Hoses are generally constructed of synthetic rubber and reinforcing material, and are designed to withstand high pressures, while providing flexibility to give the operator freedom of movement. Oxygen hoses are black or blue and the fittings at each end of the hose have right-hand threads. Fuel gas hoses are red or maroon and the fittings have left-hand threads. One of the major problems in selecting the proper bore dimensions for rubber hose is that a pressure drop occurs when gas flows through the hose over any distance. For instance, if you introduce gas at, say, 700 kPa at the inlet of the hose, friction losses cause the pressure at the outlet end to be much less. Pressure loss will occur in hose lengths over 3.5 m and allowances must be made.

A 10 mm bore hose should be used for all large flow applications and where extra-long lengths are required. Hoses are available in the following sizes: 5 mm, 8 mm, 10 mm, and 13 mm. Constant attention should be given to hoses and their connections because old hoses and poorly fitting connections are a potential source of danger. After lengthy use, hoses may become cracked due to rough handling, or the rubber perishes and the nipples become worn. Hence it is wise to renew the hoses as required to prevent fires or explosions due to oxygen or acetylene leaking from the equipment at any point.

4.3.2 Powder supply unit

The powder feeding unit is actually not the component that is purchased during the procurement of the oxy-acetylene welding system package especially in the context of this particular research.

Even though it can be purchased from foreign market, it is difficult to find the powder supply unit from local market. In this research, the powder supply system is added to the conventional oxy-acetylene cutting torch for carrying out the coating activity by using the heat generated by the combustion formed by the mixing of oxygen with acetylene in the blow pipe. We obviously know that the cutting torch only mixes oxygen and acetylene in the desired proportions, burns the mixture at the end of the tip, and provides a means for the lean flow of the flame.

a)

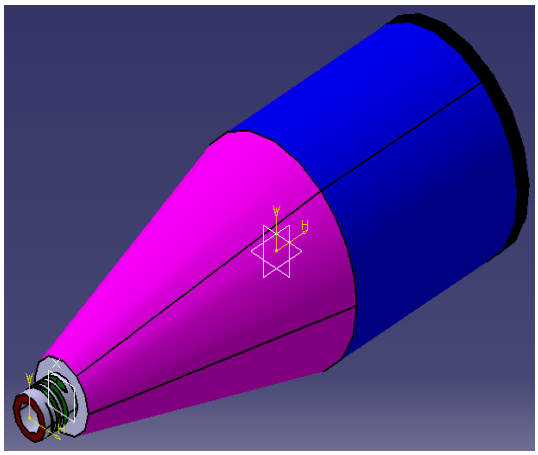

b)

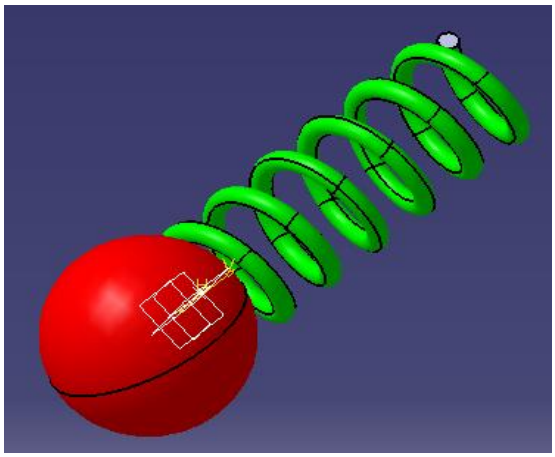

Figure 15 CATIA V5 3D designs of (a) Feed-hopper unit used for the supply of powder alloy (c) Bearing ball-reinforced spring

c)

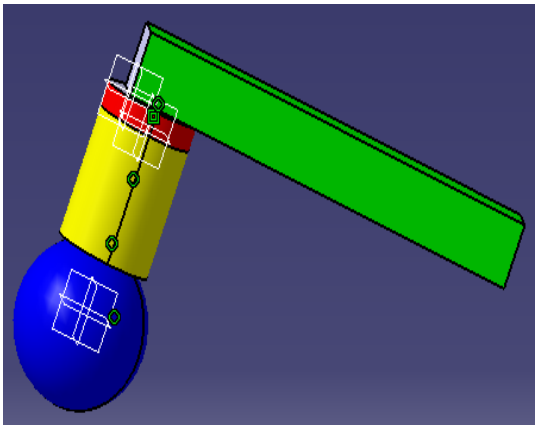

d)

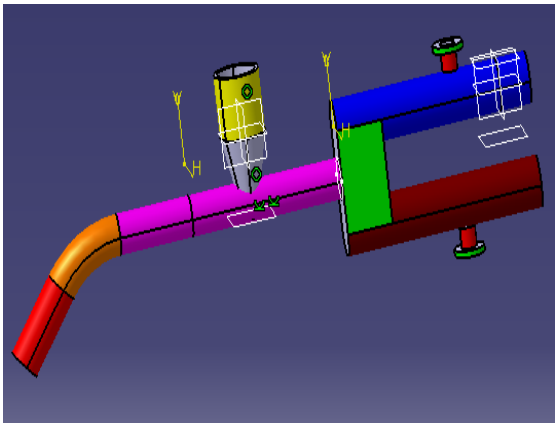

Figure 16 CATIA V5 3D designs of (c) Bearing ball reinforced spring and control valve unit, and (d) Assembly drawing of the powder supply control valve unit

The powder flame thermal spraying system with oxy-acetylene system was designed to generate a maximum temperature of 3, 160 ˚C, a particle speed of 50 m/sec, and a deposition flow rate of 1-6 kg/hr. With this capacity, the system is designed to deposit a powder alloys spraying in two layers. The properties of the applied coating are a dependent on the feedstock material, the thermal spray process and application parameters, and post treatment of the applied coating.

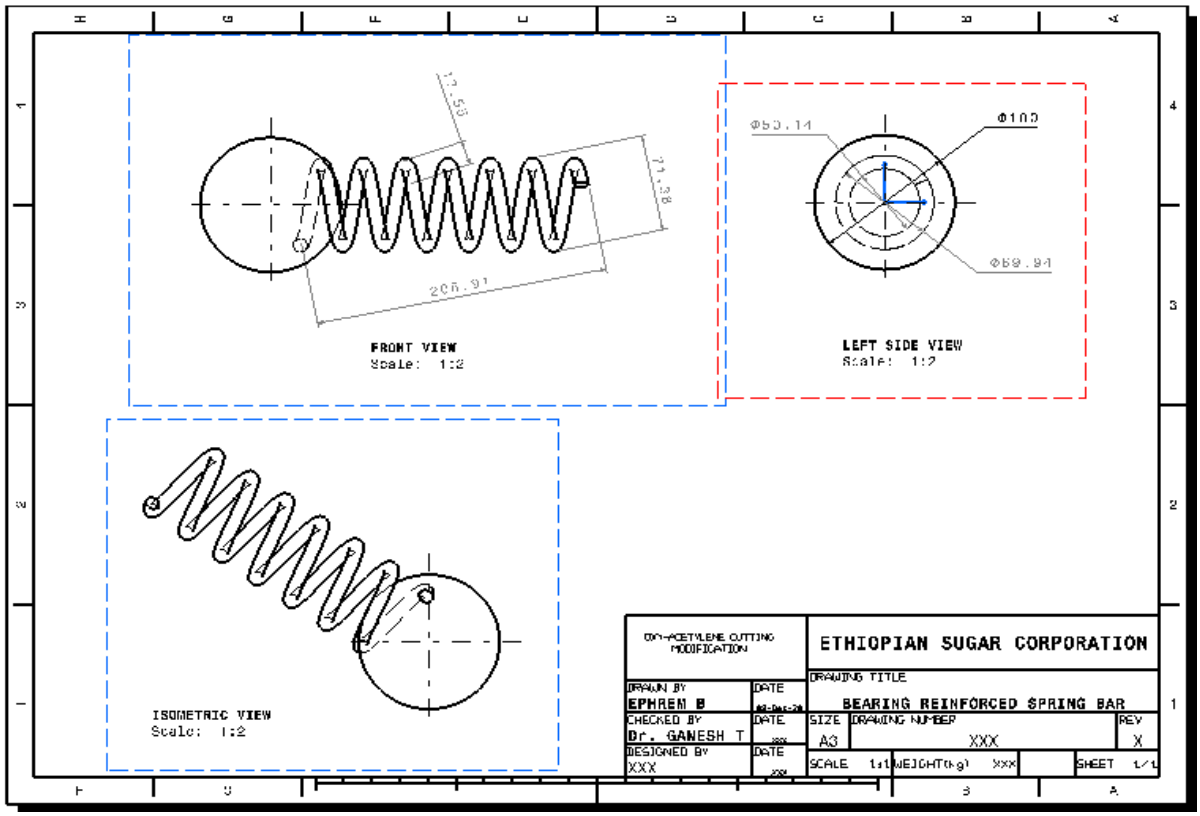

Figure 17 Bearing ball reinforced spring for cutting torch valve

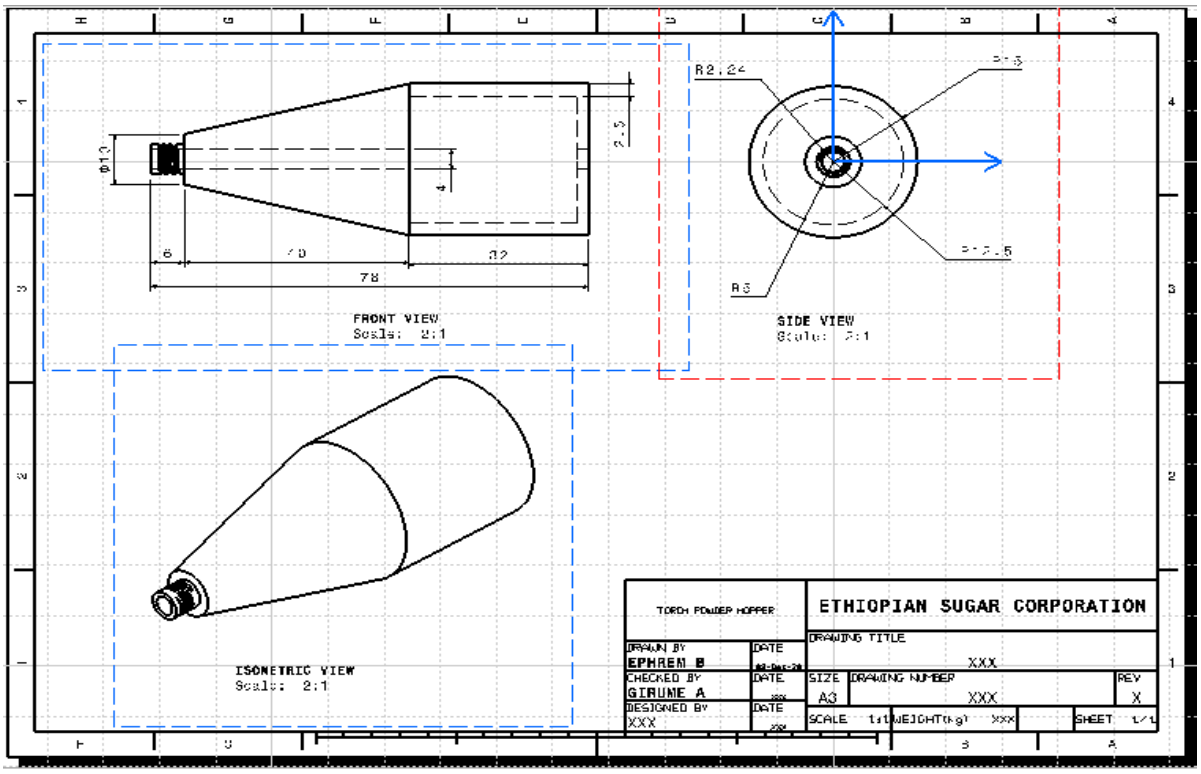

Figure 18 Powder supply hopper for cutting torch control valve

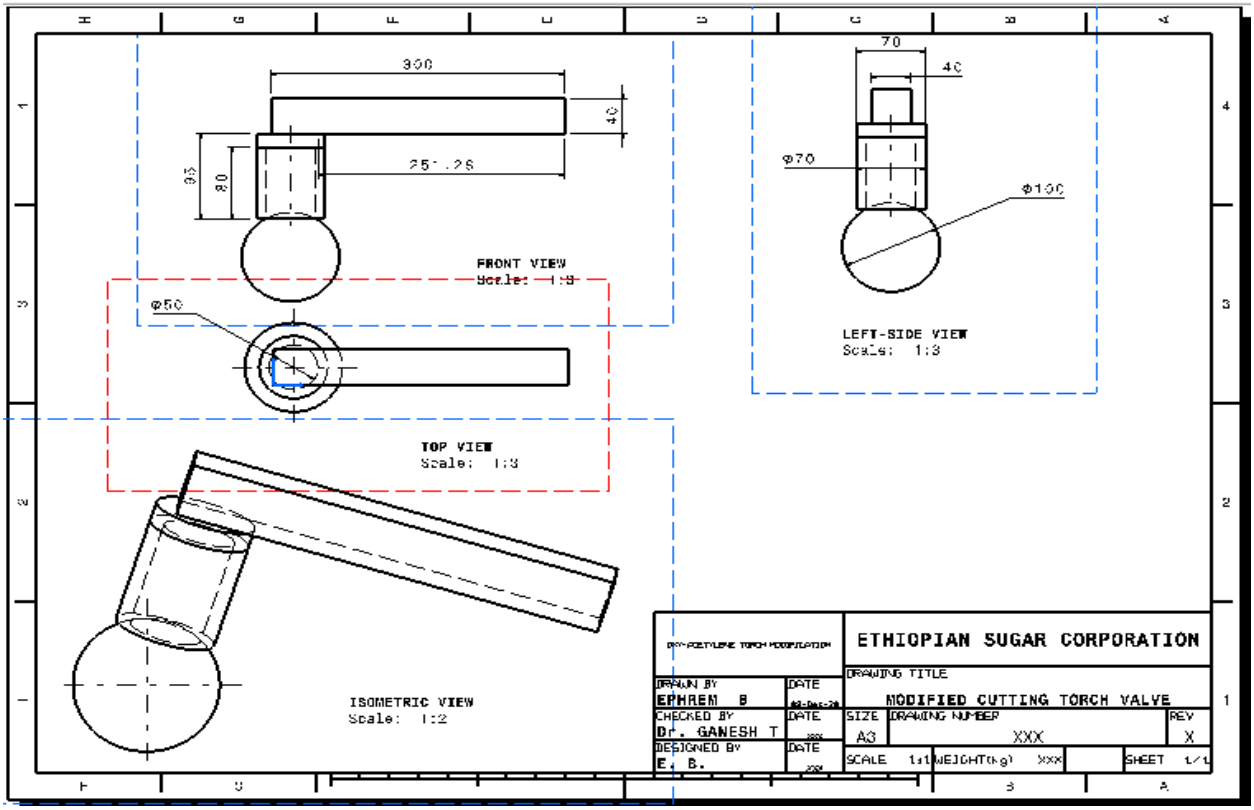

Figure 19 Assembly drawing of cutting torch powder supply control valve

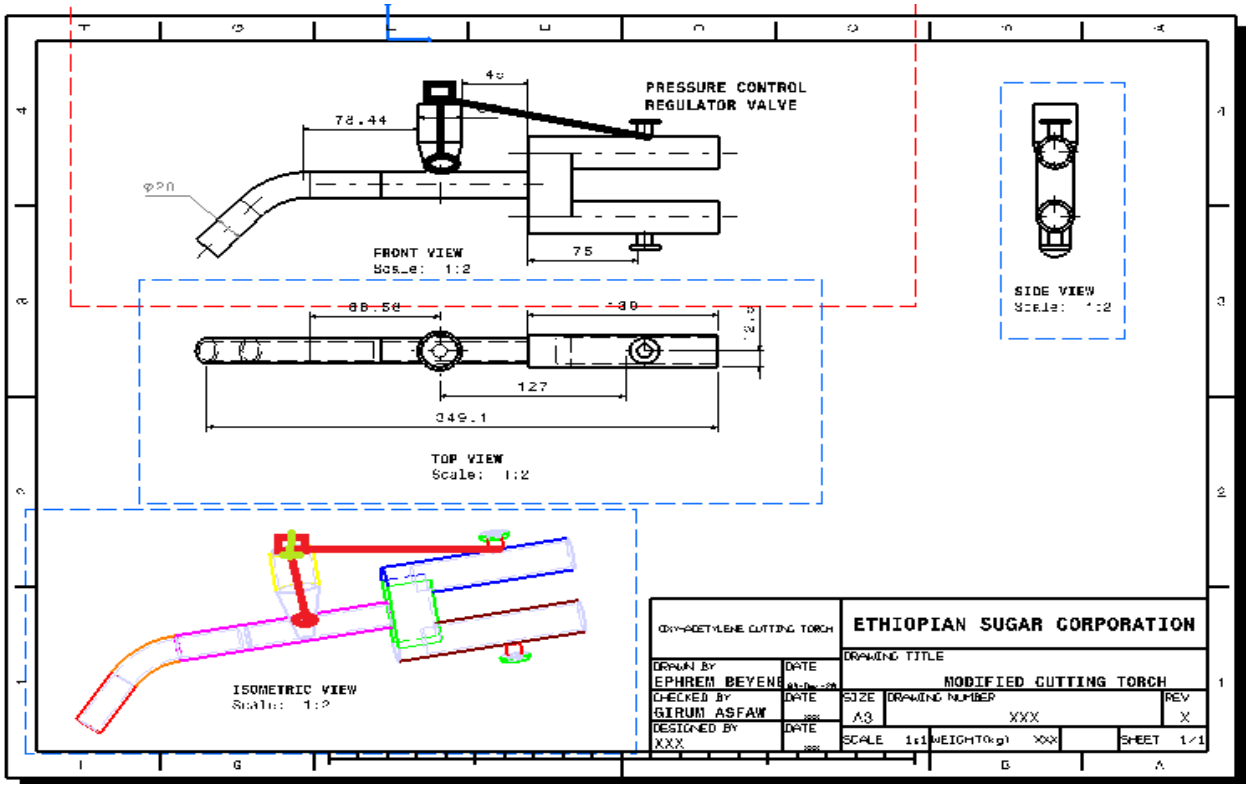

Figure 20 Assembly drawing of modified oxy-acetylene cutting torch spray system

Figure 21 Modified oxy-acetylene cutting torch with powder supply and control valve

This modified oxy-acetylene welding torch, see **Figure 21** is executed in WSSF electromechanical workshop after the design is completed by **CATIA V5** software (**Figure 15-20**). The procedures which were followed in the design, parts fabrication, and assembly of the conventional cutting torch is illustrated in **Figure 22.**

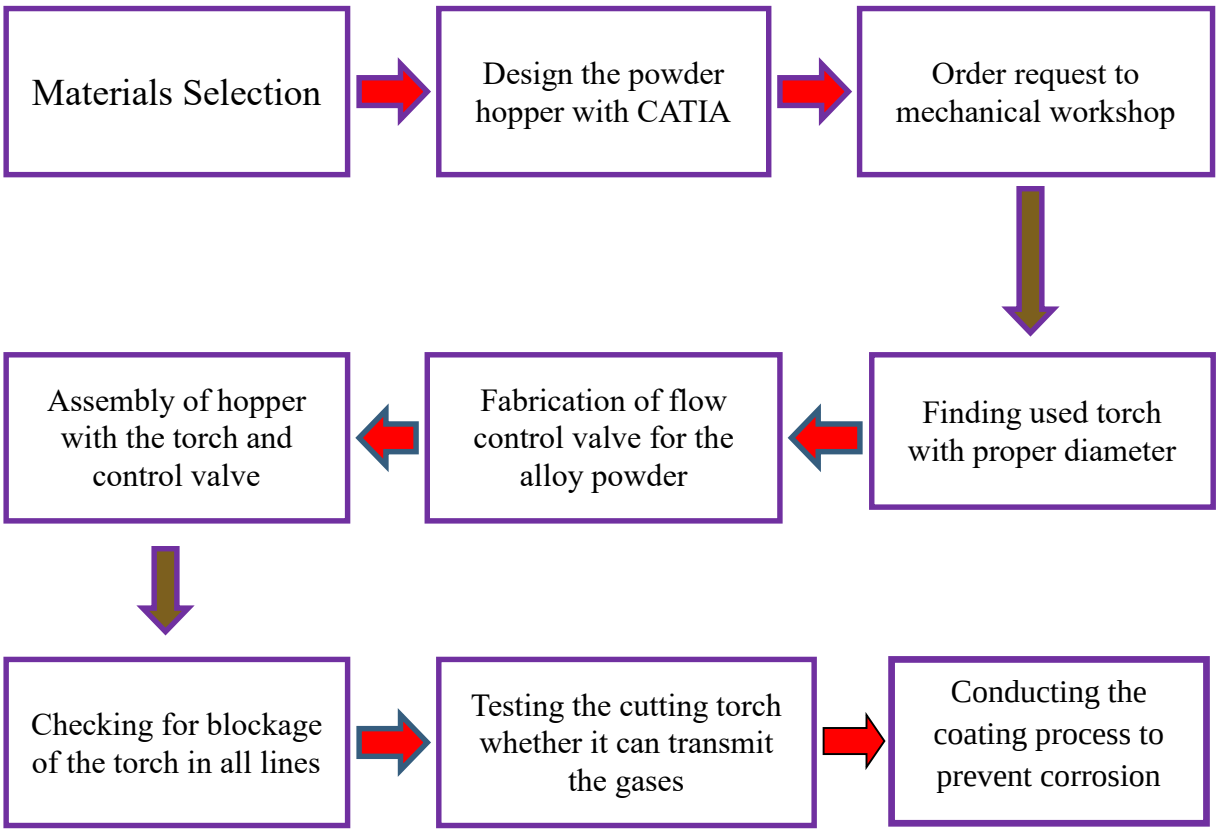

Figure 22 Steps followed in the modification of the conventional cutting torch

4.3.3 Pressure Regulators

The pressure of the gases obtained from cylinders is considerably higher than the gas pressure used to operate the welding torch. The purpose of using a gas pressure regulator is:

- To reduce the high pressure of the gas in the cylinder to a suitable working pressure, and
- To produce a steady flow of gas under varying cylinder pressures.

A pressure regulator is connected between the cylinder/generator and the hose leading to welding torch. Desired pressure at the welding torch may be somewhere up to 35 psig for oxygen and 15 psig for acetylene in the ratio of 1.5:1.

Table 4 Standard operational parameters of oxygen and acetylene cylinders

Cylinder	Cylinder pressure (psi)	Working pressure (psi)	Max. on the gauge	Flame temperature (˚C)
Oxygen	2200	1 to 35	150	3,200
Acetylene	250	1 to 12	30	

4.3.4 Welding Torch & Blow Pipe

A welding torch mixes oxygen and acetylene in the desired proportions, burns the mixture at the end of the tip, and provides a means for moving and directing the flame. There are two types of welding torches, namely:

(a) High pressure (or equal pressure) type;

(b) Low pressure (or injector) type.

High pressure blowpipes or torches are used with (dissolved) acetylene stored in cylinders at a pressure of 117 psi. Low pressure blowpipes are used with acetylene obtained from an acetylene generator at a pressure of 8 inch - head of water (approximately 0.3 psi). In high pressure blow torch, both the oxygen and acetylene are fed at equal pressures and the gases are mixed in a mixing chamber prior to being fed to the nozzle tip. The high pressure torch also called the equal pressure torch is most commonly used because:

(i) It is lighter and simpler;

(ii) It does not need an injector;

(iii) In operation, it is less troublesome since it does not suffer from backfires to the same extent.

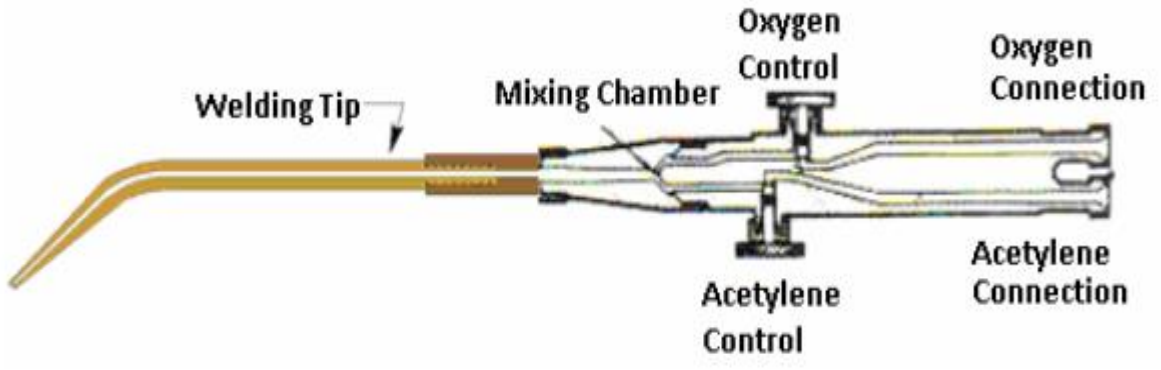

Figure 23 Typical schematic diagram of oxy-acetylene welding torch [41]

To change the power of the welding torch, it is only necessary to change the nozzle tip (size) and increase or decrease the gas pressures appropriately.

Note: The real tool of the oxy-acetylene welding process is the flame, NOT the torch. When we come to oxygen cutting, we must consider the pure oxygen jet as a second tool, working hand-in-hand with the flame. To produce only the flame, we use a welding torch, fitted with the appropriate size welding head or tip. To produce both flames and the oxygen jet, we use a cutting torch or cutting attachment, equipped with the appropriate cutting nozzle or tip.

The welding nozzle or tip is that portion of the torch which is located at the end of the torch and contains the opening through which the oxygen and acetylene gas mixture passes prior to ignition and combustion. Depending upon the design of the welding torch, the interchangeable nozzles may consist of:

(a) Either, a set of tips which screw onto the head of the blowpipe, or

(b) As a set of gooseneck extensions fitting directly onto the mixer portion of the blowpipe.

A welding nozzle enables the welder to guide the flame and direct it with the maximum ease and efficiency. To provide for different amounts of heat, to weld metals of different thicknesses, welding tips are made in various sizes. The size of a welding tip is determined by the diameter of the opening or orifice in the tip. As the orifice size increases, greater amounts of the welding gases pass through and are burnt to supply a greater amount of heat. For welding thicker material large sized tip is used which will supply more combustible gases and more heat. A chart giving sizes of tips for welding various thicknesses of metal along with oxygen and acetylene pressures used is generally provided by the manufacturers.

4.3.5 Oxygen and acetylene cylinders

The oxygen cylinder valve is made largely of brass with right hand threads. Its outlet is threaded and machined to comply with standards set by the Compressed Gas Association (CGA) and the American National Standards Institute (ANSI). All oxygen regulators sold in the U.S and Canada for use on industrial oxygen cylinders carry a mating inlet nut and nipple. The connection is designated "CGA 540". Every oxygen cylinder valve is also equipped with a bursting disk which will rupture and release the contents of the cylinder if cylinder pressure should approach cylinder test pressure (as it might in case of a fire). In order to protect cylinder valve from getting damaged, a removable steel cap is screwed on the cylinder at all times when the cylinder is not in use. The cylinder valve is kept closed when the cylinder is not in use.

An acetylene cylinder is also a solid drawn steel cylinder and the common sizes are 300, 120 and 75 cubic feet. Cylinder pressure is 250 Psi when filled. An acetylene cylinder is painted maroon and the valves are screwed left handed (with grooved hex on nut or shank).

Acetylene is extremely unstable in its pure form at pressure above 15 Psi. This instability places special requirements on the storage of acetylene. Acetylene cylinders are packed with porous material (balsa wood, charcoal, corn pith) that is saturated with acetone to allow the safe storage of acetylene. These porous filler materials aid in the prevention of high-pressure gas pockets forming in the cylinder. Acetone, a colorless, flammable liquid, is than added to the cylinder until about 40 percent of the porous material is saturated. Acetone is a liquid chemical that dissolves large portions of acetylene under pressure without changing the nature of the gas and is a liquid capable of absorbing 25 times its own volume of acetylene gas at normal pressure. Being a liquid, acetone can be drawn from an acetylene cylinder when it is not upright. If acetylene is withdrawn too rapidly, quite a lot of acetone may come with it, in vapor or droplet form, and the cylinder may cool down so much that it cannot sustain the high rate.

4.4 Coating Materials

As illustrated before, the coating materials utilized in this research are summarized in **Table 5**. These alloys were selected through systematic study, starting from simple binary alloys to more complex ones containing both alumina and chromia formers. The essential thing is that all the selected materials are good candidates for high temperature corrosion protection especially in harsh boiler conditions. The coating powders are all purchased from local chemicals market and are not synthesized in the laboratories.

Table 5 Chemical (%wt.) of powders utilized for powder spray coating

S/n	Composition	Quantity [g]	Manufacturer
1	Ni-Powder	500	Loba Chemie, India
2	Cr-Powder	500	Loba Chemie, India
3	Ni50Al	500	Loba Chemie, India
4	Ni20Cr	500	Loba Chemie, India
5	Ni50Cr	500	Loba Chemie, India
6	Cr_3C_2-30(Ni20Cr)	500	Loba Chemie, India

4.5 Oxy-Acetylene Spraying Procedure

The flame spraying process can be utilized to produce good quality coatings if correct optimization of parameters is utilized in the oxygen fuel combination and the supply of coating powders. In general, the oxy-acetylene flame thermal spray process can be divided into two main steps: specimen preparation and spraying process. Specimen preparation is the phase where the work pieces are prepared for the coating process to be carried out. The spraying process is the stage where all the modification is carried out on the conventional oxy-acetylene torch.

4.5.1 Specimen Preparation

The substrate workpiece (ASTM SA210-A1) used in this particular research were round coupons (height = 25mm, diameter = 16mm, and thickness = 5mm) cut from furnace-wall tube of a boiler in FSF. The nominal chemical composition of the boiler tube material is given in **Table 6**.

Table 6 The chemical composition of the ASTM SA210-A1 carbon steel [118]

Substrate	ASTM code	C	Mn	Si	P	S	Cr	Fe
Gr-A1	ASTM SA210	0.2	0.93	0.5-1.0	0.025	0.035	0.055	Bal.

Figure 24 The specimens prepared for the flame spray coating process

In many of the surface coating processes, the integrity of the deposit is critically dependent on the substrate surface condition. The powder flame thermal spraying is no exception, but unlike other methods, it is applied onsite in ambient atmosphere. Thus surface cleanliness in the true scientific sense is never achieved. Cleaning the surface is carried out by polishing the substrate surface by a harder material i.e. by filing and polishing by using sand paper. Since the coating is carried out on the external surface other advanced cleaning methods are not employed for this research.

4.5.2 Flame Spraying Process

Preheating is utilized for removing moisture from the substrate, reducing the thermal stress that may arise due to the difference in the coefficient of thermal expansion between the workpiece material and the coating material [65]. Preheating can also improve coating adhesion by encouraging more diffusion between the substrate and the coating [65]. Preheat temperature for aluminum substrate is 50˚C which was attained by a single pass of the spray gun, according to **METCO** [119].

Table 7 Powder flame spraying parameters in oxy-acetylene gun system

S/n	Cylinder pressure	Working pressure	Oxygen to fuel ratio	Spraying distance	Powder feed rate	Number of layers	Coating thickness
O_2 gas	2200 psi	35 psi	2:1	15-20 cm	-	2	[2±0.05] mm
C_2H_2 gas	250 psi	12 psi			-		
Powders	-	-			0.6-1g/s		

The as-sprayed coatings are seldom ready for use. In most practical applications they have to be ground and polished to get required surface roughness. Heat treatment of the sample may be necessary to change coating phase composition, to decrease porosity and residual stress or to improve other coating properties. Among the heat treatment processes, furnace treatment seem s to be the most usually applied, especially in research laboratories [65].

4.6 Coatings Synthesis and Characterization

Coating materials deposited by any type of technique must be scientifically characterized before they go into service. Visual inspection (either macro or microscopic) is the primary characterization technique used to gain coating micro structural information such as chemical composition, grain morphology and orientation, defects and so on. Mechanical properties such as coating adhesion can also be measured using the optical techniques [120]. Before optical examination is carried out, the coating surface should be prepared properly by grinding and polishing. Blemishes, such as scratches, deformation, pull-out, cracks, contamination and so on

can result from poor surface preparation according to Glancy [56]. Mechanical and thermal properties (hardness, thermo-gravimetric analysis (TGA), and scratch test) was also be evaluated.

4.6.1 Synthesis of Coating Materials

The coating powders will be used for the formulation of protective coatings on the boiler tube surface. The appropriate powder (Ni20Cr, Ni50Cr, Ni50Al, and Cr_3C_2-(30Ni20Cr)) coating materials selected for the corrosion prevention was carried out inside the ASTU laboratory.

Figure 25 The coating alloys prepared for the flame spray coating process

4.6.2 Characterization Techniques

Initially, visual and photographic examination of uncoated and coated corroded specimen was undertaken for the differentiating the external color changes that would be visible on the furnace wall tubes FWTs. The color variation because of the swelling of the scales can easily be identified with visual examination when the tube blisters. For sample preparation for microscopy, metallographic workpiece preparation is essential for characterization of thermally sprayed coatings. The preparation process can be divided into four different areas; sectioning, mounting, grinding, polishing, and finally etching the sample.

4.6.2.1 Optical Microscope (OM)

The light microscope is the first basic tool of material analysis used to examine, evaluate and quantify the micro structure of various materials. Its main advantage being relatively cheap in its simplest form compared to other microscopic observation instruments and easy to operate. Operating in its reflecting mode, it is well capable of revealing polished and etched material specimens. It comprises of an illumination system, condenser, light filters, objective lens, eyepiece, stage and stand. The optical microscope enables analyzing of the [121]:

1. Microstructure and constitutes of any surface including coatings;
2. Fraction and size of voids in the coating;
3. Fraction and size of unmelted particles in the coating;
4. Distribution of phases in the coating if an etchant is used;
5. Deformation (mechanical or thermal) of the substrate near the coating.

As the total field of microscopic observation is no greater than a few square millimeters, it is important to select a typical part of the surface of the material to get representative information about the material. **"Huvitz HRM-300"** universal camera optical microscope was used in the current research to obtain microstructure of the sample carbon steel.

4.6.2.2 Scanning Electron Microscope (SEM)

The light microscope discussed above is used for small scale material characterization. As the sophistication of investigations increased, either the Transmission Electron Microscope (TEM) or the Scanning Electron Microscope (SEM) often replaces the optical microscope. Both of those instruments have superior resolution and depth of focus. Because of its reasonable cost and wide range of application that it provides, the SEM is the preferred instrument used in material studies. The SEM provides the investigator with a highly magnified image of the surface of a material that is very similar to what one would expect if one could actually "SEE" the surface visually. The resolution of the SEM can approach a few nm (nanometer) and it can operate at magnifications from about 10X to 300000X. There are various applications of the SEM, such as [121]:

1. Examinations of metallographically prepared samples at magnifications well above the useful magnification of the optical microscope;
2. Examination of fractured surfaces and deeply etched surfaces requiring depth of field well beyond that possible by the optical microscope;
3. Evaluation of crystallographic orientation of features on a metallographically prepared surface;
4. Evaluation of the composition gradients on the surface of bulk samples over distances approaching 1μm.

Samples used in a scanning electron microscope can be of any form, as in any solid or liquid having a low vapor pressure. Electrically conductive materials can be prepared using standard metallographic polishing and etching techniques. Non-conducting materials are generally coated with a thin layer of carbon, gold or gold alloy. Samples must be free from water, organic cleaning solutions, and remnant oil-based film s and must be electrically grounded to the holder. Fine

samples, such as powder as in the case of this particular project, are dispersed on an electrically conducting film. Japan made, bench-top scanning electron microscope found in the biology department- "**JCM-6000PLUS**" was used in this in this research.

4.6.2.3 X-Ray Powder Diffraction (XRD)

XRD, that is, X-ray diffraction, refers to a method of analyzing the diffraction pattern of material by X-ray diffraction to obtain information on the composition of the material, the structure or morphology of atoms or molecules inside the material. It is a powerful material characterization technique used to identify structural properties such as strain state, grain size, phase composition and orientation and so on. Polycrystalline materials are made up of individual crystal, which in turn made up of families of identical plane of atoms, with a fairly uniform interplaner spacing d. X-ray beams will be diffracted from a given family of planes at a certain angles of incident known as Braggs' angle. So diffraction occurs at an angle of 20˚, defined by Bragg's law [122],

$$n\lambda = 2dsin\theta \quad (4.1)$$

Where N = integer, D = lattice spacing of crystal planes (mm), θ = the angle of diffraction (˚), λ = wavelength of X-ray beam (mm).

For diffraction to be observed, the detector must be positioned so as to receive the diffracted ray at angle of 2θ. The crystal must be oriented so that the normal to the diffracting plane is coplanar with the incident and diffracted beam.

One of the most important uses of XRD is phase identification of materials. Identification is done by comparing the measured d spacing in the diffraction pattern and, to a lesser extent, their integrated intensities with known standards in the JCPDS (Joint Committee on Powder Diffraction Standards, 1986) Powder Diffraction software, attached to the DIFFRACT+ Measurement Part 2002 X-ray diffraction system. In the current work, XRD was used to identify phases present in the virgin and corroded carbon steel material used as a substrate. The phase and crystallinity of the corroded, pristine, and coated boiler tube carbon steel samples were determined by x-ray diffraction (XRD) (**Shimadzu XRD- 7000**).

The X-ray diffraction data obtained from the ASTU laboratory has been done for the pristine, corroded, and coated samples and graphically illustrated with Origin software. The phases and crystallinity of the substrate and coatings have been executed and finally the crystallite sizes of the coatings have been determined using Scherer's equation.

4.6.2.4 Ultrasonic Thickness Measurements

The other important tool that was used for characterization was ultrasonic thickness gauge (UTG) which can nondestructively test the wall thickness of the FWTs without destroying the tubes. An ultrasonic thickness gauge is a measuring instrument for the non-destructive investigation of a material's thickness using ultrasonic waves.

The usage of an ultrasonic thickness gauge for non-destructive testing to check material properties such as thickness measurement is regular in all areas of industrial measurements. Some ultrasonic coating thickness gauges require that a couplant in gel (propylene glycol) format be used to eliminate gaps between the transducer and the workpiece. The thickness of the samples was measured by using "**GM100"** intelligent ultrasonic thickness gauge and Vernier Caliper in FSF workshop. The thickness loss samples were taken for a range of six months with every two months differences on four furnace wall tube samples to show thickness variation.

4.6.2.5 Weight Loss Method Measurements

The simplest way of measuring the corrosion rate of a metal is to expose the sample to the test medium and measure the loss of weight of the material as a function of time. Corrosion rate may be expressed in mils per year (mpy) of metals degraded.

$$R_{Corr}(mpy) = \frac{534W}{D * A * T} - (4.2)$$

Where W = weight loss, mg, D = Density of specimen, A = Area of Specimen, sq. in, and T = exposure time, hr.

4.6.2.6 Potentiostatic Polarization Measurements

In this technique, the polarization curves are obtained by applying potential of ±250 mV with respect to open circuit potential as shown in **(Figure 26)** below. Resulting Tafel plots contain anodic and cathodic branches. Resulting Tafel plots contain anodic and cathodic branches.

Figure 26 Electrochemical cell for Tafel Polarization Experiments [162]

Stearn and Geary (1957) [123] first presented the relationship between polarization resistance R_p (Equation 4.3), and corrosion current, $i_{corr.}$, (Equation 4.4) [124]. The anodic and cathodic Tafel slopes, and β_a *and* β_c, can be estimated as follows:

$$R_p = \frac{\Delta E}{\Delta i} \quad (4.3)$$

Where E is applied potential (often in mV) and I is the current flow (often in A). Theoretically, the corrosion current is determined from cathodic and anodic Tafel slopes β_c and β_a (the slopes of cathodic and anodic polarization curves in Tafel linear regions):

$$I_{corr} = \frac{1}{2.303R_p} \times \left(\frac{\beta_a \beta_c}{(\beta_a + \beta_c)}\right) \quad (4.4)$$

Therefore, corrosion rate (Equation 4.5) in milli inches per year (mpy) for carbon steel in a corrosive solution given the corrosion current (I_{corr}), density (d), and equivalent weight (EW) will be calculated from the following equation:

$$CR = \frac{0.13 \times I_{corr} \times EW}{d} \quad (4.5)$$

4.6.2.7 Electrochemical Impedance Spectroscopy Measurements

Electrochemical Impedance Spectroscopy (EIS) which is a highly sensitive characterization technique will be used to establish the electrical response of chemical systems in a nondestructive manner. EIS systems characterize the time response of chemical systems using low amplitude alternating current (AC) voltages over a range of frequencies. Using an electrode setup consisting of a working, reference, and counter electrodes a known voltage is passed from the working electrode through an electrolytic solution and into the counter electrode. During electrochemical impedance spectroscopy, Bode plots, Nyquist plots, are utilized to measure the corrosion resistance capacities of the coated samples.

CHAPTER 5

RESULTS & DISCUSSION

5.1 Introduction

A typical powder flame thermal spraying executed where Nickel-based alloys are utilized as coatings to deal with oxidation and corrosive environments at high temperatures. When Nickel is alloyed with chromium, the element oxidizes to form a protective surface oxide of Cr_2O_3 at rates which could make it suitable for use up to about 1473˚K [125]. When the formation of the surface oxide layer is faster, the protection offered will be much better. Therefore, there is an increasing interest in the coating deposition of Ni-based metallic alloys for protection against corrosion. Ni-based coatings are used in various applications, where corrosion resistance combined with wear and abrasion resistance is given the highest priority.

In this particular research, powder flame thermal spray coating is applied to deposit Nickel-chrome and Nickel-aluminum alloy coatings onto the outer surfaces of the furnace wall tubes of boilers to increase the corrosion resistance capacity of the boiler tubes. The coating process is carried out by utilizing the oxy-acetylene welding torch, where minor modification is carried out between the welding-tip and mixing chamber of the torch. In between these, a hopper gate that is used to supply a corrosion resistant powder is designed with **CATIA V5** and fabricated along with a control valve that regulates the amount of powder supplied for the coating process. The hopper and control valve assembly was then mounted on the welding torch internal-threaded hole in between torch tip and the mixing chamber leaving sufficient gap for powder flow.

The remaining fittings for the supply and control of oxygen and acetylene gas were mounted on the mixing chamber of the cutting torch along their pressure regulators. For the coating to be uniform, a uniform holding time, two layer coating, and a spraying distance of 8cm is applied for all the samples. Based on the exact operating conditions, deposition rates varied from 5.6 to 6.5 µm/pass. Deposition efficiencies were measured between 50 and 58% at spray distances up to 10.5 cm. Coating thickness attained in the process were in the range of [2.2 – 2.5]mm measured by ultrasonic thickness gauge **(UTG)** before and after the coating is carried out. Despite the fact that coatings were produced at different stand-off distances under similar conditions, an increase in spray distances leads to a rise in porosity of about 10%.

5.2 Visual Examinations

The macrographs for uncoated steel based alloy (SA210-A1) and PFTS sprayed Ni20Cr, Ni50Cr, Ni50Al, and Cr_3C_2-30(Ni20Cr) coatings on SA210 after 720 hours exposure to the muffle furnace at a temperature of 600 ˚C are depicted in **Figure 27** below.

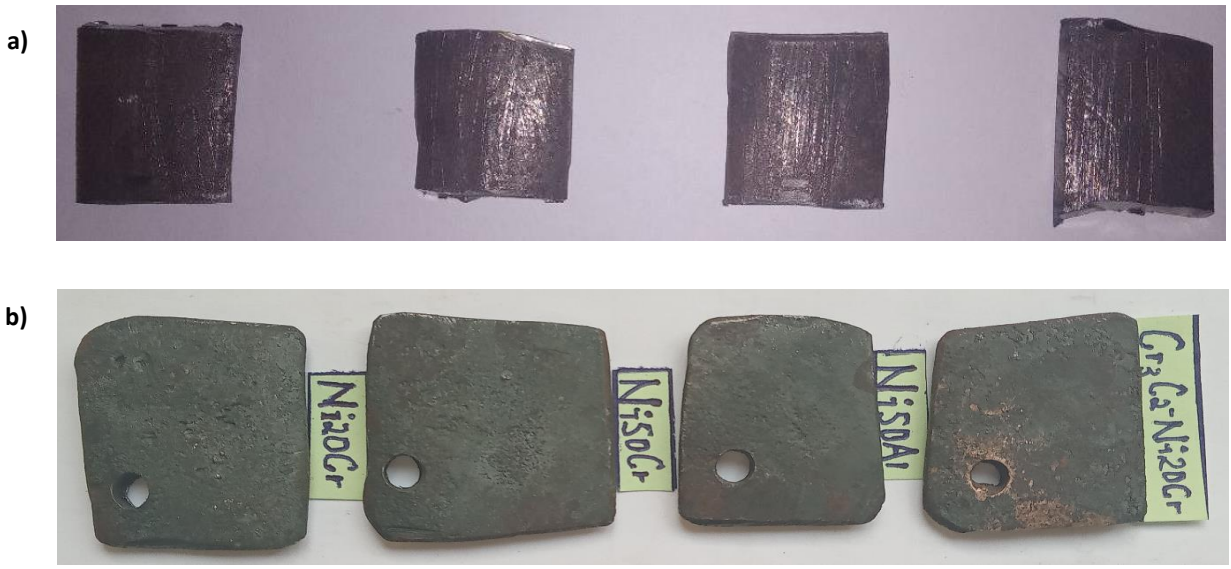

Figure 27 a) Sample pristine tubes photographed from water-wall tubes in FSF **b)** Coated tube samples after exposure to simulated boiler environment (600˚C)

5.3 Optical Microscope

Microstructural examination of the longitudinal and transverse tube oriented sections were conducted. The samples were taken from the bent zone as well as from the straight zone of the boiler tubes. The material is composed of corroded particles and returned to its original ore form. Thin inclusions with indexes A1-sulfites and D2-oxides were identified in the material, according to method A of ASTM E45 [12]. The other yellowish-blue spots revealed places that are very prone/susceptible to corrosion.

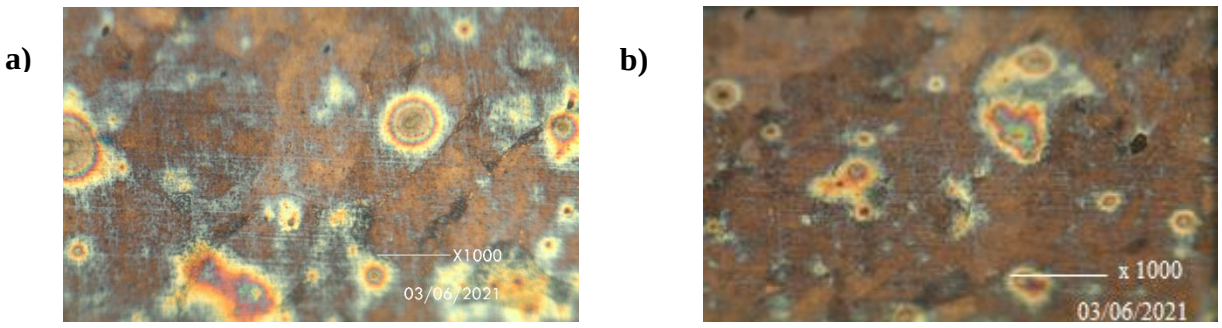

Figure 28 OM images of SA210-A1 etched with Nital reagent at different locations

The crack originated on the inner surface of the tube and grew across the tube wall until it reached the other surface. The micrographs revealed the presence of corrosion pitting, uniform corrosion, and intergranular cracking occurring at the boundaries **(Figure 28).**

5.4 Scanning Electron Microscope

SA210-GrA1 furnace wall boiler steel from *fivescail*- India was selected as substrate material and it was prepared to the required size. The scanning electron microscope picture taken for the corroded and pristine carbon steel tube material is given below.

a) **b)**

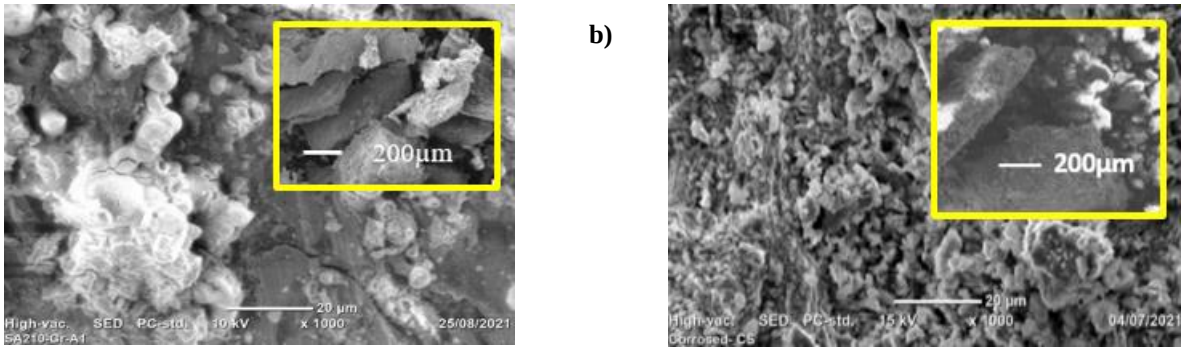

Figure 29 SEM images of carbon steel SA210-A1 (a) Pristine sample, X20µm and (b) Corroded sample X20µm

The surface microstructure of the samples is shown **Figure 29** (a) is for pristine sample with similar morphology as (b) for corroded sample which is an interconnected porous and powdery structure with small particle size. The SEM image of (a) and (b) samples clearly shows the existence of porous material porosity is one of the essential characteristics of the samples during coating process for better bond strength between the tubes and good tendency of adhesion.

5.4 Weight Loss Measurements

Weight change measurements of bare, Ni20Cr, Ni50Cr, Ni50Al, and Cr_3C_2-30(Ni20Cr) ASME SA210 GrA1 subjected to cyclic oxidation for 10 cycles at 600˚C were performed. The substrate workpiece (ASTM SA210-A1) used in this particular research were round coupons (height = 25mm, diameter = 16mm, and thickness = 5mm) cut from furnace-wall tube of a boiler in FSF. Weight gained by Ni20Cr was minimum and weight gained by bare SA210 steel alloys was maximum. **Table 8** shows the data between weight changes of the samples and number of cycles for the uncoated and coated SA210-A1 samples subjected to 720 hours cyclic exposure to mid-temperature water-wall zone of bagasse-fired boiler at 600˚C. **Table 9** shows the column chart for

uncoated and coated SA210-A1 samples of the four coating alloys used in the project (where S1 = Ni20Cr, S2 = Ni50Cr, S3 = Ni50Al, and S4 = Cr_3C_2-30(Ni20Cr).

Weight loss measurement is still the most widely used means of determining corrosion loss, despite being the oldest method currently in loss determination has a number of attractive features that account for its sustained popularity: *Simple* – No sophisticated instrumentation is required to obtain a result. *Direct* – A direct measurement is obtained, with no theoretical assumptions or approximations. *Versatile* – It is applicable to all corrosive environments, and gives information on all forms of method is commonly used as a calibration standard for other means of corrosion monitoring, such as linear polarization and electrical resistance.

Table 8 Weight measurements [g] taken before and after corrosion of the tubes

S/Tube	Pristine Sample [g]	Corroded Sample [g]			
		Month-2	Month-4	Month-6	Month-8
SN1	212	211.46	210.15	209.82	208.14
SN2	212	211.73	209.93	209.21	208.31
SN3	212	210.85	209.71	208.96	208.25
SN4	212	211.68	210.17	209.73	208.53
Average	212	211.43	209.99	209.43	208.31

SN = Sample Number, **g** = gram

From the **Table 8**, it can be easily understood that in a period of 6 months, the actual weight of the sample tubes has decreased. The simplest way of measuring the corrosion rate of a metal is to expose the sample to the test medium and measure the loss of weight of the material as a function of time. Corrosion rate may be expressed in square centi per hour (cph) of metals degraded [126]:

$$\mathrm{R_{Corr}} = \frac{534 \times (\mathrm{W_{blk}} - \mathrm{W_{inh}})}{(\rho_{wp} \times \mathrm{A} \times \mathrm{T})} \quad (5.1)$$

Where W_{blk} = weight of blank sample, W_{inh}. = weight of inhibited sample, $\boldsymbol{\rho}_{wp}$ is density of work piece, g/cm^3, A is area of specimen, sq. cm, and T is duration of exposure, hr.

Moreover, the inhibition efficiency (IE) when immersed in 0.5N H_3PO_4-NaOH and degree of surface coverage (θ) in **Table 9** are calculated by using **equation 5.2** and **5.3** as follows:

$$\%IE = \frac{W_{blk} - W_{inh}}{W_{blk}} \times 100 \quad (5.2)$$

$$\theta = \frac{W_{blk} - W_{inh}}{W_{blk}} \quad (5.3)$$

Table 9 Weight loss method for corrosion rate and inhibition efficiency measurements

Coating Materials	W_{blk} [g]	W_{inh} [g]	Weight loss ΔW [g/cm^2]	Corrosion Rate CR [g.cm^2.hr^{-1}]	IE [%]
Uncoated	230	140	90	2.2801	
Ni20Cr	12.74	12.48	0.26	0.0065	99.71
Ni50Cr	12.93	12.65	0.28	0.0071	99.68
Ni50Al	12.87	12.51	0.36	0.0091	99.60
Cr_3C_2-30[Ni20Cr]	12.59	12.05	0.54	0.0136	99.41

From the table, the weight loss (ΔW), corrosion rate (CR) and inhibition efficiency (%IE) values measured after one month of immersion indicate that the corrosion rate of the studied coatings can be given by the descending order (Ni20Cr > Ni50Cr > Ni50Al > Cr_3C_2-30[Ni20Cr]).

5.5 Thickness Loss Measurements

Corrosion rate for thinning damage mechanisms is determined by the difference between two thickness readings divided by the time interval between the readings measured by ultrasonic thickness gauge (UTG), **[GM100]**. The determination of corrosion rate may include thickness data collected at more than two different times. Suitable use of short-term versus long-term corrosion rates is determined by the inspection of the sample at different points. Six month data has been collected from FSF boiler furnace wall tubes for corrosion study before and after corrosion.

a) **b)**

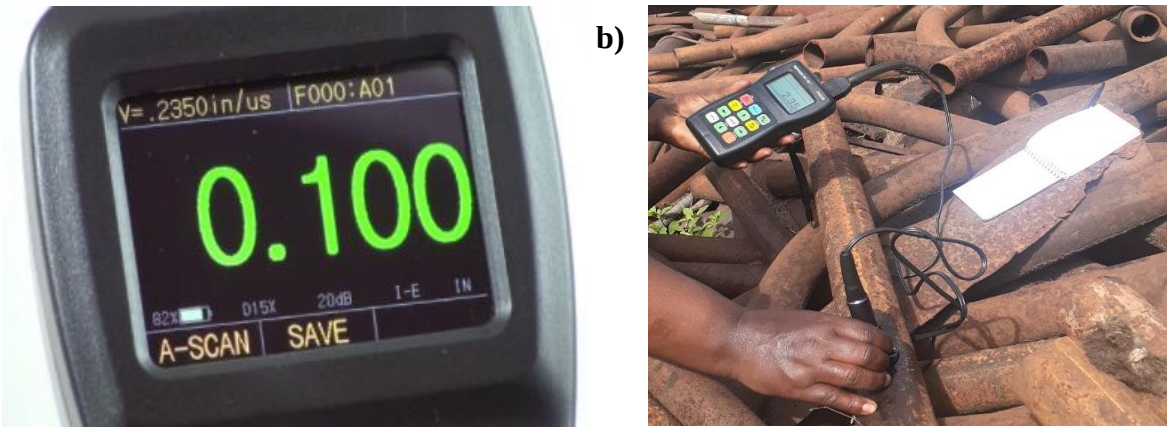

Figure 30 Calibration and Measurement of Ultrasonic Gauge (UTG)

Thinning and diminution of the wall thickness of four different sample tubes were monitored in a space of six months to establish their corrosion rate (both short term and long term) and the

remaining life. These parameters are considered as part of the prediction and rejection criteria used to ascertain the life span and usage worthiness of the furnace wall tubes.

Table 10 Thickness difference taken before and after corrosion of the tube material

S/Tube	Pristine Thickness [mm]	Corroded Sample Thickness [mm]			
		Month-2	Month-4	Month-6	Month-8
SN1	5.73	5.34	4.82	4.17	3.82
SN2	5.73	5.25	4.73	4.20	3.75
SN3	5.73	5.17	4.91	4.32	3.91
SN4	5.73	5.28	4.85	4.16	3.78
Average	5.73	5.26	4.83	4.21	3.82

SN = Sample Number, **mm** = millimeter

With this data in hand, we were able to calculate corrosion rates according to the following:

$$\text{Metal loss} = T_o - T_a \quad [5.4]$$

Where, T_o is original thickness, T_a is actual thickness.

5.6 X-Ray Diffraction Analysis

The diffraction patterns of the tube material are shown in (**Figure 31 - 36)**. The various phases identified from X-ray diffraction patterns of surface oxides formed on and the inside-corroded, outside-corroded, and pristine carbon steel alloys of SA210-A1 are illustrated below. The XRD graph of the pristine sample is verified to be conformed to ICDD number 006-0696. The main phases identified for the pristine and corroded grade A-1 alloy are FeO, Fe_2O_3 and Fe_3O_4 **[Figure 31 - 34]** which are in accordance with the EDS results. In **Figure 32** the diffraction peaks at angles of 2θ = 26.54º, 35.6º, 43.34º, 48.61º, 53.31º, 57.35º, 62.95º correspond to the (001), (002), (100), (101), (102), (004), (112), crystallographic plane, indicating the presence of iron oxides.

The existence of large amount Fe_2O_3 on corroded SA210-A1 steel alloys indicates the diffusion of Fe from the substrate during oxidation at a temperature of 600˚C. These outputs are complied with results reported in reference [127]. The XRD pattern of the outside-corroded boiler tube steel material SA210-A1 was also illustrated by comparing with XRD pattern of standard carbon steel materials. No considerable change has been observed even on the outside-corroded carbon steel XRD results depicted in **Figure 33** where the diffraction peaks were observed at angles of 2θ = 21.09˚, 35.63˚, 44.87˚, 53.28˚, 62.92˚, and 68.35˚ which correspond to the (001), (002), (100), (101), (102), (111) crystallographic planes.

The crystallite size of the coatings (Ni20Cr, Ni50Cr, Ni50Al, Cr_3C_2-30(Ni20Cr)) particles was calculated using Scherer's equation by assuming the crystallites were cubic and mono-disperse in

size [76]. The lesser the crystallite size, the better tendency of coatings to the substrate and better inter-particle bond strength of the coating materials. The crystalline size was calculated according to equation (5.5) below and presented in **Table 11**. It is obviously known that as particle size decreases, the surface area of the material increases and the possible active sites parallel increases which may promote high bonding strength.

$$D = \frac{K\lambda}{\beta Cos\theta} \quad \text{----------} \quad (5.5)$$

Where, λ = 0.154 nm (wavelength of X-ray), K = 0.9 (Scherer's constant), D = Crystalline size (nm) and β = FWHM.

Furthermore, the XRD pattern of the coated samples have been executed and has shown that the uncoated sample XRD has been camouflaged the peaks of the coated because of the two layer thickness (~2mm) of the coatings applied on the substrate tube material.

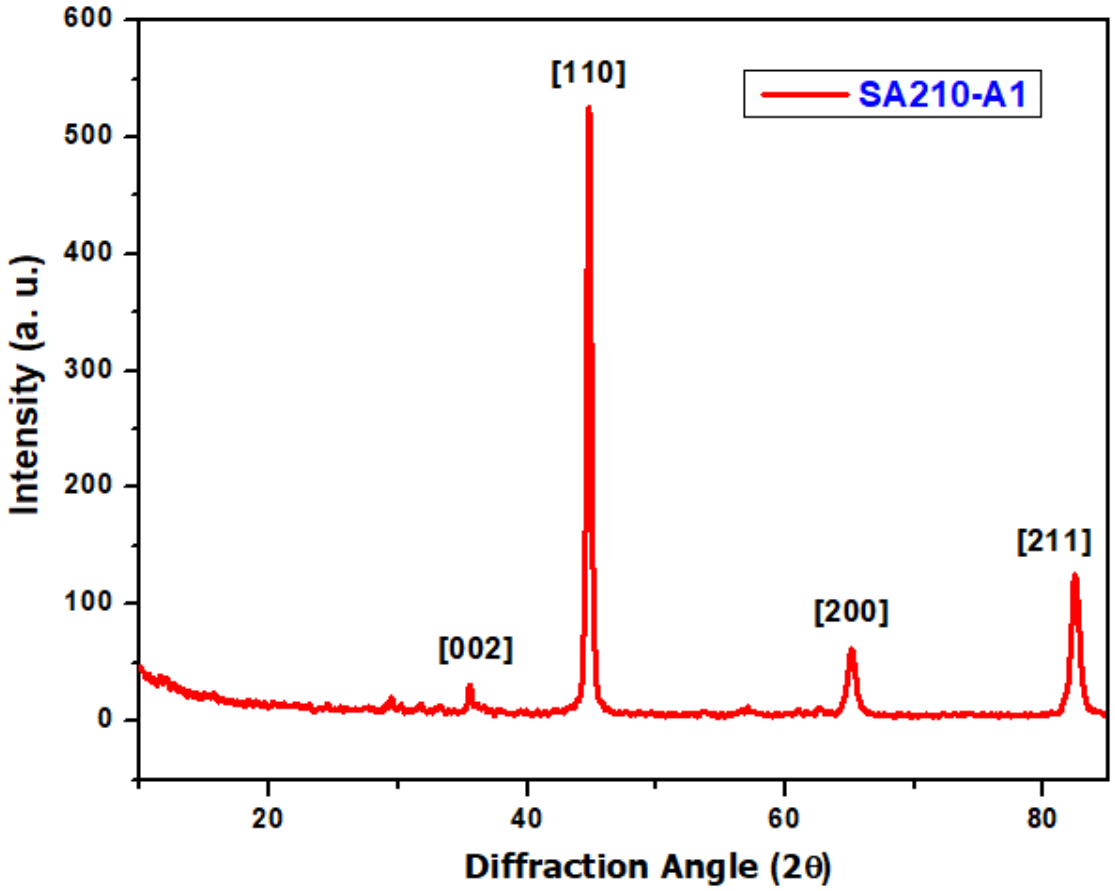

Figure 31 X-ray diffraction patterns of intensity of pristine boiler tube sample

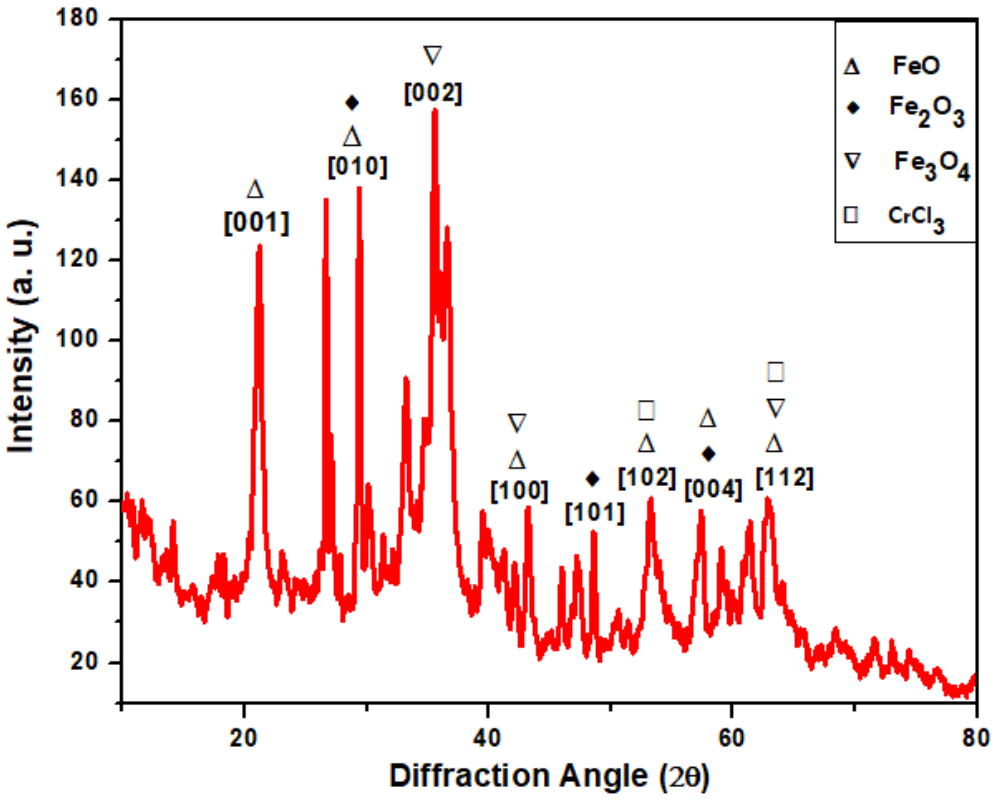

Figure 32 X-ray diffraction patterns of intensity of inside-corroded boiler tube

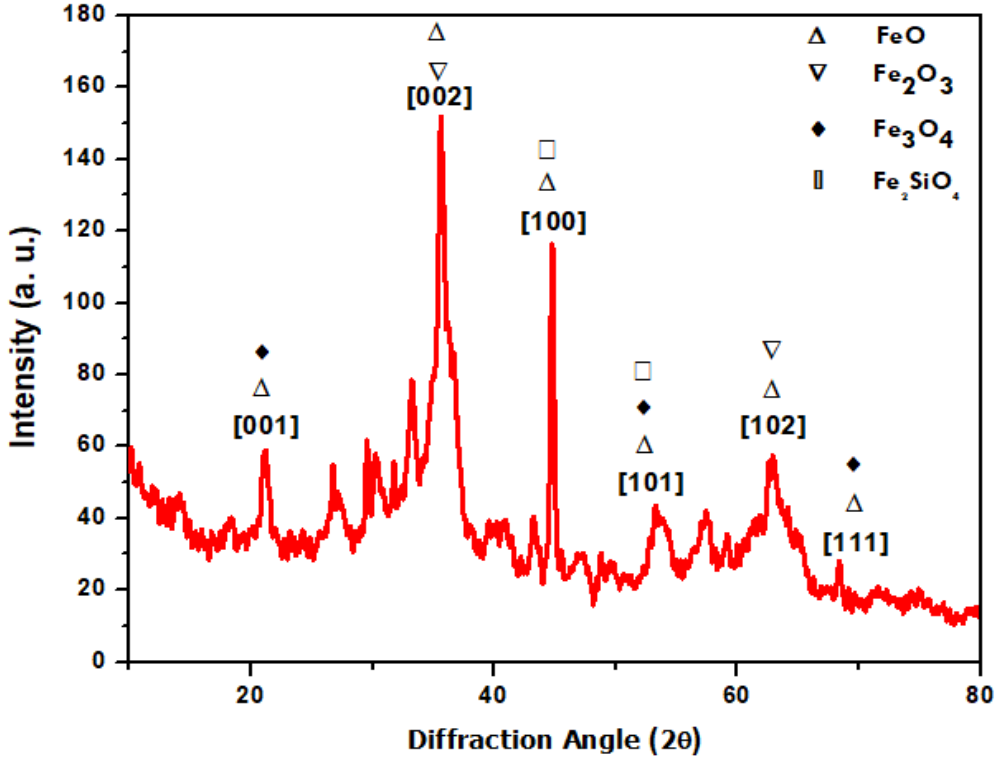

Figure 33 X-ray diffraction patterns of intensity of outside-corroded boiler tube

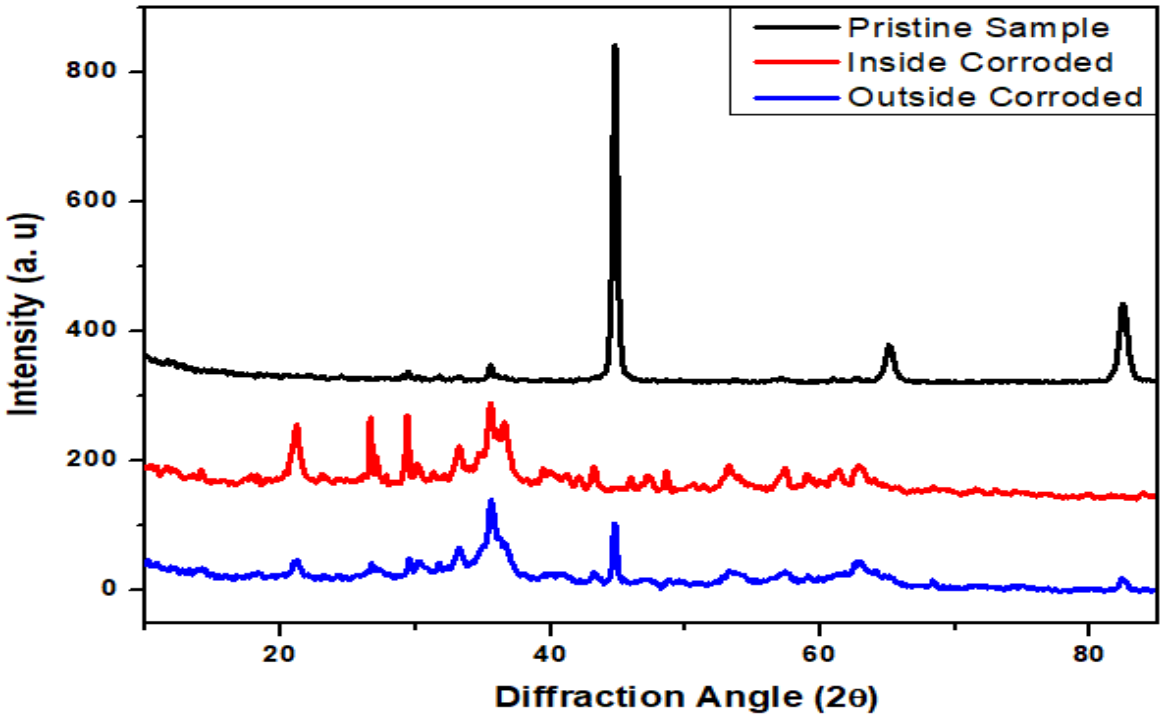

Figure 34 X-ray diffraction patterns of pristine, inside, and outside-corroded boiler tubes

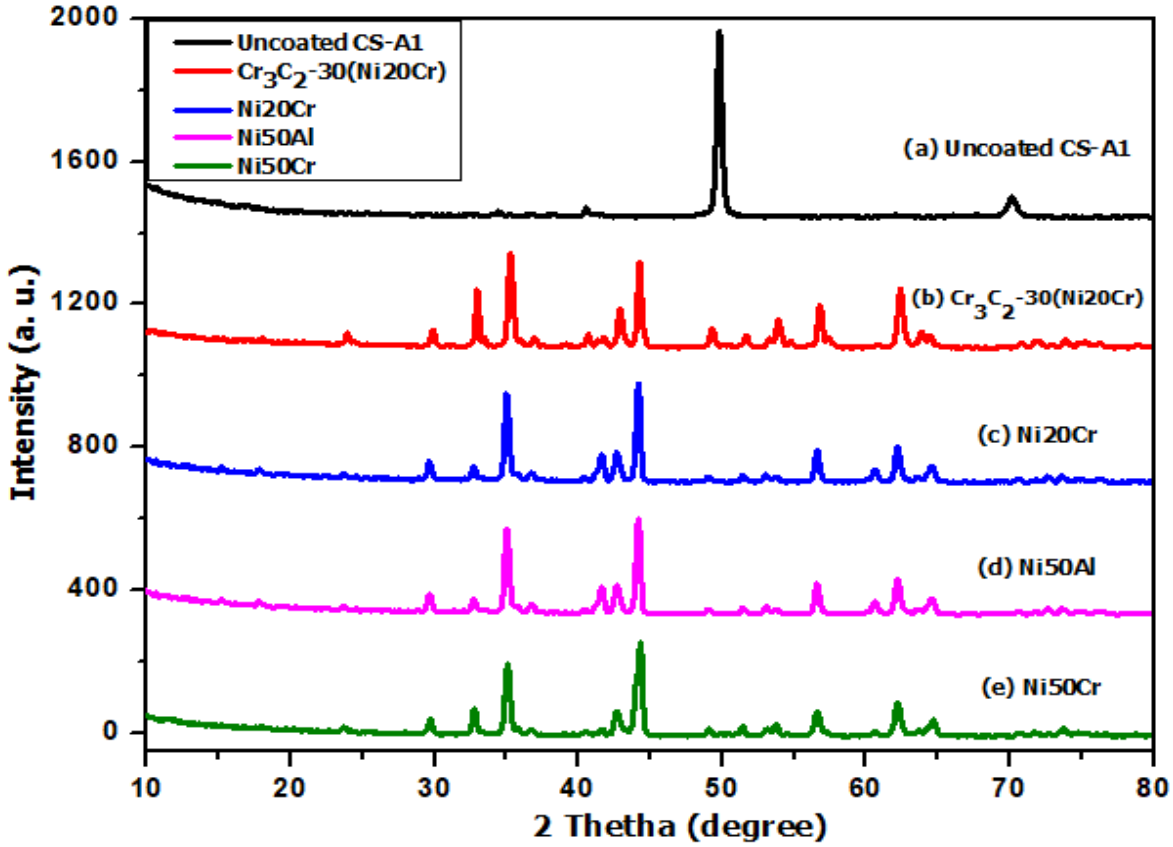

Figure 35 X-ray diffraction patterns of intensity of coated and uncoated boiler tubes

Table 11 The average values of the crystallite size of the coated samples

S/n	Coating Alloys	Crystal sizes, D (nm)
1	Ni20Cr	0.3562
2	Ni50Al	0.4371
3	Ni50Cr	0.4135
4	Cr_3C_2-30(Ni20Cr)	0.5283

Despite the similarities in the peaks obtained for all the coatings utilized in the research, the D-spacing and full width at half maximum (FWHM) vary from one another. The major peak that is seen in the pristine sample have been veiled by the coating materials and not sensed by the XRD due to the limitation of XRD penetration depth and coating thickness attained i.e. ~2mm.

5.7 Particle Density Analysis

Numerically, density represents the mass per unit volume of a matter. The volume of an object increases with increasing temperature, because of the matter's volumetric thermal expansion. Therefore, in general, the density of an object depends on its temperature, with higher temperature resulting in lower density. The density of a gas further depends on the pressure as well. Nevertheless, this effect is negligible in a case of liquid and/or solid matter. There are several experimental methods used for density determination of liquids. In this particular research, the density is analyzed using pycnometer method of density determination.

The pycnometer (from the Greek 'puknos', meaning "density", also called pyknometer or specific gravity bottle), is a flask with a close-fitting ground glass stopper with a fine hole through it, so that a given volume can be accurately, by reference to an appropriate working fluid such as water or mercury, using an analytical balance. The particle density of a powder, to which the usual method of weighing cannot be applied, was determined with pycnometer in Sugar Research Center Laboratory. The powder is added to the pycnometer, which is then weighed, giving the weight of the powder sample [128]. The pycnometer is then filled with a liquid of known density, in which the powder is completely insoluble. The weight of the displaced liquid has been determined, and thence the specific gravity of the powder (in this case the corroded and pristine carbon steel). The density of the corroded sample was found to be less than the densities of the pristine samples. The calculation was carried out as illustrated as follows:

Observations:

Weight of empty pycnometer (R.D. bottle) = W_1

Weight of empty R.D. bottle + water = W_2

Weight of R.D. bottle + rust + water = W_3

Weight of corroded boiler tube taken = 10 g

Calculation:

Weight of water displaced by tube-rust = $(W_2 + 10) - W_3$

Particle density of tube-rust $= \frac{10}{(W_2 + 10) - W_3}$ ---------- [5.6]

Table 12 Particle density measurement of corroded and pristine CS SA210-A

S/n	W_1	W_2	W_3	$\rho^p_{corrod.}$	ρ^p_{virgin}
Month- 2	**10.000**	**161.789**	**169.152**	**3.792**	**7.358**
Month- 4	**10.000**	**162.312**	**170.013**	**3.511**	**6.736**
Month- 6	**10.000**	**160.614**	**168.241**	**4.214**	**7.642**
Month- 8	**10.000**	**163.731**	**169.463**	**2.343**	**7.853**
Average	**10.000**	**162.112**	**169.217**	**3.565**	**7.397**

5.8 Thermal Property Analysis

5.8.1 Thermogravimetric (TGA) Analysis

TG curves pristine and corroded samples was conducted and the results are given in **Figure 36**. Two distinct stages have been observed in these research, 100-600˚C and 600-1,000˚C, were observed for the pristine samples. **Step I**, the constant phase from 100-600˚C indicates a constant phase where the sample adsorbing heat from the sample material. **Step II**, the increase in temperatures of TGA baseline shows an apparent weight gain due to buoyancy. As temperature increases, the gas surrounding the sample pan becomes less dense, so the pan experiences less buoyant lift (per Archimedes' principle). On the other hand, the **Phase I** (100-600˚C) for the corroded sample shows a declining phase which indicates the dehydration of the corroded sample, resulting from evaporation of physically adsorbed water in the rust and **Phase II** is a constant phase where heat energy is absorbed with negligible mass change (**Figure 37**).

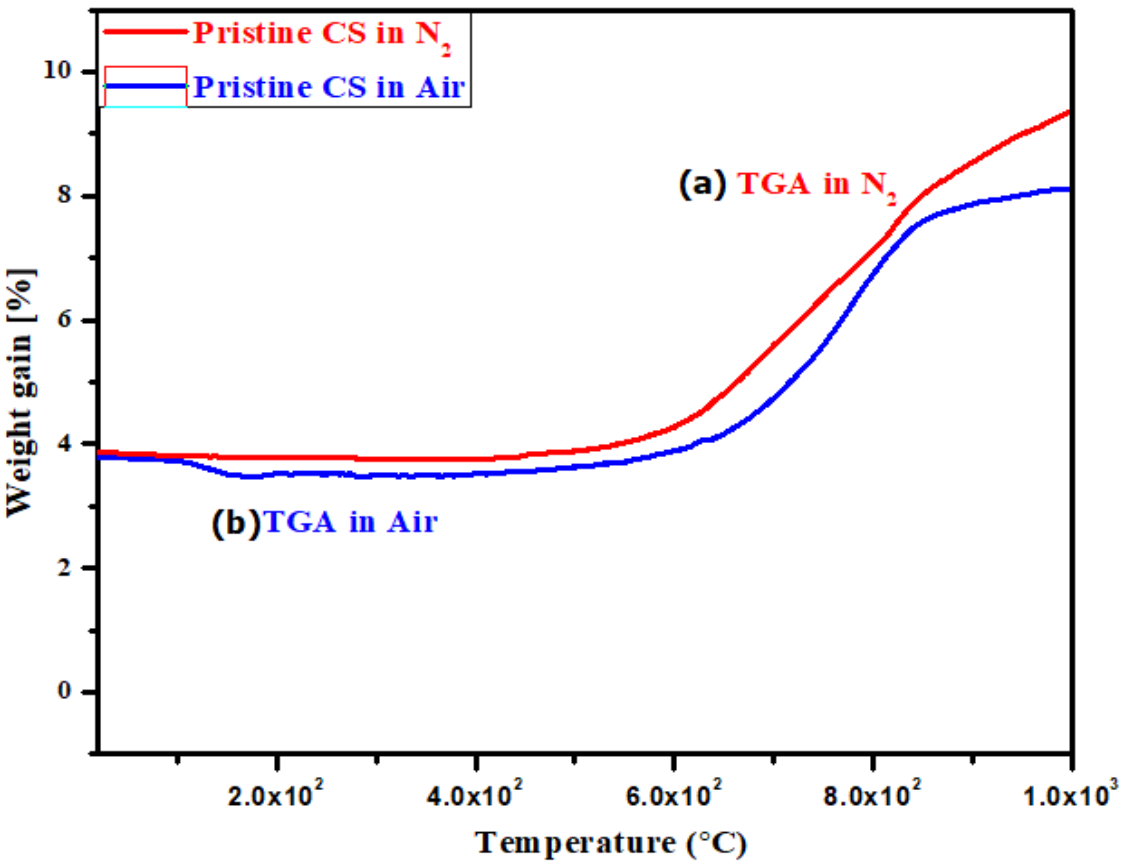

Figure 36 Thermal Analysis (TGA) of Pristine Carbon Steel in (a) N_2, and (b) Air

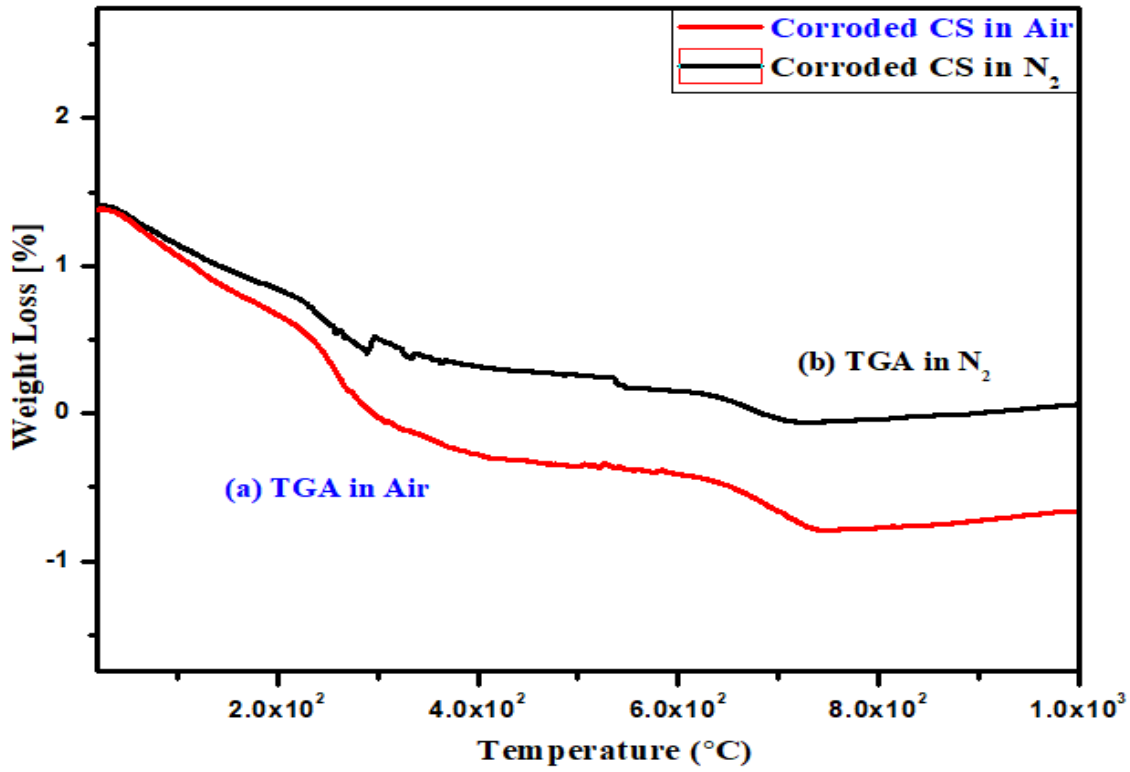

Figure 37 Thermal Analysis (TGA) of Corroded CS in (a) N_2, and (b) Air

5.8.2 Differential Thermal Analysis (DTA)

During the thermal treatment process, in **Stage-I** the DTA curves showed slight increase for the pristine sample and spike real time spike for the corroded sample before it reaches 300˚C **(Figure 38**). During the first endothermic reactions which corresponds to evaporation the physically absorbed water from the sample in **Stage-II**, the sample has undergone relatively high energy is absorbed at 300-500˚C for the corroded than for the pristine sample. Later, in **Stage-III** (500-800˚C) the decline shown with a deeper concave indicates a serious absorption of energy during the last endothermic reaction, which corresponds to the dehydration process, i.e., the hydroxyl in the hydroxyl-oxide is destroyed. Greater energy is absorbed during the second endothermic reaction, the more the percentage of hydroxy-oxide contained in the corroded sample. The exothermic spike followed is due to the oxidation of magnetite for the corroded sample while the endothermic decline is observed in the pristine sample due to reduction (**Figure 39**).

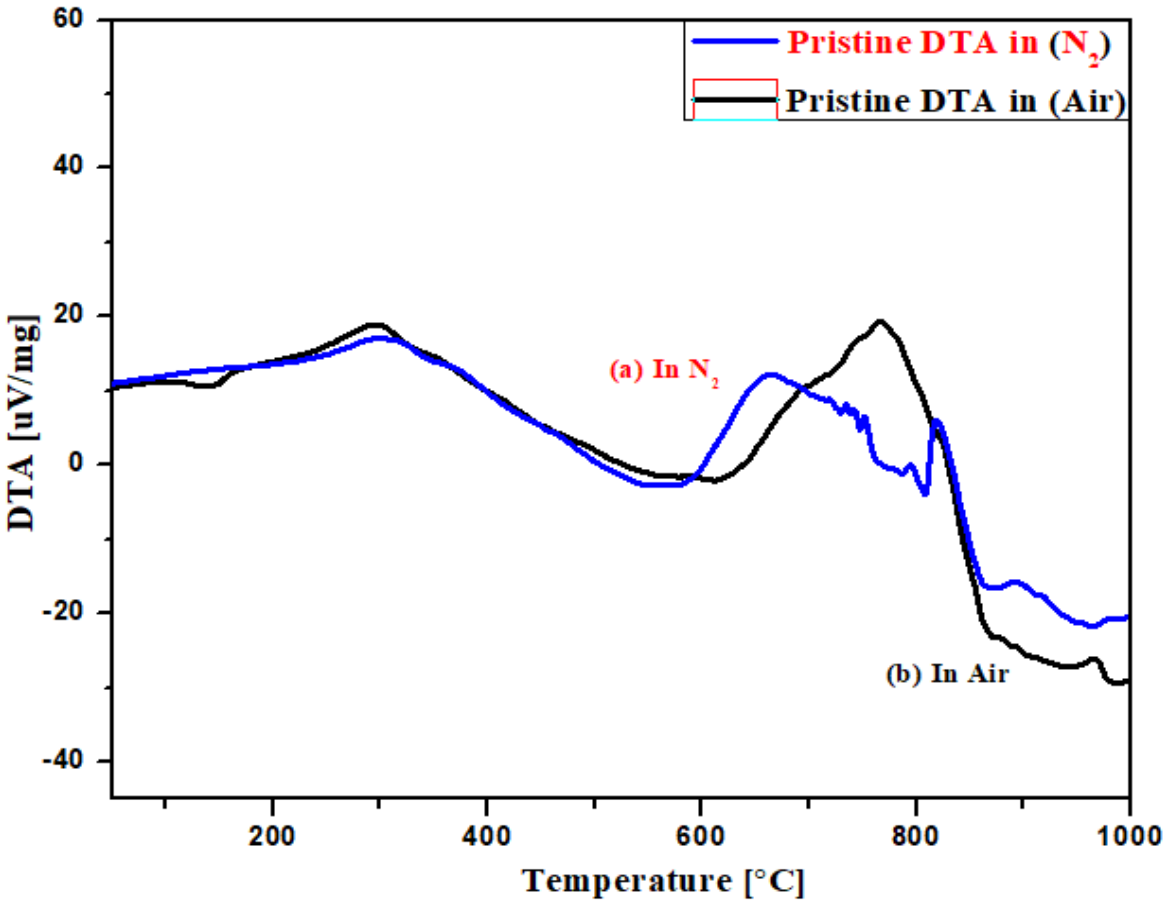

Figure 38 Differential Thermal Analysis (DTA) of Pristine CS in (a) N_2, and (b) Air

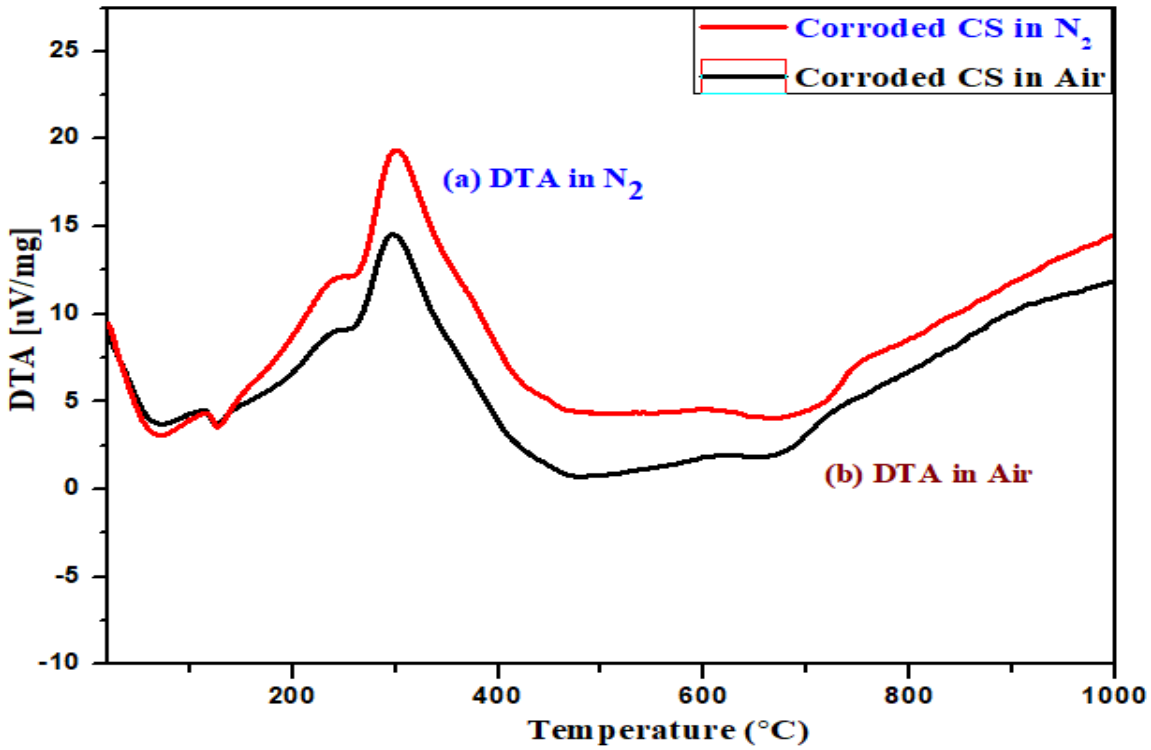

Figure 39 Differential Thermal Analysis (DTA) of Corroded CS in (a) N_2, (b) Air

5.9 Hardness Test Results

Vickers hardness test was conducted on the samples at the bent and straight sections of the boiler tubes using Vickers hardness tester **HVS-50**, which uses a square-based pyramid diamond indenter with an angle of 136˚ between the opposite faces at the vertex, which is pressed into the surface of the workpiece at a test load of 10kgf. The results are shown in **Table 13**. According to B31.1 ASME code [129], the boiler tubes must be heat treated after bending to a holding temperature of 600–650 °C for 15–60 min. In order to verify if the heat treatment prior to service was the adequate, a sample of the boiler tube was heated to 600 °C for 20 min. The hardness measurements after the heat treatment are shown in **Table 13, Figure 40** calculated by dividing the kgf load (P) by the square mm (d) area of indentation.

$$VHN = \frac{2P \times sin\left(\frac{136}{2}\right)}{d^2} \quad \text{----------} \quad (5.7)$$

In general, the hardness of all the samples is > 100 HV/10, which is the maximum value required by the norm for SA210-A1 seamless steel [130]. This situation could have made the material susceptible to cracking. Furthermore, after the heat treatment, the average hardness of the bent sample decreased considerably in comparison with the non-treated sample (see **Table 13**). This

suggests that the boiler tubes were not heat treated properly before the boiler commenced its operation campaign during its commissioning.

Table 13 Hardness of the sample CS SA210-A1 measured according to ASTM E18-15

Sample	**S-1**	**S-2**	**S-3**	**S-4**	**Avg.**
Straight Section	150.5	146.3	150.6	148.4	148.9
Bent Section	151.7	150.5	152.2	151.8	151.6

a) **b)**

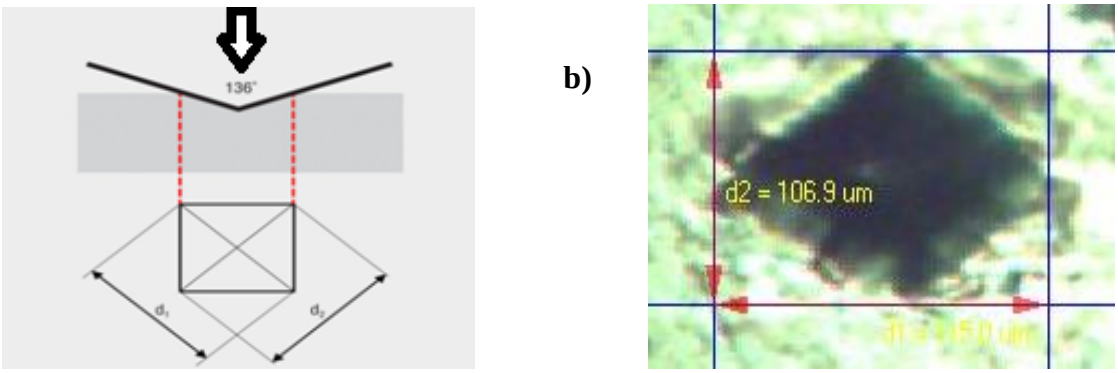

Figure 40 Vickers Hardness Test Measurements, according to ASTM E18-15

5.10 Electrochemical Impedance Tests

5.10.1 Linear Polarization Resistance

The conventional three-electrode electrochemical cell consisting of platinum counter electrode, Ag/AgCl reference electrode and the specimen as working electrode was used. A potentiostat of **Model SP-300** electrochemical interface analyzer equipped with **EC-lab 10.40** was used for potentiostatic polarization. Before the electrochemical measurements, the working electrodes were reduced potentiostatically at -800 mV vs open circuit potential (OCP) for 30 minutes to remove the surface oxide film formed while immersing the specimens into the electrolyte. The time taken for removing the corroded oxide film from the corroded sample is much greater than the time take for the pristine sample to reach the stable region, see **Figure 43**. The stable region of equilibrium is the state where the substrate will neither experience cathodic nor anodic reaction.

Each of the electrochemical experiment started with a freshly polished working electrode. The electrode was first allowed to equilibrate at the OCP conditions for 1 hr. Then, the first LPR was recorded. The evolution of Rp and the OCP measurements with time for the carbon steel SA210-A1 specimens, in the absence and in the presence of 3.5% NaCl and 0.5N H_3PO_4-NaOH as displayed in **Figure 41** is given for pristine and corroded specimens was carried out.

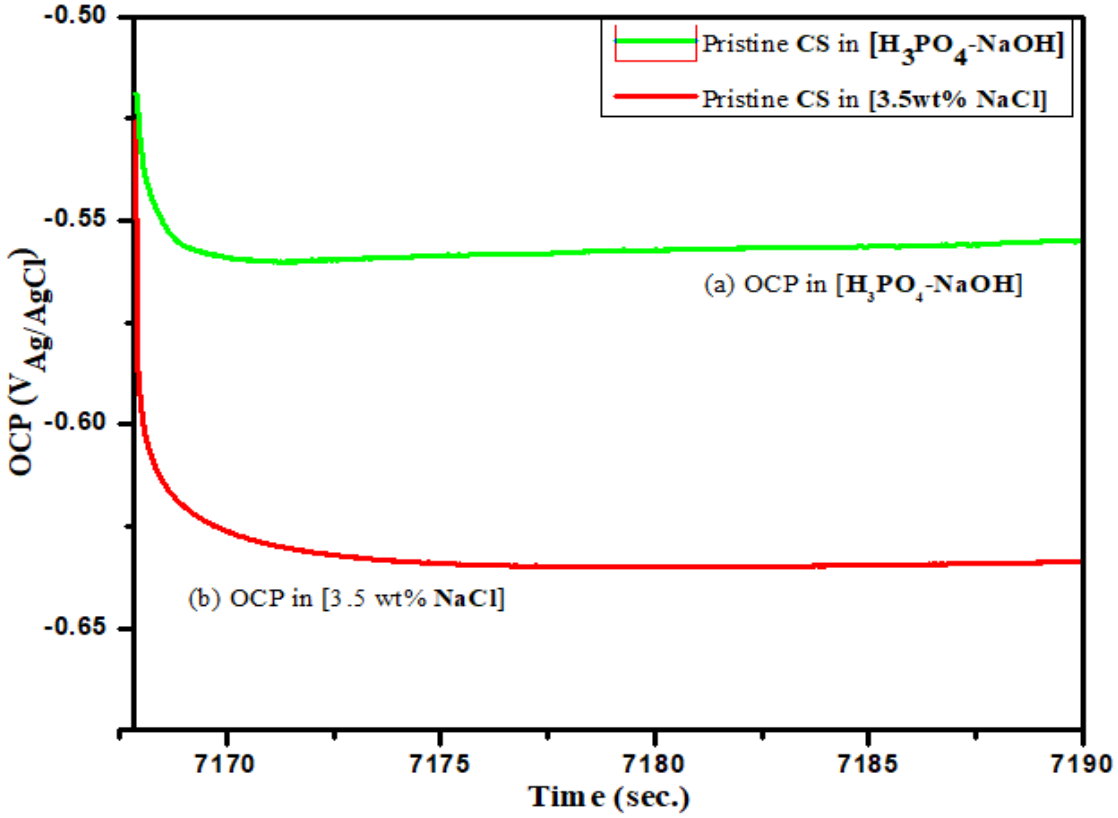

Figure 41 OCP Pristine Carbon Steel SA210-A1 immersed in (a) 0.5N H_3PO_4-NaOH, pH = 11, (b) 3.5 wt% NaCl

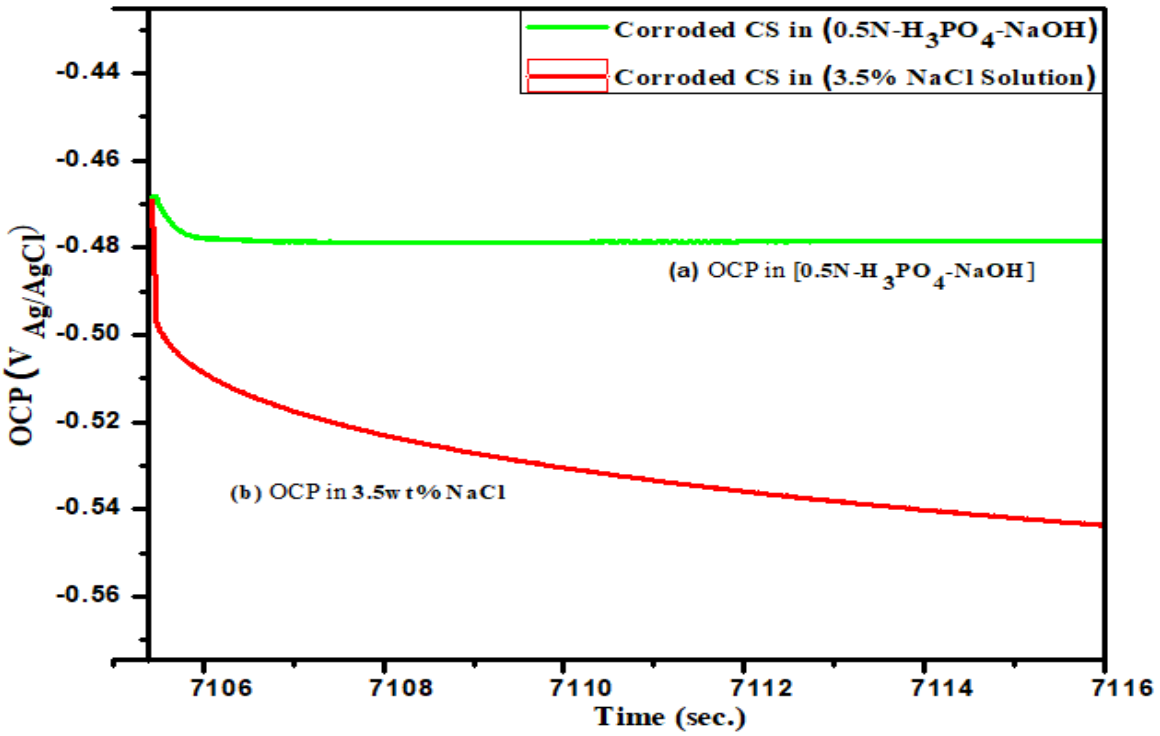

Figure 42 OCP of Corroded CS SA210-A1 immersed in (a) 0.5N H_3PO_4-NaOH, pH = 11, (b) 3.5 wt% NaCl

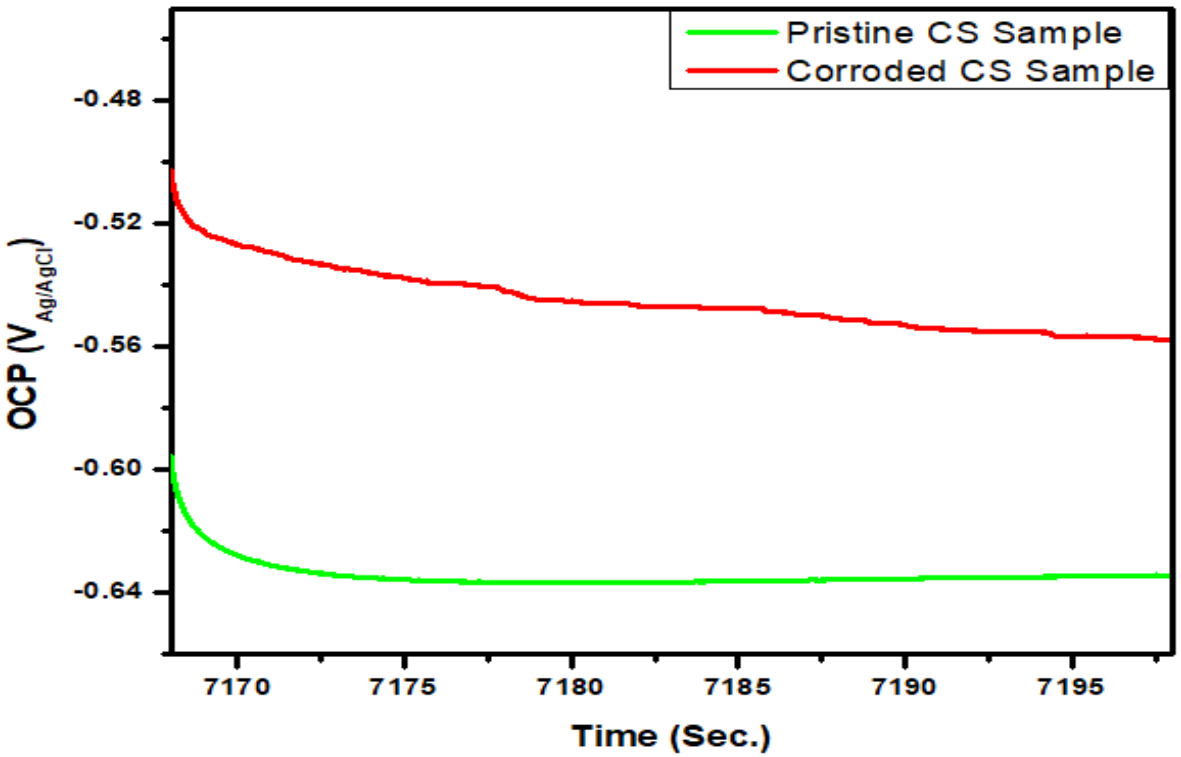

Figure 43 OCP of Pristine and Corroded Carbon Steel in 3.5 wt. % NaCl

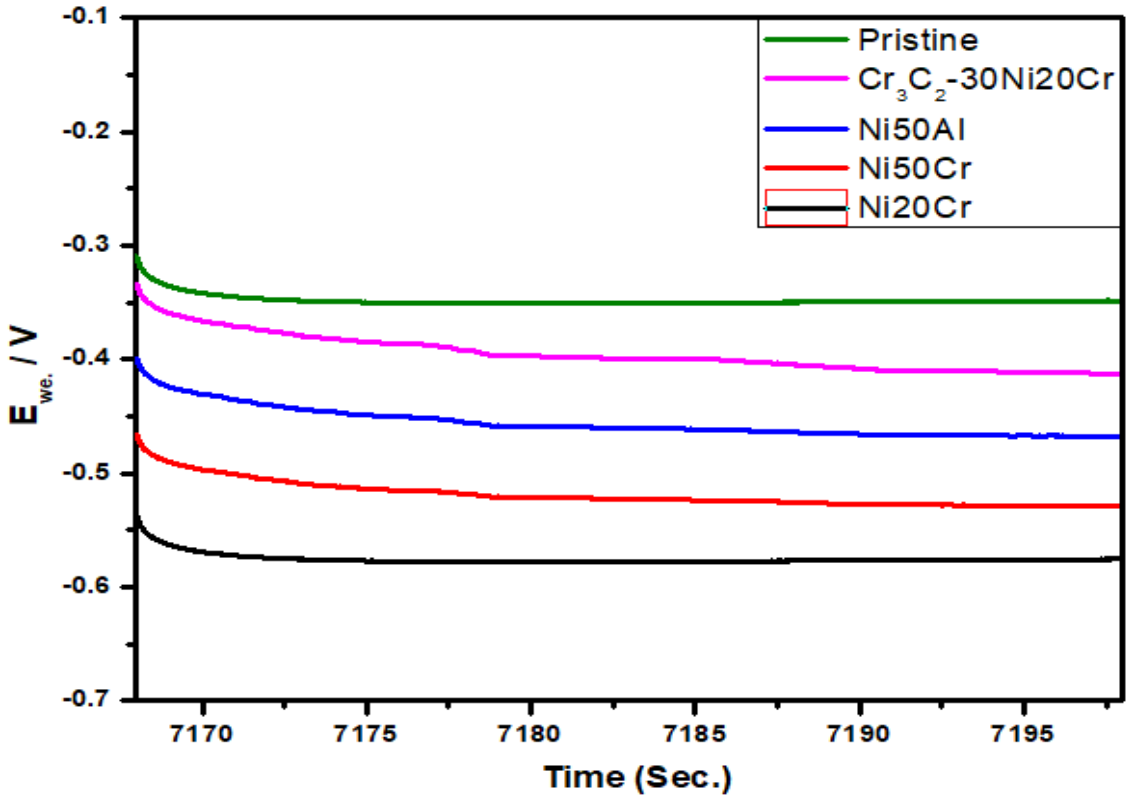

Figure 44 OCP of Pristine and Coated Carbon Steels immersed in 3.5 wt. % NaCl

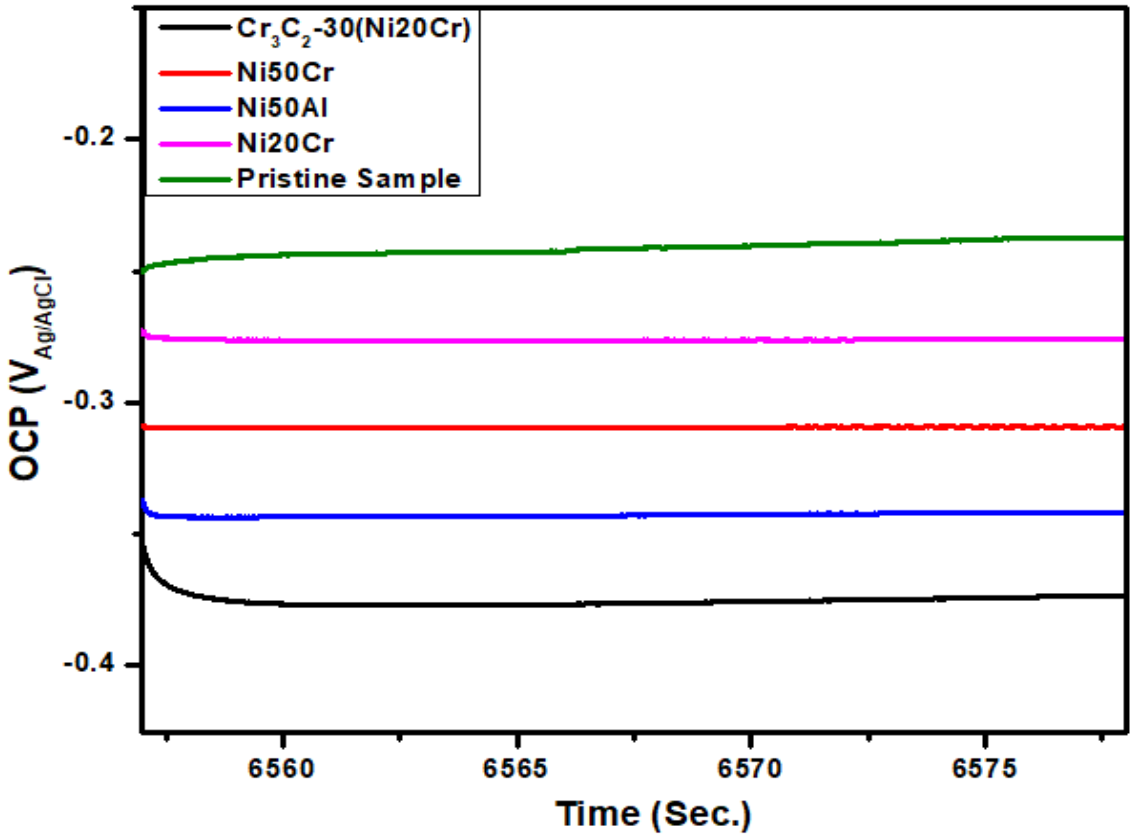

Figure 45 OCP of Pristine and Coated CS immersed in 0.5N H_3PO_4-NaOH, pH = 11

5.10.2 Electrochemical Impedance Measurements

An electrochemical cell can be represented by a purely electronic model since an electrode interface during an electrochemical reaction is analogous to an electronic circuit consisting of resistors and capacitors. This allows, to characterize the electrochemical system in terms of its 'equivalent circuit'. In a system, where carbon steel is used as substrate material passivated by coating alloys the equivalent circuit can be represented as in **Figure 46** where R_p is polarization resistance at electrode/solution interface, R_Ω is the uncompensated resistance between the working and reference electrode, and C_{dl} is double layer capacitance at the electrode/solution interface. R_p and C_{dl} are used to calculate the corrosion rates and inhibitor efficiency.

Electrochemical Impedance Spectroscopy (EIS) methods was conducted to do qualitative comparison between impedances in 3.5 wt. % NaCl solution and 0.5 N H_3PO_4-NaOH solutions. The result obtained from the methods were Nyquist plots of materials in different electrolyte solutions, which showed the impedance measured as comparison to observe corrosion resistance in different condition. Nyquist plot was formed from the impedance of alternating current flowing

back and forth on both samples interface. Greater impedance correlates with less corrosion rate, as current flow decreases with increasing resistance in the system. The graph showed that linear straighter lines correlates with better corrosion resistance, as the lines have greater impedance to corrosion due to lesser tendency of charge transfer.

It is crystal clear that the LPR results were consistent with EIS measurements. Results obtained for the electrochemical impedance analysis coated samples in a 3.5 wt% NaCl and 0.5 N H_3PO_4-NaOH solutions, after 6 h immersion at the corrosion potential (E_{corr}) are presented in Nyquist and Bode plots **Figures (47 - 48)** and **Figures (49 - 50)** respectively. In the absence of inhibitors and at the E_{corr}, the working electrode exhibits single depressed semicircles at high to medium frequencies range. Similar results have been reported in the literature [113].

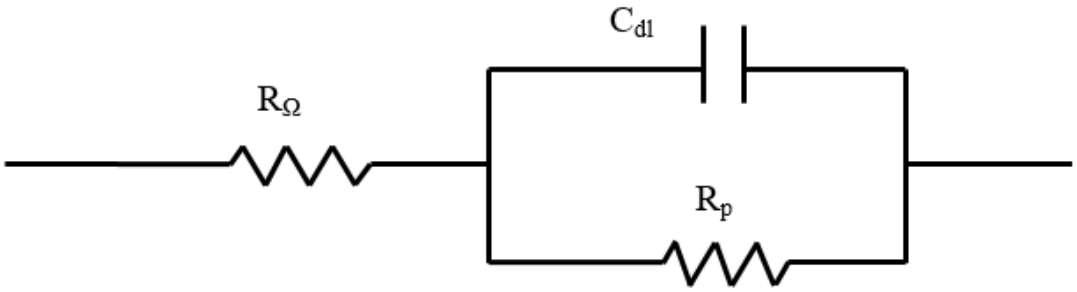

Figure 46 Equivalent Circuit for Corrosion in Inhibited 3.5wt. % NaCl Solution

In conducting the EIS experiment after opening the potentiostat software, we selected "Potentiostatic EIS" test option or equivalent and adjusted the test parameters to meet testing requirements **(Table 14)** for recommended parameters, which are adequate for most measurements. Then, OCP has been monitored to ensure the system is at a steady state, i.e. the OCP is not increasing or decreasing systematically. An acceptable allowance for potential drift is $\pm$ 50 mV per 100 sec, assuming the raw value is between $+500$ and -1500 mV vs SCE.

Table 14 Recommended EIS Parameters and inputs utilized

S/n	EIS Parameters	Input
1	Start Frequency	10^5 KHz
2	End Frequency	10^{-2} Hz
3	Voltage Amplitude	10 mv
4	Points per Decade	6
5	Sample Area	11.2cm^2
6	Total time	4,800 sec
7	Electrolyte solution	3.5wt% NaCl, 0.5N H_3PO_4-NaOH

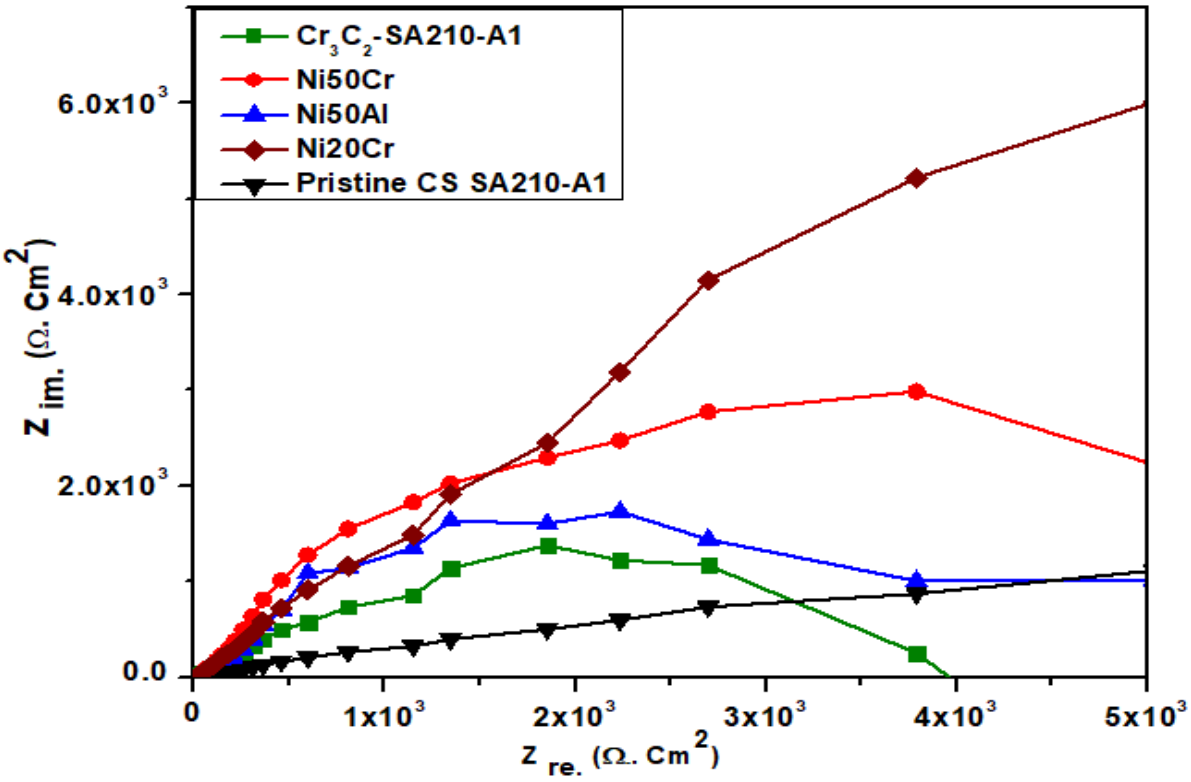

Figure 47 Nyquist Plot of Coated Carbon Steel Immersed in 0.5N H_3PO_4-NaOH

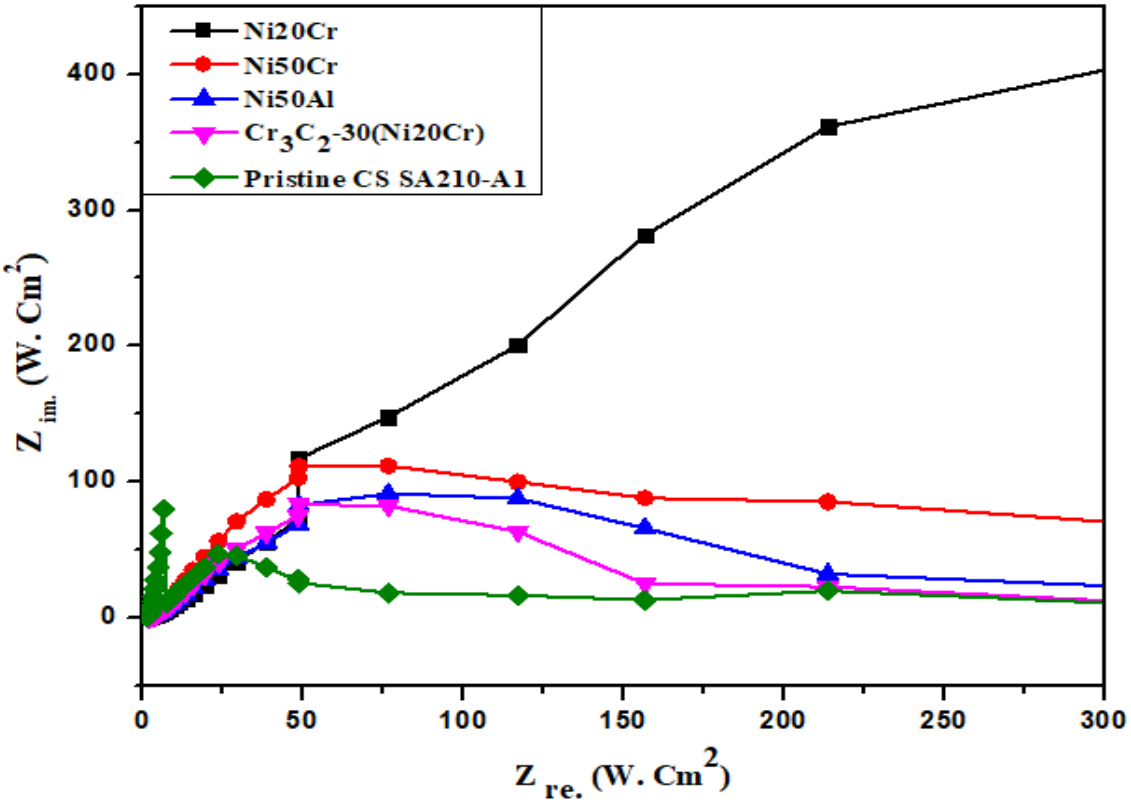

Figure 48 Nyquist Plot of Coated Carbon Steels Immersed in 3.5%wt NaCl Solution

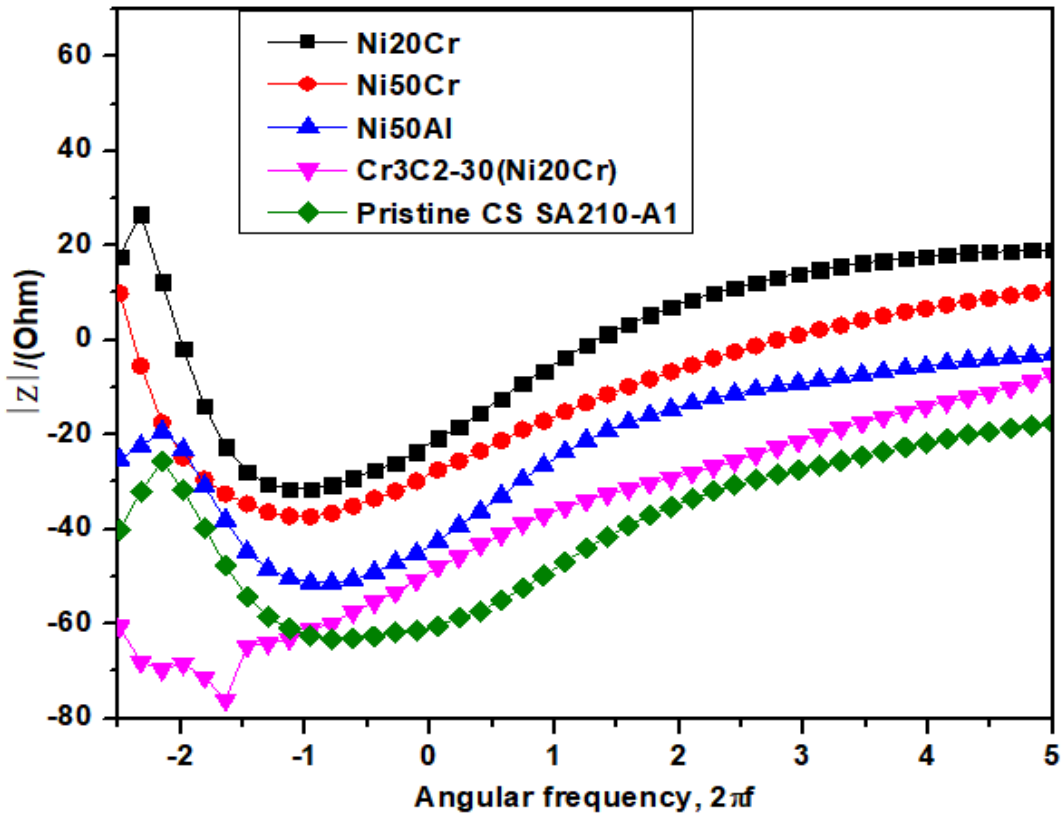

Figure 49 Bode plot of Pristine and Coated Carbon Steels in 3.5wt% NaCl solution

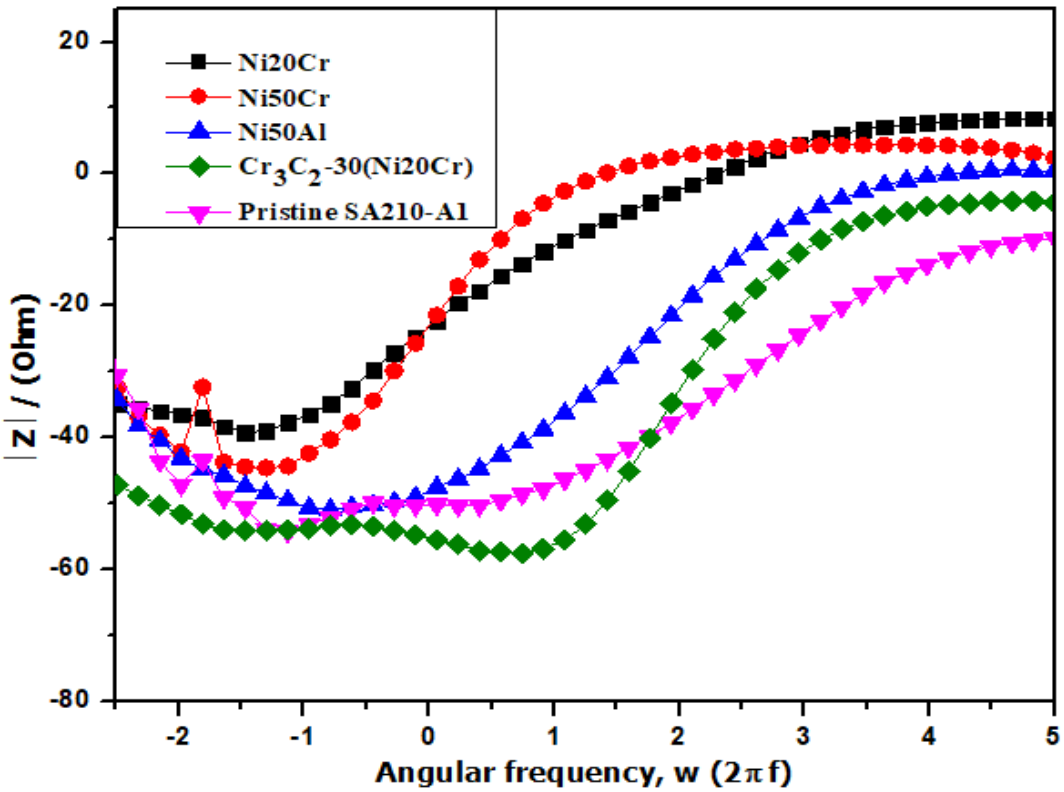

Figure 50 Bode Plot of Pristine and Coated CS immersed in 0.5N H_3PO_4-NaOH Solution

5.10.3 Corrosion Fits and Simulation

It was clear that, the presence of the coatings causes a markedly decrease in the corrosion rate, i.e. shifts the anodic curves to more positive potentials and the cathodic curves to more negative potentials. This may be ascribed to adsorption of the coatings over the corroded surface. Electrochemical corrosion kinetic parameters, such as corrosion potential (E_{corr}), cathodic (β_c) and anodic (β_a) Tafel slopes, corrosion current density (I_{corr}), coverage surfaces (θ) and the inhibition efficiency (*IE*) were obtained from the Tafel extrapolation (**Figure 51**) of the polarization curve where the Tafel plot for the pristine sample is sketched alone because it is out of the range of the coated samples. This parameters were summarized in **Table 15**.

Besides the qualitative method conducted in this experiment, quantitative data was also provided by doing fit and simulation on provided Nyquist graphs. Fit and simulation is a process that shows electrochemical equivalent circuit presenting the surface condition of the samples. Some of the elements that could be presented are the solution resistance (R_s), polarization resistance (R_p), double layer capacitance (CPE/C_{dl}), and constant phase element (Q). The difference between R_p and R_s is that the value of R_s is influenced by the condition of environment and material positioning, thus, the value of R_s does not represent the corrosion resistance of the sample. Thus, R_p should be considered as the corrosion resistance of the sample.

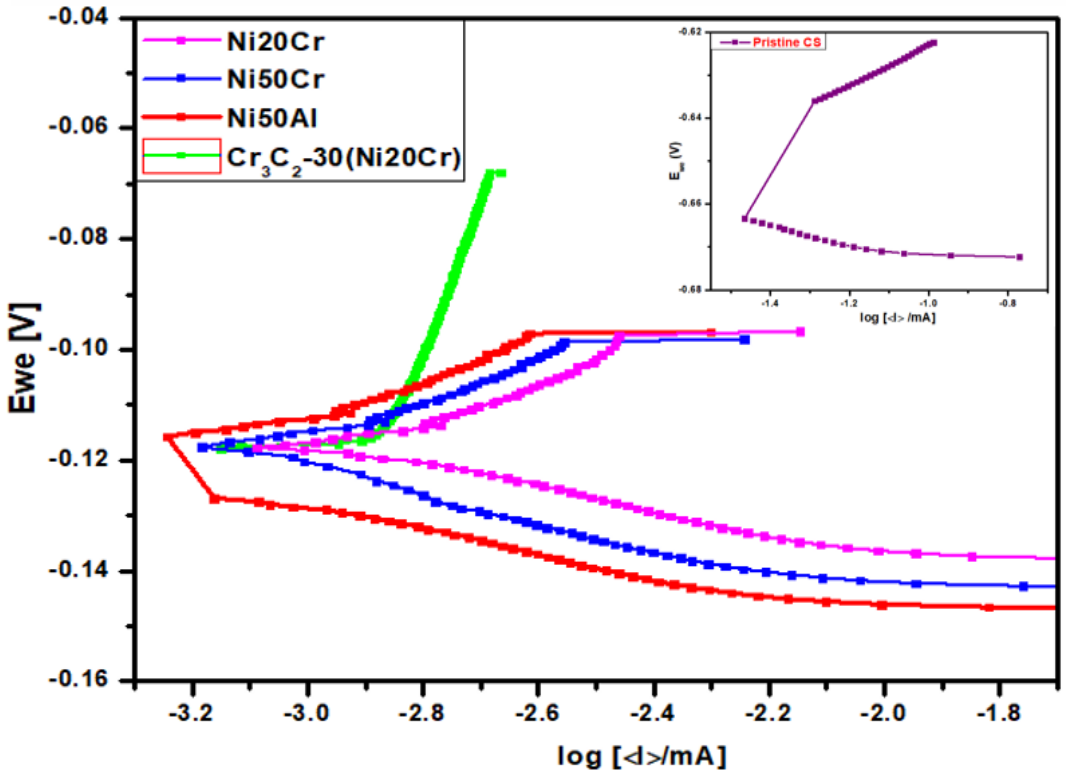

Figure 51 Tafel Plot of Pristine and Coated CS SA210-A1 in 3.5 wt% NaCl solution

Table 15 Potentiodynamic polarization measurements of CS immersed in 3.5 wt% NaCl solution in the absence and presence of coatings (25˚C, ρ = 7.87 g/cm^3 & EW = 27.925).

Coatings	**-E_{corr} [mV]**	**$I_{corr.}$ [µA]**	**R_p [23]**	**β_a [mV]**	**β_c [mV]**	***CR* *[mpy]***
Ni20Cr	-485.59	21.42	339.00	0.018	0.230	9.8790
Ni50Cr	-494.27	27.68	149.00	0.010	0.201	12.767
Ni50Al	-500.12	38.51	117.67	0.011	0.212	17.762
Cr_3C_2-30[Ni20Cr]	-516.21	41.74	106.03	0.010	0.200	19.252
Uncoated	-542.05	46.31	85.71	0.010	0.120	21.360

From the table, the corrosion rate (CR) values indicate that the inhibitive properties of the studied coatings can be given by the descending order (Ni20Cr > Ni50Cr > Ni50Al > Cr_3C_2-30[Ni20Cr]) which conforms to the results obtained from the weight loss method which complies with study results obtained from previous coating research results [52].

6. Conclusions

This research has detailed the high temperature corrosion resistance of the powder flame oxy-acetylene sprayed Ni-based coatings in simulated bagasse fired power-plant conditions. The coating technique and materials utilized can be recommended for corrosion protection and, hence, for increasing the lifetime/service-life of carbon steel tube substrates in bagasse-fired water-tube boilers. Out of all the significant outcomes of the research, some of the major ones are stated:

- Ni-based alloys particularly Ni20Cr, Ni50Cr, Ni50Al, and Cr_3C_2-30(Ni20Cr) coatings have been found to be effective for corrosion protection of carbon steel boiler tubes.
- Oxy-acetylene cutting torch has been utilized for the powder-flame thermal spray coating of Ni-based alloys with little modification at the tip of the torch.
- The oxidation behaviour was strongly dependent on the amount of passive-forming elements such as Cr or/and Al in the coating, which can develop a protective alumina or chromia scale at the test temperature of (600˚C).
- A significant percentage drop in the corrosion rate of 11.48% was attained with coating alloy performed by Ni20Cr.
- In ambient air environment, the corrosion resistance of the coatings based on weight loss and EIS studies showed the following ranking in their performance (in the descending order): (Ni20Cr > Ni50Cr > Ni50Al > Cr_3C_2-30[Ni20Cr]).
- The corrosion rate of coated substrate material obtained from the weight loss method is consistent and correlated with the corrosion rate values obtained from the electrochemical impedance spectroscopy results.

Therefore, modified oxy-acetylene cutting torch can be utilized for effective powder flame spray coating of Ni-based alloys of boiler water-wall tubes for enhancing corrosion prevention capacity. Not only water-wall tubes, but other boiler tubes like economizers, superheaters, and bank tubes can also be coated with this method to prevent the impact of corrosion upon the tubes and the longevity of the boiler service life. Furthermore, powder-flame thermal spraying can also be used for wear and tear applications in machineries where rotating components are involved.

7. Recommendations

This particular research is specifically targeted to devise, fabricate, and test a powder flame thermal spray method utilizing oxy-acetylene cutting torch for coating Ni-based alloys on carbon steel substrate of boiler tube material for reducing the effect of corrosion. Much work remains to be performed both on optimizing the spraying method for increasing the bond strength, reducing porosity, and improving particle speed and on getting better coating materials so that the performance of coating alloys on the tube material can yield optimal result and duration.

i. The Spraying Technology Utilized:

The spraying technology utilized in the present study was oxy-acetylene torch that is modified at the tip for the supply of the coating powder alloys for the prevention of corrosion. Advanced coating guns like plasma spray coating, high velocity oxy-fuel coatings could be used.

ii. Effect of post treatment on corrosion behavior:

Post-spray treatments are recommended to be investigated for different purposes. For instance, mechanical treatment like shot peening can be used for splat-size control in order to unify the diffusion of protective elements the surface. Heat treatment can be implemented in order to pre-oxidize the coating to ensure formation of a highly protective Cr_2O_3 on the surface.

iii. Advanced characterization techniques:

State-of-the-art characterization techniques such as X-ray photoelectron spectroscopy (XPS) and facilities such as Broad Ion Beam (BIB) milling could be implemented. The advanced characterization techniques will help to better understand the formation of different complex corrosion products during corrosion processes and the interaction between chlorine and the various alloying elements and how this affects the scale growth. In the thermal spray coatings, the influence of passivation elements such as Cr can be studied by XPS as this technique is a highly surface sensitive research tool in corrosion science.

References

1. Guo, R.Q.Z., C.; Yang, Y.; Peng, Y.; Liu, L. , *Corrosion and wear resistance of a Fe-based amorphous coating in underground environment.* . Intermetallics 2012. **30**: p. 94-99.
2. Liu, X.Q.Z., Y.G.; Chang, X.C.; Hou, W.L.; Wang, J.Q.; Tang, Z.; Burgess, A. , *Microstructure and properties of Fe-based amorphous metallic coating produced by high velocity axial plasma spraying.* Journal of Alloys Compound. , 2009. **484**: p. 300 - 307.
3. Lu, W.W., Y.; Zhang, J.; Hong, S.; Zhang, J.; Li, G. , *Microstructure and Corrosion Resistance of Plasma Sprayed Fe-Based Alloy Coating as an Alternative to Hard Chromium.* . Journal of Thermal Spray Technology, 2010. **20**: p. 1063-1070.
4. Tillman, D.A., *Biomass cofiring: The technology, the experience, the combustion consequences.* Biomass Bioenergy, 2000. **19**(6): p. 365-384.
5. H. P. Nielsen, F.J.F., K. Dam-Johansen, and L. L. Baxter, *Implications of chlorine-associated corrosion on the operation of biomass-fired boilers.* 2000. **26**(3): p. 283-298.
6. D. Fähsing, M.R., L. Konrad, and M. C. Galetz, *Fireside Corrosion of Chromium- and Aluminum-Coated Ferritic–Martensitic Steels.* Oxid. Met., 2017. **88**(1-2): p. 155-164.
7. Crook, P., *Corrosion resistance Nickel alloys.* Advanced materials and processes, 2007.
8. D. Leclerc, W.L.D., and M. Vessey, *Effects of combustion and operating conditions on PCDD/PCDF emissions from power boilers burning salt-laden wood waste.* 2006. **63**(4): p. 676-689.
9. Hasan, M., *High Velocity Oxy-Fuel (HVOF) Thermal Spray Deposition of Functionally Graded Coatings.* PhD Dissertation, 2005: p. 1-2.
10. Couch, K.W., et al., *Studies of the Flame Spraying of Polymers.* Proceedings of the 9th National Thermal Spray Conference, Ohio, USA, 1996: p. 251-255.
11. Nakano, A., et al., *Production o f Heat and Corrosion-Resistant Plastic Coatings.* Proceedings o f the 9th National Thermal Spray Conference, Ohio, USA, 1996: p. 257-262.
12. D. Fantozzi, V.M., M. Uusitalo, H. Koivuluoto, and P. Vuoristo, *Chlorine-induced high temperature corrosion of Inconel 625 sprayed coatings deposited with different thermal spray techniques.* Surf. Coat. Technol., 2017. **318**: p. 233-243.
13. M. Oksa, P.A., J. Salonen, and T. Varis, *Nickel-based HVOF coatings promoting high temperature corrosion resistance of biomass-fired power plant boilers.* Fuel Process. Technol., 2014. **125**: p. 236-245.

14. E. Sadeghimeresht, N.M., M. Huhtakangas, and S. Joshi, *Isothermal oxidation of HVAF-sprayed Ni-based chromia, alumina and mixed-oxide scale forming coatings in ambient air.* Surf. Coat. Technol., 2017. **316**: p. 10-21.
15. E. Sadeghimeresht, N.M., and S. Joshi, *Isothermal oxidation behavior of HVAF-sprayed Ni and NiCr coatings in H2-H2O environment.* Surf. Coat. Technol., 2017. **317**: p. 17-25.
16. K. A. Habib, M.S.D., J. J. Carpio, I. Cervera, and J. J. Saura, *Performance of NiCrAlY Coatings Deposited by Oxyfuel Thermal Spraying in High Temperature Chlorine Environment.* J. Mater. Eng. Perform., 2014. **23**(10): p. 3511-3522.
17. B. Song, Z.P., K. T. Voisey, and T. Hussain,, *Gas and liquid-fuelled HVOF spraying of Ni50Cr coating: Microstructure and high temperature oxidation.* 2017. **318**: p. 224-232.
18. Metco, S., *An Introduction to Thermal Spray*. 2013(4).
19. Mareceau, J.A., & Adjorlolo, A. A., *Commercial Aircraft" in ASTM, Corrosion Tests and Standards: Application and Interpretation.* American Society for Testing and Materials Society, , 1995: p. 574-578.
20. Seki, M., et al., *Application of Thermal Spray Coatings to Prevent Corrosion of Construction in Japan.* Proceedings of the 5th National Thermal Spray Conference, California, USA, 1993: p. 679-684.
21. Zhao, L., et al., *Influence of the Spraying Processes on the Properties of 316L Stainless Steel Coatings.* Surface and Coatings Technology, 2002. **162**: p. 6-10.
22. Nakagawa, P.M., et al., *Trends in Automotive Applications of Thermal Spray Technology in Japan.* Proceedings of the 7th National Thermal Spray Conference, Boston, USA., 1994: p. 1-6.
23. Ohmori, A., *Thermal Spraying: Current Status and Future Trends.* Proceedings of the 14th International Thermal Spray Conference; Kobe, Japan,, 1995: p. 1241-3047.
24. Emilio Cano, D.L.a.D.M.B., *Use of EIS for the evaluation of the protective properties of coatings for metallic cultural heritage: a review.* 2010. **14**: p. 381-391.
25. Dehghanghadikolaei, A.M., B.; Namdari, N.; Fotovvati, B. , *Abrasive Machining Techniques for Biomedical Device Applications.* Journal of Material Science, 2018. **5**: p. 1-11.
26. Hailing, J., *Recent Developments in Surface Coating and Modification Processes.* 1985.
27. Chapman, B.N., & Anderson, T. C., *Science and Technology of Surface Coating" , Academic Press, UK.* 1974.

28. Behzad Fotovvati, N.N., and Amir Dehghanghadikolaei, *On Coating Techniques for Surface Protection: A Review.* Journal of Manufacturing and Materials Processing, 2019.
29. Hillery, R.V., *Coatings for High-Temperature Structural Materials, Trends and Opportunities.* National Academy Press, Washington, 1996.
30. Holmberg, K., & Matthews, A., *Coatings Tribology: Properties, Techniques and Applications in Surface Engineering.* 1994.
31. A.M. Beltran, D.A.S., *Study of oxidation and hot corrosion of nickel-base superalloys.* 1980. **24**: p. 4289-4296.
32. Anees U. Malik, S.A.A.-F., M. Mobin and Mohammad Al-Hajri and *Studies on the Failure of Economizer Tubes Involving Acid Dew-Point Corrosion in High Pressure Boilers* International Journal of Scientific & Engineering Research,, September-2013. **4**(9).
33. METCO, S., *Product Information.* www.sulzermetco.com, 2001.
34. Heimann, R.B., *Plasma-Spray Coating, Principles and Applications.* VCH Publishers, New York, USA, 1996.
35. Bhatia, A., *Thermal Spraying Technology and Applications.* Engineer Manual, Continuing Education and Development, Inc., 1999.
36. Dorfman, M.R., *Advanced Materials Processing.* 2000. **160**: p. 66-68.
37. H. Herman, S.S., R. McCune, *MRS Bull.* 2000. **25**: p. 17-25.
38. Onlene Sulzer METCO documen, *www.sulzermetco.com/tech/pr-ts.html*.
39. Document, O.E.W.C., *http://www.ewi.org/technologies/ arcwelding/thermalspray.asp.*
40. Stokes, J., *The Theory and Application o f the HVOF Thermal Spray Process, School o f Mechanical and Manufacturing Engineering.* 2003.
41. Bhatia, A., *Fundamentals of Gas Cutting and Welding.* 2005.
42. L. Schultz, K.S., J. Wecker, M. Katter, and C. Kuhrt, J, *Applied Physics.* 1991. **70**: p. 6339.
43. M. Kumar, H.S., N. Singh, Joshi,, *Erosion-corosion behaviou of cold-spray nanostructure Ni-20Cr coatings in actual boiler environment.* Wear, 2015: p. 1035-1043.
44. Motoki A, Y.M., *Japan Society of Corrosion Engineering.* 1990. **39**(192).
45. P. Goel, R.K., L.K Singhal, and R.K. Goyal,, *Role of stainless steel to combat corrosion in the Indian sugar industry.* 2007. **38**(12): p. 39-46.
46. S. Karlsson, L.-E.Å., and J. Liske,, *'Reducing high-temperature corrosion on high-alloyed stainless steel superheaters by co-combustion of municipal sewage sludge in a fluidised bed boiler'.* 2015. **139**: p. 482-493.

47. Key, J.F., et al., *Use of De Laval Nozzles in Spray Forming.* 1993: p. 75-80.
48. Thorpe, R.J., & Thorpe, M . L., *High Pressure HVOF: An Update.* 1993: p. 199-204.
49. Kowalsky, K.A., et al., *HVOF: Particles, Flame Diagnostics and Coating Characteristics.* 1990: p. 587-596.
50. Thorpe, M.L., & Richter, H. J., *A Pragmatic Analysis and Comparison of HVOF Processes.* 1992: p. 137-147.
51. Stokes, J., & Looney, L., *Properties of WC-Co Components Produced using the HVOF Thermal Spray Process.* 2000: p. 263-270.
52. Jaswinder Singh, H.V., Sharanjit Singh, *Performance of different coating materials against high temperature oxidation in boiler tubes – A review*. Materials Today, 2020.
53. Online EWI W eldnet Company Document, 2004.
54. Learning Resource, E., *Basic Gas Welding and Cutting, Metals and Engineering.* 2016.
55. C. Monticelli, A.F., and F. Zucchi, , *Investigation on the corrosion process of carbon steel coated by HVOF WC/Co cermets in neutral solution.* 2004. **46**(5): p. 1225-1237.
56. Glancy, S.D., *Preserving the Microstructure of Thermal Spray Coatings.* Journal of Advanced Materials and Processes, 1995. **148**(1): p. 37-40.
57. Yamada K, O.M., Ohtuka T, Koyama M, *High Temperature Society of Japan, Proceedings of the Third Thermal Spray Division.* 1994: p. 6-7.
58. Wilcox, B.a., *Boiler tube Analysis, Babcock and Wilcox Power Generation Group.* 2005.
59. Cail, F., *Operation and Maintenance Manual for 110TPH Bagasse Fired Boiler.* 2015.
60. L. L. Baxter et al., *'The behavior of inorganic material in biomass-fired power boilers: Field and laboratory experiences'.* 1998. **54**(1-3): p. 47-78.
61. P. Henderson, P.S., R. Pettersson, C. Andersson, and J. Högberg,, *'Reducing superheater corrosion in wood-fired boilers'.* 2006. **57**(2): p. 128-134.
62. J.O. Bello, R.J.K.W., and J.A. Wharton,, *Synergistic effects of micro-abrasion–corrosion of UNS S30403, S31603 and S32760 stainless steels.* 2007. **263**(1-6): p. 1-866.
63. L. Tengur, a.B.Y.R.S., *Corrosion Problems in Sugar Factories in Mauritius.* Journal Mechanical and Aerospace Engineering, 1984.
64. M. Campo et al., *Corrosion resistance of thermally sprayed Al and Al/SiC coatings on Mg'.* 2009. **203**(20-21): p. 3224-3230.
65. Pawlowski, L., *The Science and Engineering of Thermal Spray Coatings, Wiley and Sons, UK.* 1995.

66. P. Marcus, P., *Corrosion mechanisms in theory and practice.* 2002: p. 680-718.
67. Perrigo, D.L., *Evaluating corrosion resulting from repeated chemical cleaning. MCB UP Ltd.* 1964. **11**(12): p. 21-25.
68. I. Obernberger, T.B., and G. Bärnthaler, , *Chemical properties of solid biofuels-significance and impact.* 2006. **30**(11): p. 973-982.
69. A. Miltner, G.B., and A. Friedl,, *Preventing the chlorine-induced high temperature corrosion in power boilers without loss of electrical efficiency in steam cycles.* 2006. **26**(16): p. 2005-2011.
70. A. Zahs, M.S., and H. J. Grabke, *Chloridation and oxidation of iron, chromium, nickel and their alloys in chloridizing and oxidizing atmospheres at 400-700°C.* 2000. **42**(6): p. 1093-1122.
71. T. Sharobem and M. J. Castaldi, *The effect of SO_2/HCl ratio on superheater high temperature corrosion.* 2012: p. 23-27.
72. J. Kalivodova, D.B., M. Schütze, and V. Rohr,, *Gaseous corrosion of alloys and novel coatings in simulated environments for coal, waste and biomass boilers.* 2005. **56**(12): p. 882-889.
73. M. Spiegel, A.Z., and H. J. Grabke, *Fundamental aspects of chlorine induced corrosion in power plants.* 2003. **20**(2): p. 153-159.
74. Y. Y. Lee and M. J. McNallan, *Ignition of nickel in environments containing oxygen and chlorine.* 1987. **18A**(6): p. 1099-1107.
75. S.C. Srivastava, K.M.G., M.K. Banerjee, *HVOF thermal spray coating on boiler tubes.* Surface and coatings technology, 2010.
76. Zhang, H., et al., *Enhanced adsorption of molecules on surfaces of nanocrystalline particles.* 1999. **103**(22): p. 4656-4662.
77. M. Spiegel, *Reactions between gas phase, deposits and metallic materials in chlorine containing atmospheres.* 1997. **14**(3): p. 221-226.
78. Berge, M.J.P., *Stress and Strain Caused by Chemical Attack, Corrosion of Steels and Stainless Steels in Water Vapor at an Elevated Temperature (Surface Treatment).* 1988.
79. A. J. López, M.P., V. Utrilla, E. Otero, and J. Rams,, *High-temperature corrosion behavior of Ni–50Cr coating deposited by high velocity oxygen–fuel technique on low alloy ferritic steel.* 2014. **59**: p. 94-102.

80. M. Kumar, H.S., and N. Singh, *Study of Ni-20Cr Coatings for High Temperature Applications – A Review.* 2013. **58**(2): p. 523-528.
81. Arden, T.V., Journal of Chemical Society, 1950. **882**.
82. Imkolthoff, D.L.L., Journal American Chemical Society, 1953. **75**(24-76).
83. H. Hooshyar, T.J., J. Hall, J.-E. Svensson, L. G. Johansson, and J. Liske, *The Effect of H_2 and H_2O on the Oxidation of 304L-Stainless Steel at 600 °C: General Behaviour (Part I).* 2015: p. 1-22.
84. P. L. Fauchais, J.V.R.H., and M. I. Boulos,, *Industrial Applications of Thermal Spraying Technology.* 2014: p. 1401-1566.
85. V. A. D. Souza and A. Neville, *Linking electrochemical corrosion behaviour and corrosion mechanisms of thermal spray cermet coatings (WC–CrNi and WC/CrC–CoCr).* 2003. **352**(1-2): p. 202-211.
86. J. Saaedi, T.W.C., H. Arabi, S. Mirdamadi, and J. Mostaghimi, *Effects of HVOF process parameters on the properties of Ni-Cr coatings.* 2010. **19**(3): p. 521-530.
87. M. Rodriguez, M.S., L. Gil, F. Arenas, and A. Scagni,, *Effect of heat treatment on properties of nickel hard surface alloy deposited by HVOF*. 2000. **16**(5): p. 415–420.
88. T. S. Sidhu, S.P., and R. D. Agrawal,, *Studies on the properties of high-velocity oxy-fuel thermal spray coatings for higher temperature applications.* 2005. **41**(6): p. 805-823.
89. K. A. Unocic et al., *High-temperature behavior of oxide dispersion strengthening CoNiCrAlY*. 2017. **35**(3): p. 108-119.
90. Oksa, M.T., E.; Suhonen, T.; Varis, T.; Hannula, S. P., *Optimization and Characterization of High Velocity Oxy-fuel Sprayed Coatings: Techniques, Materials, and Applications.* 2011. **1**: p. 17-52.
91. M. A. Uusitalo, P.M.J.V., and T. A. Mäntylä,, *High temperature corrosion of coatings and boiler steels in reducing chlorine-containing atmosphere'.* 2002. **161**(2-3): p. 275-285.
92. T. Hussain, T.D., N. J. Simms, and J. R. Nicholls,, *Fireside corrosion behavior of HVOF and plasma-sprayed coatings in advanced coal/biomass co-fired power plants.* 2013. **22**(5): p. 797-807.
93. R. Viswanathan, D.G., K. Coleman, *Advances in materials technology for fossil power plants.* 2008: p. 1-15.
94. Sridhar, D.C.A.a.N., *Nickel and nickel-base alloys for corrosion applications.* 2011.
95. George E. Totten, L.i., Kiyoshii Funatani, *Handbook of Mechanical Alloy Design.* 2004.

96. Davis, J.R., *Heat-Resistant Materials, ASM Specialty Handbook,* . 1997: p. 3-30.
97. A. Zahs, M.S., and H. Grabke, *The influence of alloying elements on the chlorine-induced high temperature corrosion of Fe-Cr alloys in oxidizing atmospheres.* 1999. **50**(10): p. 561-578.
98. Sadeghimeresht, E., *Ni-Based Coatings for High Temperature Corrosion Protection.* Production Technology, 2018.
99. Israelsson, N., *High Temperature Oxidation and Chlorination of FeCrAl alloys.* 2014.
100. Pawel Jozwik, W.P., and Zbigniew Bojar, *Applications of Ni_3Al Based Intermetallic Alloys-Current Stage and Potential Perceptives* 2001.
101. Liu C.T., S.V.K., *Nickel Aluminides for Structural Use.* Journal of Metallurgy, 1986. **38**: p. 19-21.
102. Plucknett, K., *Cermets and Hardmetals.* 2018.
103. Dominique Poirier, J.-G.L., and Rogerio S. Lima, *Engineering HVOF-Sprayed Cr_3C_2-NiCr Coatings: The Effect of Particle Morphology and Spraying Parameters on the Microstructure, Properties, and High Temperature Wear Performance.* Journal of Thermal Spray Technology, 2013. **22**(280): p. 2-3.
104. Davis, J.R., *Handbook of Thermal Spray Technology, ASM International,.* 2004.
105. Nurbas, E.N.A.D.a.M., *Corrosion Behavior of Different Thermal Spray Coatings and Hard Chromium Electroplating on A286Super Alloy.* 2010. **154-155**: p. 226-229.
106. C. Xu, L.D., B. Yang, and W. Zhang, *Study on salt spray corrosion of Ni–graphite abradable coating with 80Ni20Al and 96NiCr–4Al as bonding layers.* May 2011. **205**(17-18): p. 4154-4161.
107. Z. Zhou, L.W., F. Wang, and Y. Liu, *Formation and corrosion behavior of Fe-based amorphous metallic coatings prepared by detonation gun spraying.* Dec. 2009. **19**(3): p. 634-638.
108. Y. Tao et al., *Microstructure and corrosion performance of a cold sprayed aluminium coating on AZ91D magnesium alloy.* 2010. **52**(10): p. 3191-3197.
109. Talbert, R., *Porosity Causes on Powder-Coated Surfaces.* 2014.
110. Sadeghimeresht, E., *Ni-Based Coatings for High Temperature Corrosion Protection.* 2018(23).

111. A. Milanti, V.M., H. Koivuluoto, G. Bolelli, L. Lusvarghi, and P. Vuoristo, , *Effect of spraying parameters on the microstructural and corrosion properties of HVAF-sprayed Fe–Cr–Ni–B–C coatings.* 2015. **277**: p. 81-90.
112. D. Zhang, S.J.H., and D. G. McCartney, *Microstructure formation and corrosion behaviour in HVOF-sprayed Inconel 625 coatings,.* 2003. **344**(1-2): p. 45-56.
113. G. Bolelli, L.L., and R. Giovanardi,, *A comparison between the corrosion resistances of some HVOF-sprayed metal alloy coatings.* 2008. **2002**: p. 4793-4809.
114. J. M. Guilemany, J.F., J. Delgado, A. V. Benedetti, and F. Climent,, *Effects of thickness coating on the electrochemical behaviour of thermal spray Cr_3C_2–NiCr coatings.* 2002. **153**(2-3): p. 107-113.
115. S. D. Zhang, J.W., W. B. Qi, and J. Q. Wang,, *Effect of porosity defects on the long-term corrosion behaviour of Fe-based amorphous alloy coated mild steel.* 2016. **110**: p. 57-70.
116. R. Arrabal, A.P., M. C. Merino, M. Mohedano, P. Casajús, and S. Merino, , *Al/SiC thermal spray coatings for corrosion protection of Mg–Al alloys in humid and saline environments,.* 2010. **204**: p. 2767-2774.
117. N. Espallargas, J.B., J. M. Guilemany, A. V. Benedetti, and P. H. Suegama, , *Cr_3C_2–NiCr and WC–Ni thermal spray coatings as alternatives to hard chromium for erosion–corrosion resistance.* 2008. **202**(8): p. 1405-1417.
118. Amandeep Singh, V.C., and NeelKanth Grover, *Oxidation Behavior OF CNT Reinforced Al_2O_3 Coated Grade A-1 Boiler Steel In Air at 900°C.* International Journal of Engineering Science Invention Research & Development. **Volume III**(Issue VIII).
119. METCO/Perkin-Elmer, 1989.
120. Smith, M.F., et al., *A Comparison of Techniques for the Metallographic Preparation of Thermal Sprayed Samples.* 1991: p. 97-104.
121. Brundle, C.R., et al., , *Encyclopaedia of Materials Characterization.* 1992.
122. Cullity, B., D., *Elements of X-Ray Diffraction.* 1978.
123. Stern, M., Geary, A.L., *A Theoretical Analysis of the Shape of Polarization Curves. Journal of the Electrochemical Society,.* Electrochemical Polarization, 1957. **104**: p. 56-63.
124. Kelly, R.G., Scully, J. R., Shoesmith, D., and Buchheit, R. G., *Electrochemical Techniques in Corrosion Science and Engineering.* 2002: p. p. Chapter 4.
125. Coward, G.W., *Overview: protective coatings—purpose, role, and design.* 1986(2): p. 194-200.

126. A. Torres-Islas, B.C., S. Serna, J. Uruchurtu, J. G. Gonzalez-Rodriguez, *Corrosion inhibition efficiency study in a microalloyed steel for sour service at 50 C.* Journal of Applied Electrochemistry, 2010. **40**: p. 1483-1491.
127. Camilo A. Duarte, E.E., Juan Carlos Martinez, *Failure analysis of the wall tubes of a water-tube boiler.* 2017(79): p. 704-713.
128. Gupta, P.K., *Soil, Plant, Water, and Fertilizer Analysis*. 2016. p. 66-67.
129. B31.1, A., *ASME Code for Pressure Piping,* . 1999: p. 105.
130. AST, A.A., *Standard Specification for Seamless Medium-Carbon Steel Boiler and Superheater Tubes.* 2002.